DEUTSCHES ELEKTRONEN-SYNCHROTRON DESY

DESY 86-041
March 1986

HEAVY QUARK PHYSICS AT LEP

by

A. Ali

Deutsches Elektronen-Synchrotron DESY, Hamburg

ISSN 0418-9833

NOTKESTRASSE 85 · 2 HAMBURG 52

To be sure that your preprints are promptly included in the
HIGH ENERGY PHYSICS INDEX ,
send them to the following address (if possible by air mail) :

DESY
Bibliothek
Notkestrasse 85
2 Hamburg 52
Germany

DESY 86-041
March 1986

ISSN 0418-9833

HEAVY QUARK PHYSICS AT LEP*

A. Ali
Deutsches Elektronen-Synchrotron, DESY
Hamburg, Federal Republic of Germany

Contents

1) Introduction

2) The standard model predictions in $e^+e^- \to$ hadrons
   2.1 Hadronic cross sections, σ_{tot}, and the forward-backward charge asymmetry, A_{FB}^f.
   2.2 QCD and quark mass corrections to $\sigma(e^+e^- \to \gamma,Z \to X)$ and A_{FB}^f.
   2.3 Weak decays of heavy quarks
   2.4 Semileptonic decay distributions of heavy quarks and hadrons
   2.5 Top quark polarization effects

3) The Cabibbo-Kobayashi-Maskawa Matrix

4) Weak mass mixings and their implications at LEP
   4.1 $D^0-\bar{D}^0$ mixings
   4.2 $B^0-\bar{B}^0$ mixings
   4.3 Inclusive dilepton rates in $e^+e^- \to b\bar{b} \to llX$
   4.4 Weak mixing effects in the forward-backward bottom quark charge asymmetry
   4.5 Weak mixing effects in $\sigma(e^+e^- \to l^\pm K^\mp K^\mp X)$
   4.6 Direct and induced mixing effects in top hadrons

5) CP-violation in bottom hadrons and prospects of measurements at LEP

6) Summary and conclusions

---

* To be published in the proceedings of the LEP-Physics-Jamboree, CERN, Geneva, Switzerland.

Abstract:

The theory and phenomenology of heavy quark production and decays at LEP and SLC energies are discussed. We particularly emphasize the bottom quark physics because of the anticipated large event rates on the Z^0 peak, and top quark physics for obvious reasons. A good part of the calculations presented here is of interest also for experiments at lower e^+e^- energies.

1. Introduction

The past and present experience with e^+e^- storage rings as precision tools in the studies of heavy quark physics strengthens our hope that LEP and SLC would continue this illuminating tradition. This hope is certainly well founded since one expects a cross section for $e^+e^- \to Z^0 \to$ (hadrons, leptons) of $\sim$ 30 nb at the Z^0-peak, $\sqrt{s} = m_Z \simeq 93$ GeV. With an estimated integrated luminosity of $\sim 100\ pb^{-1}$ in a typical year at LEP, one expects per year 3×10^6 Z^0 events[1]. Thus, the interest in LEP lies primarily in its capability of studying rare processes. This aspect has already been emphasized in the context of Higgs and Higgs - like particle searches[2]. We would like to concentrate here on the heavy quark physics, especially the rare processes in the weak decays of heavy quarks.

Let us briefly take stock of the situation in weak decays of the charmed and bottom hadrons. As of now $\sim$ 85 % of the D^0 and $\sim$ 88 % of the D^+ exclusive decays have been measured, mostly from the ψ'' (3.77) decays[3]. The inclusive measurements of the processes $(D^0, D^+) \to K^\pm X$, their semileptonic decays as well as measurements of a large number of Cabibbo suppressed decays have put the Cabibbo - GIM current in charmed hadron decays on a firm footing. The inclusive lepton spectra are well reproduced by the QCD - improved quark decay model[4]. The experimental situation about the $F^\pm$ decays is not quite as satisfactory. There are only a few $F^\pm$ decay modes established and even inclusive measurements of the type $BR(F^\pm \to l^\pm X)$, $BR(F^\pm \to K^\pm X)$, $BR(F^\pm \to \eta X)$ etc are not yet measured. This circumstance is both due to the relatively small statistics of the $e^+e^- \to F^\pm X$ sample as well as due to the formidable background from the much more frequent processes $e^+e^- \to D^0X$, $D^\pm X$. Since, one expects a branching ratio $BR(Z^0 \to c\bar{c}) \simeq 11$ % in the standard model, this would lead to $O(10^5)$ events of the type $Z^0 \to CX \to F^\pm X$ in a typical year at LEP. This is large

enough a sample to address detailed questions about $F^{\pm}$ decays. However, the real difference at LEP and SLC and their counterparts at PETRA and PEP lies in the improved vertex detection capability at LEP and SLC with typical resolutions of $O(20)\mu$[5]. This should provide a reasonable detection efficiency for the $F^{\pm}$ mesons at LEP and SLC, something which is missing in lower energy e^+e^- experiments at PEP, PETRA, CESR and DORIS. The interest in tagging the $F^{\pm}$, apart on its own right, is also due to the expected decays of the bottom mesons B_s^0 and weak mixings $B_s^0 \leftrightarrow \bar{B}_s^0$ giving $B_s^0 \to F^{\pm}X$[6]. Thus, an understanding of the $F^{\pm}$ decay properties and an improved detection efficiency at LEP and SLC would be at a premium.

There is another latent interest in the studies of the charmed meson decays, namely in the $D^0 \leftrightarrow \bar{D}^0$ oscillations. The present best limit on the probability of $D^0 \leftrightarrow \bar{D}^0$ oscillation is: $P(D^0 \leftrightarrow \bar{D}^0) \leq 4.7\times10^{-3}$[7]. We do expect some improvement on this limit by the ongoing experiments before the LEP turnon. In the standard model one expects Prob. $(D^0 \leftrightarrow \bar{D}^0) \sim O(10^{-3})$, though there is considerable uncertainty in the numerical prediction due to non-perturbative effects[8]. The large number of events in the process $Z^0 \to D^0X$ and the sizeable detection efficiency for the D^0 mesons at LEP and SLC experiments should make it possible to detect $D^0 \to \bar{D}^0$ mixings at the 10^{-3} level. The vertex detection efficiencies for the charmed and bottom mesons at LEP are discussed separately by R. Settles in a companion report[9].

Turning to the present status of bottom hadron decays, probably the most significant result so far has been the measurement of their average lifetime, $\langle\tau_B\rangle = (1.26 \pm 0.16) \times 10^{-12}$ sec. The long bottom lifetime is a boon for LEP and SLC experiments and would enable them to detect bottom mesons at a rather handsome rate (see refs. (9) and (10) for calculations of detection efficiencies at LEP and SLC). The other significant information from the CESR and DORIS experiments is the present upper limit on the bottom quark coupling constant ratio: $\bar{R} \equiv \Gamma(b\to u l\nu_l)/\Gamma(b\to c l\nu_l) < 0.08$ % (90 % confidence level.)[11]. In addition to the inclusive measurements, the experiments at CESR and DORIS have put upper bounds on a number of two - body or quasi two - body decays of the B^0 and $B^{\pm}$ mesons, which are typically at the level of $O(10^{-4})$, for example $BR(\bar{B}^0 \to \pi^+\pi^-) < 0.02$ %[11]. For the Cabibbo - Kobayashi - Maskawa (CKM)[12] allowed transition $b \to c$, the inclusive measurements of the semileptonic branching ratios and lepton spectra are in agreement with perturbative QCD - improved quark decay model. On the other hand, the

B_s^0 meson has yet to be discovered. The discovery of the B_s^0 meson and the anticipated large $B_s^0 \leftrightarrow \bar{B}_s^0$ oscillation may have to wait the onset of the LEP and SLC machines, though we do expect significant advances elsewhere on these fronts in the intervening period[13]. Extrapolating in time, probably the most important questions in bottom decays at the time of the LEP turnon would be the determination of the CKM suppressed transition $b \to u$, the observation (confirmation?) of $B_s^0 - \bar{B}_s^0$ oscillation, the measurement of individual bottom hadron lifetimes and semileptonic branching ratios. Since the branching ratio $BR(Z^0 \to b\bar{b}) \simeq 15$ %, we expect a production of $O(10^6)$ bottom hadrons per detector at LEP per year. This should enable the experiments at LEP to study most if not all of these questions. Whether one would be able to detect CP violation in bottom hadron decays is a question that depends on a number of fortunate circumstances. Dedicated LEP runs over a long period, however, would provide the statistics and the measuring environment to at least meaningfully probe the predictions in several extensions of the standard model in the CP violation sector. In most extensions of the standard model, the CP violation effects in the bottom sector are enhanced[14].

The standard model predicts a sixth quark, top, to complete the bottom doublet. Present evidence for the top quark is rather fragile. The UA1 - collaboration have reported evidence for a signal in the canonical topology expected in the t-quark decays with the mass in the range $m_t \simeq 30$-50 GeV[15]. The top landscape is otherwise flat and it is virgin land for experimenters at LEP and SLC. Obviously, if $m_t > m_{Z/2}$, then top will not be accessible in the Z^0 decays but only in the higher energy e^+e^- continuum where the $t\bar{t}$ cross section is not large. For $m_t < m_{Z/2}$, there certainly is some phase space suppression in top quark production rates. These rates have been estimated by the working group on toponium physics[16], which we have also used here. We shall restrict ourselves here to some of the interesting issues in the decays of the top quark. In the CKM model, the present bound on the matrix element V_{ub} and unitarity predicts $|V_{tb}| \gg |V_{ts}| \gg |V_{td}|$. The question is whether it would be possible to measure the transitions $t \to s$ and $t \to b$ at LEP, leading to an independent determination of the matrix element V_{ts} and V_{td}. Since V_{ts} is already known in the CKM model via the relation $V_{ts}^2 = 1 - V_{us}^2 - V_{cs}^2$, this would provide a check on the 3-family CKM model. The method to determine V_{ts} is through the measurement of the $l^{\pm}$ energy spectrum in the semileptonic decays $t \to sl^+\nu_l$, which would result in harder momentum spectrum compared to the decays $t \to bl^+\nu_l$. However, since already $|V_{ts}|/|V_{tb}| \sim O(\lambda)^2$, where $\lambda = \sin\theta_c$, measuring this ratio

would require a very large top hadron sample, which may or may not be available at the Z^0 peak. A lower value of m_t , say m_t = 30-35 GeV, would be very welcome in this respect.

There is no compelling reason to believe that quarks heavier than the top exist. However, they may exist in their own right. The most stringent constraint on the heavier fermion masses is due to their contribution to the so called ρ-parameter defined for example by $\rho \equiv m_W^2/m_Z^2\cos^2\theta_W$ .The value of ρ found from the deep inelastic ν_μ and $\bar{\nu}_\mu$ data is $\rho = 1.02 \pm 0.02$ [17]. At 1σ level therefore one has $\Delta\rho < 0.04$, which translates into the following bounds on the fermion masses [18]

$$(m_{Qu} - m_{Qd})^2 + \frac{1}{3}(m_{\nu L} - m_L)^2 < (310\ \text{GeV})^2$$

where the notation is obvious. This gives a fairly large allowed mass range for the search of heavy fermions. If the heavy fermion mass $m_F < E_{beam}$, then e^+e^- machines would be suitable tools to produce these fermions and study their properties. We shall, however, restrict ourselves to 3-families and refer to detailed calculations presented in refs. (22) and (23) for phenomenological implications of heavier than top quark production at LEP.

This paper is organized as follows. In section 2, we discuss the production cross sections for the process $e^+e^- \to \gamma,z \to f\bar{f}$ and review the forward - backward charge asymmetry. The cross sections estimates take into account both the perturbative QCD corrections in $O(\alpha_s)$ as well as the quark mass effects for heavy quarks. This then provides the branching ratios for $Z^0 \to f\bar{f}$. We review the present status of the weak decays of heavy quarks, presenting estimates for their lifetimes, semileptonic branching ratios and some exclusive decay modes of the bottom hadrons which have a special theoretical interest. We also discuss the perturbative QCD corrections to the $l^\pm$ energy spectra in the semileptonic decays of the charm, bottom and top quarks and present a method to determine the ratio V_{bu} / V_{bc} in the continuum e^+e^- (or on the Z^0 pole) through the $l^\pm$ transverse - energy distributions. In section 3, we review the present status of the CKM matrix elements and the potential of LEP experiments to determine some of the undetermined entries in the CKM matrix. In section 4, we review the theory and phenomenology of B-$\bar{B}$ oscillations [19]. We present rates for the dilepton final states in the decays $Z^0 \to b\bar{b} \to l^\pm l^\pm x$, l^+l^-x [20] and for the inclusive lepton-kaon-kaon final states in

$e^+e^- \to \gamma,Z^0 \to l^\pm K^\mp K^\mp x$, $l^\pm K^\pm K^\pm x$, $l^\pm K^+ K^- x$, which also provide useful signatures for the B_s - $\bar{B}_s$ oscillations. In section 5, we briefly review the prospects of CP-violation in the bottom hadron decays, remaining mainly in the standard model framework and briefly mentioning variations on this theme [6,14,22]. Finally, section 6 contains a brief summary and an outlook.

2. THE STANDARD MODEL PREDICTIONS in $e^+e^- \to$ HADRONS

2.1 Cross sections and the forward backward charge asymmetry

We start this section by reviewing some of the standard formulae for the processes $e^+e^- \to Z^0,\gamma \to f\bar{f}$ where f is either a lepton or a quark. In the Born approximation, and ignoring for the time being fermion mass corrections, the differential cross section (averaged over initial and summed over final spins) can be written as

$$\frac{d\sigma}{d\cos\sigma}(e^+e^- \to Z,\gamma \to f\bar{f}) = \frac{\pi\alpha^2 Q_f^2 N_f(1+\cos^2\theta)}{2s}$$

$$- \frac{\alpha Q_F N_f G_F (1 - s/m_Z^2)D^{-1}}{2\sqrt{2}}\left[v_e v_f (1+\cos^2\theta) + 2a_e a_f \cos\theta \right]$$

$$+ \frac{G_F^2 N_f s D^{-1}}{16\pi}\left[(v_e^2 + a_e^2)(v_f^2 + a_f^2)(1+\cos^2\theta) + 2a_e a_f v_e v_f \cos\theta \right] \qquad (2.1)$$

where $D = (1 - s/m_Z^2)^2 + (\Gamma_Z/m_Z)^2$, Q_f is the electric charge and the parameters of the standard model a_f, v_f and N_f are given in table 1. As is well known the interest in the $\cos\theta$ distribution is in the electroweak forward-backward charge asymmetry defined as

$$A_{FB}^{f} \equiv \frac{\int_{0}^{1} \frac{d\sigma}{dcos\theta} dcos\theta - \int_{-1}^{0} \frac{d\sigma}{dcos\theta} dcos\theta}{\int_{0}^{1} \frac{d\sigma}{dcos\theta} dcos\theta + \int_{-1}^{0} \frac{d\sigma}{dcos\theta} dcos\theta} \equiv \frac{\Delta_f^{(0)}}{\sigma_f^{(0)}} \qquad (2.2)$$

The numerator in the integrated asymmetry, Δ_f, and the cross section, σ_f, in the denominator are given by (the superscript (0) denotes lowest order)

$$\sigma_f^{(0)} = \sigma_{VV}^{f} + \sigma_{AA}^{f} \qquad (2.3)$$

$$\Delta_f^{(0)} = \Delta_{z\gamma}^{f} + \Delta_{zz}^{f}$$

where

$$\sigma_{VV}^{f} = \frac{4}{3s}\pi\alpha^2 Q_f^2 N_f - \frac{4\alpha Q_f N_f G_F (1 - s/m_z^2) D^{-1} v_e v_f}{3\sqrt{2}} + \frac{G_F^2 N_f s D^{-1} v_f^2 (v_e^2 + a_e^2)}{6\pi}$$

$$\sigma_{AA}^{f} = \frac{G_F^2 N_f s^{-1}}{6\pi} a_f^2 (v_e^2 + a_e^2) \qquad (2.4)$$

$$\Delta_{z\gamma}^{f} = -\frac{4\alpha}{\sqrt{2}} Q_f N_f G_F (1 - s/m_z^2) D^{-1} a_e a_f$$

$$\Delta_{zz}^{f} = \frac{G_F^2 N_f}{2\pi} s D^{-1} a_e a_f v_e v_f$$

from where it is straightforward to read off the expressions for the cross sections and the asymmetry. Distinguishing here between the (i) PETRA/PEP range $s \ll m_z^2$ and (ii) at the Z^0-peak, $s = m_z^2$, one has the following expressions for the two regions

(i) $s \ll m_z^2$

$$A^{f} \approx -\frac{3G_F}{\alpha\sqrt{2}\pi} \frac{s}{(1 - s/m_z^2)} a_e \left(\frac{a_f}{Q_f} \right)$$

$$\sigma_f = \sigma_{\mu\mu} \left[Q_f^2 N_f - \frac{\pi G_F}{\sqrt{2}\alpha} N_f \frac{v_e (Q_f v_f)}{(1 - s/m_z^2)} \right] \qquad (2.5)$$

where

$$\sigma_{\mu\mu} = \sigma(e^+e^- \to \mu^+\mu^-) = \frac{4}{3s}\pi\alpha^2 \qquad (2.6)$$

(ii) $s = m_z^2$

$$A_{F-B}^{f} = \frac{3 a_e a_f v_e v_f}{(v_e^2 + a_e^2)(v_f^2 + a_f^2)}$$

$$\sigma^{f} = \frac{G_F^2 N_f m_z^4}{6\pi\Gamma_z^2} (v_e^2 + a_e^2)(v_f^2 + a_f^2) \qquad (2.7)$$

We will not discuss here the electroweak radiative corrections, which have been extensively discussed by the working group on the precision tests of the standard model at LEP[24]. Our interest here is mainly in the production and decay properties of the heavy quarks. To get a quantitative estimate of the production cross sections for $e^+e^- \to Z^0 \to t\bar{t}x$, which in turn effects the branching ratios for all other Z^0 decay modes, as well as for the theoretical interpretation of precision measurements of the forward backward asymmetries for the quark sector, we need to evaluate both the QCD corrections and the effects of including the quark masses.

2.2 QCD and quark mass corrections to $\sigma(e^+e^- \to \gamma,z \to x)$ and A_{FB}^q

We shall first discuss the QCD corrections to the production cross section, σ^q, for $e^+e^- \to Z^0 \to q\bar{q}$. It is well known that ignoring the quark masses, the perturbative QCD corrections to the electroweak cross section $\sigma(e^+e^- \to \gamma,z \to q\bar{q}x)$ are the same as for the purely electromagnetic production process $e^+e^- \to \gamma \to q\bar{q}x$. These later corrections have been calculated upto terms of order α_s^2 a long time ago, giving[25]

$$\sigma = \sigma_0 \left(1 + \frac{\alpha_s^{(2)}(Q^2)}{\pi} + c_2 \left(\frac{\alpha_s^{(2)}(Q^2)}{\pi}\right)\right) \tag{2.8}$$

where σ_0 is the point like cross section in the quark parton model,

$$\sigma_0 = \frac{4\pi\alpha^2}{s} \sum_q Q_q^2 \tag{2.9}$$

$\alpha_s^{(2)}(Q^2)$ is given by the (two-loop) expression[26]

$$\alpha_s^{(2)}(Q^2) = \frac{12\pi}{(33 - 2n_q)\ln(Q^2/\Lambda^2)} \left[1 - \frac{3(306 - 38n_q)}{(33 - 2n_q)^2} \frac{\ln\ln(Q^2/\Lambda^2)}{\ln(Q^2/\Lambda^2)}\right] \tag{2.10}$$

and the constant c_2 is given by the following expression in the so called $\overline{MS}$ scheme[27]

$$c_2 = 1.98 - 0.115n_q \tag{2.11}$$

$$\sim 1.4 \text{ for } n_q = 5$$

For the massless case going over from $e^+e^- \to \gamma \to q\bar{q}x$ to $e^+e^- \to \gamma,z \to q\bar{q}x$ amounts to replacing σ_0 by σ_f which is given in Eqs. (2.3) and (2.4). In other words σ_{VV}^q and σ_{AA}^q are normalized by the same multiplicative factor. Including quark mass correction splits the factorized form of the QCD correction terms (2.8) into two different

multiplicative factors for σ_{VV}^q and σ_{AA}^q. The quark mass corrections up to $O(\alpha_s)$ to σ_{VV}^q are the same (apart from a colour factor $c_F = 4/3$) as the ones obtained by Schwinger in QED[28]. They are well approximated by the expression[29]

$$R_V^q = \beta_q \frac{(3 - \beta_q^2)}{2} \left\{1 + \frac{4}{3}\alpha_s(Q^2)\left[\frac{\pi}{2\beta_q} - \left(\frac{3 + \beta_q}{4}\right)\left(\frac{\pi}{2} - \frac{3}{4\pi}\right)\right]\right\}$$

$$\xrightarrow[\beta_q \to 1]{} 1 + \frac{\alpha_s(Q^2)}{\pi} \tag{2.12}$$

where $\beta_q = (1-4m_q^2/Q^2)^{1/2}$

$$\alpha_s(Q^2) = \frac{12\pi}{33\ln Q^2/\Lambda^2 - 2\sum_q \ln\frac{Q^2 + 5m_q^2}{\Lambda^2 + 5m_q^2}}$$

$$\xrightarrow[\beta_q \to 1]{} \frac{12\pi}{33 - 2n_q \ln Q^2/\Lambda^2} \tag{2.13}$$

and we have indicated the relativistic limits for $s \gg 4m_q^2$ (i.e. $\beta_q \to 1$). In other words, the coupling constant $\alpha_s(Q^2)$ feels the effect of only the light flavours. The correction factor for the σ_{AA}^q part of the cross section is well approximated by[30]

$$R_A^q = \beta_q^3 \left\{1 + \frac{4}{3}\alpha_s(Q^2)\left[\frac{\pi}{2\beta_q} - \left(\frac{19}{10} - \frac{22}{5}\beta_q + \frac{7}{2}\beta_q^2\right)\left(\frac{\pi}{2} - \frac{3}{4\pi}\right)\right]\right\} \tag{2.14}$$

The expression for the cross section $\sigma(e^+e^- \to \gamma,z \to q\bar{q})$ now becomes

$$\sigma_f = \sum_q \left(R_V^q \sigma_{VV}^q + R_A^q \sigma_{AA}^q\right) + \sum_l \left(\sigma_{VV}^l + \sigma_{AA}^l\right) \tag{2.15}$$

where the cross section is now obviously split into the leptonic and hadronic parts. The expressions for σ^f_{VV} and σ^f_{AA} are given in eqs. (2.4) together with the coefficients in table (1).

There are several remarks about the determination of $\alpha_s(Q^2)$ that have been made in literature and we would like to restate them here. Suppose $m_t > m_{Z/2}$ in which case the decay $Z \to t\bar{t}$ is forbidden. Then, to an excellent approximation the total hadronic cross section $\sigma(e^+e^- \to \gamma,z \to q\bar{q}x)$ is given by eqs. (2.8). The QCD correction term amounts to approximately 4% assuming $\Lambda_{\overline{MS}} \simeq 150$ MeV[31]. With the huge statistics available, the determination of $\alpha_s(Q^2)$ at LEP will be dominated by the systematic errors. These are discussed in detail elsewhere[24]; assuming a ± 1% error on Γ_Z or on $\sigma(e^+e^- \to \gamma,z \to x)$ will allow a determination of α_s within ± 20% in a model independent way. By the same argument measurements of the leptonic branching ratio $BR(Z^0 \to l^+l^-)$ will also provide a more or less comparable sensitivity to α_s. If $m_t < m_{Z/2}$, then the contribution due to $t\bar{t}$ production becomes somewhat uncertain. It has been argued[30] that including $O(\alpha_s)$ corrections should provide a better theoretical estimate for $\sigma(e^+e^- \to t\bar{t})$ and $\Gamma(Z^0 \to t\bar{t})$. However, the topology of $t\bar{t}$ events is expected to be quite different. This is discussed in detail by G. Rudolph in a separate companion report[32]. Excluding these events and calculating $\sigma(e^+e^- \to \gamma,Z \to q\bar{q})$ for the rest of the hadronic events should again lead to a determination of $\alpha_s(Q^2)$. Clearly, such a measurement is not entirely inclusive and an additional systematic uncertainty has to be included in all such determinations of $\alpha_s(Q^2)$. We have not attempted to estimate the model dependence of nontop topological cross sections and leave it as an instructive exercise for our experimental colleagues.

We return to the discussion of the estimates for the decay width $\Gamma(Z^0)$ and the branching ratios $BR(Z^0 \to f\bar{f})$, including the branching ratio for $Z^0 \to t\bar{t}$. Normalizing the widths $\Gamma(Z^0 \to f\bar{f})$ in terms of $\Gamma(Z^0 \to \nu\bar{\nu})$, we can express the relative branching ratios as

$$\frac{\Gamma(Z^0 \to f\bar{f})}{\Gamma(Z^0 \to \nu\bar{\nu})} = 2N_f \left[v_f^2 R_V^f + a_f^2 R_A^f \right] \qquad (2.16)$$

$$\text{and } \Gamma(Z^0 \to \nu\bar{\nu}) = \frac{\alpha m_Z}{24 \sin^2\theta_W \cos^2\theta_W (1 - \Delta r_0)} \qquad (2.17)$$

with $\Delta r_0 = 0.06$ which corrects for the effect of the renormalization of α[33]. The expressions for $R^l_{V,A}$ are obtained from Eqs. (2.12) and (2.14) by setting $\alpha_s = 0$. In table 2(a) - 2(c) we present the branching ratios for the decays $Z^0 \to f\bar{f}$ for three sets of values for m_Z and $\sin^2\theta_W$. In fig. (1) we show the branching ratio $Z^0 \to t\bar{t}$ as a function of m_t[30]. Clearly, the perturbative calculations for $\Gamma(Z^0 \to t\bar{t})$ break down if the mass difference $\Delta M (Z \to t\bar{t})$ is very small (≪ 1 GeV), since non-perturbative effects become important. We note that in the standard model, with three families of quarks and leptons, the branching ratios for heavy flavour production are rather large. In particular, we expect $BR(Z \to c\bar{c}) \simeq 11\%$ and $BR(Z^0 \to b\bar{b}) \simeq 15\%$. The branching ratio for the $t\bar{t}$ mode, $BR(Z^0 \to t\bar{t})$, could be as large as ≃ 3% for $m_t \simeq 40$ GeV, where now $O(\alpha_s)$ corrections play an important role.

Next we discuss the mass and QCD corrections to the forward-backward charge asymmetry. At the Born level, the quark-mass corrections to A_F are given by $A_f = \beta^2 A_f^{(0)}$ where $A_f^{(0)}$ is given in eq. (2.3). The $O(\alpha_s)$ corrections to A^f have also been calculated[33]. One now has

$$A_q^{(1)} = A_q + \frac{\alpha_s(Q^2)}{\pi} \left[r_F \frac{4}{3} A_q^{(0)} + r_F' A_{Z\gamma}'(q) \right] \qquad (2.18)$$

where as noted in ref. (33.), the $A'_{Z\gamma}$ term originates from the imaginary part of the Z propagator interfering with the photon propagator giving,

$$A'_{Z\gamma}(q) = \frac{4}{\sqrt{2}} G_F \alpha Q_e Q_q a_e a_q \left(\Gamma_{Z/m_Z} \right) D^{-1} \qquad (2.19)$$

The functions r_F and r_F' are shown in fig. (2) as a function of [illegible]. As pointed out in ref. (33), the $O(\alpha_s)$ correction terms to A_q in eq. (2.18) are rather small. However, since σ_q changes substantially for $\beta_q \ll 1$, the forward-backward asymmetry $A_q = \frac{A_q}{\sigma_q}$ also changes substantially for the heavy quarks in the same

limit. At the Z^0-pole, however, this effect is expected to be substantial only for the top quark. In fig.3 we show the effect of the change in the asymmetry for the top quark for m_t = 25GeV as a function of the centre of mass energy. The interest in fig. (3) is twofold. First, the determination of the heavy quark electroweak coupling constants have to be corrected for the quark mass and $O(\alpha_s)$ effects which certainly are not small for the top quark. Secondly, these corrections tend to decrease the forward-backward charge asymmetry. As we are going to discuss in a subsequent section, weak mass mixing effects due to $B-\bar{B}$ mixing also tend to decrease this asymmetry. Since $B_s-\bar{B}_s$ mixing is expected to be large and the forward-backward asymmetry in $e^+e^- \to b\bar{b} \to l^{\pm}x$ has been advocated as a possible place to detect such mixings[34], it is important to take into account the corrections we have just discussed.

Before closing this section we reiterate that the measurements of the total cross section and the asymmetry in regions (i) and (ii) are sensitive to different pieces of the standard model couplings. This is obvious from Eqs.(2.3)-(2.7). In table (3) we have collected the present experimental information on the standard model coupling constants and their expected values.

The axial vector coupling constants a^e, a^μ, a^u and a^d have been measured with a typical error of ±10% at lower energies. The errors on a^τ, a^c and a^b are still large. Hopefully, more data from PETRA and PEP should also render measurements of $a^{\tau,c,b}$ at a comparable level of accuracy. There is practically no information available on a^s, for lack of a proper signal of the s-quark, and on a^t for obvious reasons. Turning to the measurement of the vector coupling constants v^q, there have been very few attempts in the past to extract them directly from data. Instead, almost always results are presnted in terms of $\sin^2\theta_w$. It would be nice to have measurements of v_q. The present status of the leptonic vector coupling constants is summarized in fig. (4) where the product $v_e v_\mu$ and $v_e v_\tau$ are presented from the measurements at PETRA and PEP energies. The forward-backward asymmetry at the Z^0 peak allows measurements of the coupling constant product $a_f v_f$ as can be seen from eq. (2.7) and σ^f measures the combination $(v_f^2 + a_f^2)$. Thus, measurements of A_{FB}^f and σ^f at the Z^0 peak would determine a_f and v_f individually.

2.3 Weak decays of heavy quarks

We shall briefly review here some of the salient features of heavy quark decays, which are relevant for studies at LEP and SLC energies. In the standard model the weak decays for heavy hadrons are governed by the Hamiltonian

$$H_W = \frac{G_F}{\sqrt{2}} \left(J_+^\mu (0) J_{-\mu} (0) + h.c \right) \tag{2.20}$$

with the charged weak current given by

$$J_{-\mu} = J^l_{-\mu} + J^q_{-\mu}$$

The leptonic and the quarkonic currents have the familiar form:

$$J^l_{-\mu} = \left(\bar{\nu}_e, \bar{\nu}_\mu, \bar{\nu}_\tau \right) \gamma_\mu \left(1 - \gamma_5 \right) \begin{pmatrix} e^- \\ \mu^- \\ \tau^- \end{pmatrix}$$

$$J^q_{-\mu} = \left(\bar{u}, \bar{c}, \bar{t} \right) \gamma_\mu \left(1 - \gamma_5 \right) V \begin{pmatrix} d \\ s \\ b \end{pmatrix} \tag{2.21}$$

where V is a 3x3 matrix, first written by Kobayashi and Maskawa for 3 quark families.

It is customary to use the free quark decay model for the processes

$$Q \to q\, l^{\pm}\, \nu_l, \quad q q_1 \bar{q}_2$$

to calculate inclusive semileptonic and nonleptonic rates and $l^{\pm}$-momentum spectra. The short distance part of the strong interaction corrections are then taken into account in QCD perturbation theory. This gives two types of corrections (i) genuine $O(\alpha_s)$ perturbation theory corrections to Γ_{SL}, Γ_{NL} and (ii) renormalization of the bare Hamiltonian for the non-leptonic interactions, H_{NL}. We discuss the corrections of type (ii) first. The renormalization group improvements lead to the multiplicative renormalization of the operators $O^{\pm}$, giving[35]

$$H_{NL}^{eff} = \frac{G_F}{\sqrt{2}} \left[c_+ \left(\alpha_s, \frac{m_W}{\mu} \right) O_+ + c_- \left(\alpha_s, \frac{m_W}{\mu} \right) O_- \right] \tag{2.22}$$

with

$$O_\pm = \frac{1}{2} \left[\left(\bar{U} V D \right)_L \left(\bar{D} V^+ U \right)_L \pm \left(\bar{U} V U \right)_L \left(\bar{D} V^+ D \right)_L \right]$$

where U(D) denotes the up(down)-type quark arrays and $(\bar{U}D)_L = \bar{U} \gamma_\mu (1 - \gamma_5) D$. In the leading log approximation, one has[34]

$$c_- = \left[\alpha_s(\mu^2)/\alpha_s(M_W^2) \right]^{\frac{12}{33-2n_f}}$$

$$c_+ = 1/\sqrt{2}$$

where μ is a reference mass scale and n_f is the number of flavours ($n_f = 4,5,6$ for c,b and t decays, respectively). Clearly, the values of $C_\pm$ are flavour (and quark mass dependent). For $\Lambda = 0.2$ GeV, numerically[35]

$$c_- (m_c = 1.7 \text{ GeV}) = 1.7 \tag{2.23}$$

$$c_- (m_b = 5 \text{ GeV}) = 1.4$$

$$c_- (m_t = 40 \text{ GeV}) = 1.07$$

This is to be compared with the free-quark decay result $c_+ = c_- = 1.0$. Thus, for the top quark, renormalization group improvements in $c_\pm$ are not very significant.

The genuine $O(\alpha_s)$ corrections to the partial widths Γ_{SL} and Γ_{NL} have also been calculated. For semileptonic decays one has the result[36]

$$\Gamma_{SL} = \Gamma_0 \sum_q I \left(0, \frac{m_l}{m_Q}, \frac{m_q}{m_Q} \right) \left[1 - \frac{2}{3} \frac{\alpha_s(m_Q^2)}{\pi} f \left(\frac{m_q}{m_Q} \right) \right] |V_{Qq}|^2$$

$$\equiv \Gamma_{SL}^{(0)} K_{SL} \tag{2.24}$$

The correction factors of type (i) and type (ii) for Γ_{NL} together give[37]

$$\Gamma_{NL} = \Gamma_0 \sum_{q_i} 3 |V_{Qq_1}|^2 |V_{q_2 q_3}|^2 I \left(\frac{m_{q1}}{m_Q}, \frac{m_{q2}}{m_Q}, \frac{m_{q3}}{m_Q} \right)$$

$$\times \left(\frac{2c_+^2 + c_-^2}{3} \right) \left[1 + \frac{2}{3} \frac{\alpha_s(m_Q^2)}{\pi} b_Q \left(0; c_\pm \right) \right] \tag{2.25}$$

$$\equiv \Gamma_{NL}^{(0)} K_{NL}$$

where $\Gamma_0 = \frac{G_F^2 m_Q^5}{192\pi^3}$

The phase space factor I(x,y,z) is given by

$$I(x,y,z) = 12 \int_{(x+y)^2}^{(1-z)^2} \frac{d\xi}{\xi} \left(\xi - x^2 - y^2 \right) \left(1 + z^2 - \xi \right) W \left(\xi, x^2, y^2 \right) W \left(1, z^2, \xi \right) \tag{2.26}$$

where $W(a,b,c) = \left[a - \left(\sqrt{b} + \sqrt{c} \right)^2 \right]^{1/2} \left[a - \left(\sqrt{b} - \sqrt{c} \right)^2 \right]^{1/2}$

and $\quad x,y,z = \frac{m_i}{m_Q}$ (i = 1,2,3).

For y = z = 0, the function I(x,y,z) has the familiar form

$$I(x,0,0) \equiv g(x) = 1 - 8x^2 - 24x^4 \ln x + 8x^6 - x^8$$

In eqs. (2.24) and (2.25), we have introduced the multiplicative QCD correction factors K_{SL} and K_{NL} for the semileptonic and non-leptonic decays, which represent the cumulative effects of all QCD corrections to the widths. The phase space functions g(x) and f(x) are shown in fig.(5) for 0<x<0.5, which is the range of interest for the t,b and c decays. The function $h_Q(0,c\pm)$, which enters the non-leptonic decays, has actually been calculated for $m_{q_i} = 0$ and so the quark mass effects in the QCD corrected form have been approximated by the free-quark decay expression. The numerical accuracy of this approximation has still to be checked. In the limit $m_{qi} = 0$, the function h(0,c±) is given by[37]

$$h(0,c\pm) = -\left(\pi^2 - \frac{31}{4}\right) + \frac{19}{4}\,\frac{c_-^2 - c_+^2}{2c_+^2 + c_-^2} + 3\,\frac{\alpha_s(m_Q^2) - \alpha_s(m_W^2)}{\alpha_s(m_Q^2)}\,\frac{2c_+^2\rho_+ + c_-^2\rho_-}{2c_+^2 + c_-^2} \qquad (2.27)$$

where

$$\rho_+ = \left(-\frac{221}{24} + \frac{5}{9}n_f\right)\frac{1}{b_1} + \left(51 - \frac{19}{3}n_f\right)\frac{1}{b_1^2}$$

$$\rho_- = \left(\frac{263}{12} - \frac{10}{9}n_f\right)\frac{1}{b_1} + \left(-102 + \frac{38}{3}n_f\right)\frac{1}{b_1^2}$$

$$b_1 = \left(\frac{33 - 2n_f}{3}\right) \qquad (2.28)$$

There is considerable amount of uncertainty in the determination of the renormalization constants c± because of the choice of the renormalization scale μ. A reasonable choice of μ is probably the parent quark mass and all our calculations are based on the assumption $\mu = m_Q$[38]. With this choice of μ and $\Lambda_{\overline{MS}}$ = 200 MeV, one gets K_{NL}(charm) = 1.46. The values of $c_\pm$ and K_{NL} for the bottom quark for the experimentally allowed bottom quark mass range[39] 4.8 GeV < m_b < 5.2 GeV are given in table 4. Typically K_{NL} (bottom) = 1.12. The corresponding quantities for the top quark in the mass range 30 GeV < m_t < 50 GeV are given in table 6. Quite amusingly K_{NL}(top) < 1, with K_{NL} (m_t = 40 GeV) = 0.94 being a typical number.

The $O(\alpha_s)$ correction factor for the semileptonic decay $Q \to q l \nu_l$ depends on the mass ratio m_q/m_Q. For the charm quark decays, m_s and m_c have been determined by the fits to the lepton energy spectra in the process $e^+e^- \to \psi'' \to l^\pm x$. This gives K_{SL}(charm) = 0.81. The corresponding K-factore for the CKM allowed bottom decays are given in table 5a for the mass range 4.8 GeV < m_b < 5.2 GeV and 1.5 GeV < m_c < 1.8 GeV.

Typically, for the $b \to c l \nu_l$ decays K_{SL}(bottom) = 0.87. The corresponding K-factors for the CKM supposed decays $b \to u l \nu_l$ are shown in table 5b for 4.8 GeV < m_b < 5.2 GeV and 0.3 GeV < m_u < 0.6 GeV. Typically, K_{SL} (b → ux) = 0.82. For the top quark decays the semileptonic K-factors are:

$$K_{SL}\ (m_t = 40\ \text{GeV}) = 0.89 \quad \text{for } t \to b l \nu_l$$
$$= 0.87 \quad \text{for } t \to s l \nu_l$$
$$\text{and } t \to d l \nu_l \qquad (2.29)$$

The dependence of K_{SL} on m_t in the range 30 GeV < m_t < 50 GeV is very mild and we don't show it explicitly here. However, we have taken this variation into account in calculating Γ(top) and the semileptonic branching ratio $BR(t \to l\overset{\pm}{x})$.

We remark that the QCD corrections we have been discussing so far pertain to the free quark decays only. How about the final state interactions, like for

example the interference effects discussed for the $D^{\pm}$ decays[40], or other non-spectator mechanisms, like for example the annihilation mechanism[41] important for D^0 decays? That these mechanisms are numerically important for the charm decays is well established through the ratio of the life-times:

$$\frac{\tau(D^+)}{\tau(D^0)} = 2.0 \pm 0.2$$

and that of the semileptonic branching ratios[42]

$$\frac{D^+ \to e^+ x}{D^0 \to e^+ x} = 2.3 \,^{+0.5}_{-0.4} \pm 0.1$$

We would like to argue here that despite the importance of the non-spectator effects in the charmed hadron decays, their analogues in the bottom and top decays are expected to be numerically unimportant, at least in the inclusive decay rates and branching ratios. We briefly review below the annihilation and interference effects for the bottom and top hadron decays.

The annihilation of a pseudoscalar meson into a pair of fermions is well known from the charged pion and kaon decays, $(K^{\pm}, \pi^{\pm}) \to \mu^{\pm}\nu_{\mu}$, $e^{\pm}\nu_e$. The matrix elements describing the decay $P \to f_1 + \bar{f}_2$ depend, due to the familiar helicity arguments, on the fermion masses m_1 and m_2, and on the overlap of the annihilating quark wave functions in the pseudoscalar meson. Thus, for the leptonic decays $P \to l^{\pm}\nu_l$, the decay width is given by

$$\Gamma\left(P(\equiv Q\bar{q}) \to l^{\pm}\nu_l \right) = G_F^2 \frac{|V_{Qq}|^2}{8\pi} f_p^2 m_p m_l^2 \left(1 - \frac{m_l^2}{m_p^2} \right)^2 \qquad (2.30)$$

where V_{Qq} is an element of the CKM matrix and f_p is the pseudoscalar meson coupling constant defined as

$$\langle 0|\bar{q}\gamma_\mu\gamma_5 Q|P\rangle = i f_p P_\mu \qquad (2.31)$$

For the decays $P \to f_1\bar{f}_2$, the decay width is obtained from the expression

$$\Gamma(P \to f_1\bar{f}_2) = C \frac{G_F^2}{8\pi} f_p^2 m_p (m_1^2 + m_2^2) I_A\left(\frac{m_2^2}{m_p^2}, \frac{m_2^2}{m_p^2} \right) \qquad (2.32)$$

where the two-body phase space factor $I_A(x,y)$ is given by

$$I_A(x,y) = \left[1 - \frac{(x-y)^2}{x+y} \right] \lambda^{1/2}(1,x,y) \qquad (2.33)$$

with $\lambda(1,x,y) = (1-x-y)^2 - 4xy$ and the factor C describes the dynamical details:

$$\begin{aligned} C &= 3\,|V_{Qq}|^2\,|V_{12}|^2 && \text{for } W^{\pm}\text{-annihilation} \quad P \to q_1\bar{q}_2 \\ &= |V_{Qq}|^2 && \text{for } P \to l^{\pm}\nu_l \\ &= \frac{1}{3}\,|V_{Q_1}|^2\,|V_{q2}|^2 && \text{for } W^{\pm}\text{-exchange} \end{aligned} \qquad (2.34)$$

The pseudoscalar coupling constant f_p and the CKM matrix elements V_{Qq} and V_{12} are needed to evaluate the contribution of the decays $P \to f_1\bar{f}_2$. The constants f_p have been evaluated in a number of papers using non-relativistic potential models[43], QCD sum rules[44] and the so called bag models of hadrons[45]. In non-relativistic potential models f_p is related to the wave-function at the origin, $\Psi(0)$, by the expression

$$f_p = \sqrt{\frac{12}{m_p}}\,|\Psi(0)| \qquad (2.35)$$

where the $Q\text{-}\bar{q}$ centre of mass wave function $\Psi(r)$ is normalized by $\int d^3r\,|\Psi(r)|^2 = 1$. In such models, $\Psi(0)$ is governed by the reduced mass

$$\mu = \frac{m_Q m_q}{m_Q + m_q}$$

which approaches the light quark mass m_q for $m_q/m_Q \ll 1$. Hence in the non-relativistic models $\Psi(0)$ approaches a constant value as m_Q increases, which would predict a decrease of f_p as

$$f_p \propto \sqrt{\frac{1}{m_p}}$$

with increasing m_p. Non-relativistic models are expected to work reasonably well when both the quark masses m_Q and m_q are not small, like for example in the $B_c^{\pm}$, $T_c^{\,0}$ and $T_b^{\pm}$ mesons. The relativistic as well as QCD corrections change the numerical values of f_p, in particular the latter corrections for the heavy-light quark mesons are expected to be significant, like for example in D^0, $D^{\pm}$, B^0, $B^{\pm}$, $T_u^{\,0}$ and $T_d^{\pm}$ mesons. The present theoretical dispersion in the estimates of f_p is at least a factor 2, with most models predicting the follwing values for f_p (in the normalization f_π = 130 MeV)

$$\begin{aligned} f_D &\sim 120 - 180 \text{ MeV} \\ f_F &\sim 130 - 220 \text{ MeV} \\ f_{B_d} &\sim 80 - 160 \text{ MeV} \\ f_{B_s} &\sim 100 - 200 \text{ MeV} \end{aligned} \qquad (2.36)$$

Thus, most probably $f_B \leq 200$ MeV for the $B_d^{\,0}$, $B_u^{\pm}$ and $B_s^{\,0}$ mesons. The corresponding coupling constants f_T for the $T_u^{\,0}$, $T_d^{\pm}$, $T_s^{\,0}$ mesons are expected to be even smaller. This would imply that the contribution of the $W^{\pm}$ -exchange and annihilation diagrams in $P \to f_1\bar{f}_2$ would become rapidly unimportant as m_Q increases. We expect these mechanisms to contribute at the rate of $\leq$ 10% to the B decays and at a completely negligible rate for the top decays. In this respect, the estimates presented in this report are substantially different than for example the ones reported in ref. (46), where a much higher value f_B = 500 MeV was used to estimate the decays $B \to f_1\bar{f}_2$. Some of the two-body decays of the charmed and bottom hadrons are quite interesting in that they provide testing grounds for the hadronic wave functions, like for example f_p ,and/or provide information on the CKM matrix elements V_{ij}. We will later present an estimate of the branching ratios for some of the two body annihilation modes.

In what follows, we shall ignore the $W^{\pm}$exchange and annihilation contribution in estimating the total widths of the bottom and top hadrons. Likewise, interference effects are also expected to become numerically small due to the large phase space available in the bottom and top decays, while the wave-function overlap, which is the measure of interference effects, is expected to be essentially constant. The effect of neglecting the non-spectator contribution on Γ_{tot} can be estimated assuming a model for the hadronic wave function. We shall however not attempt this here. Alternatively, one can get an estimate of the accuracy of the

spectator model description of inclusive widths by the predictions of the semileptonic branching ratios.

In the approximation of neglecting $W^{\pm}$exchange and interference contributions, the total width of the bottom quark can be expressed as follows[47]

$$\Gamma^b_{tot} = \frac{G_F^2 m_b^5}{192\pi^3}\left[\,|V_{bc}|^2 Z_c + |V_{bu}|^2 Z_u\,\right] \qquad (2.37)$$

The factors Z_c and Z_u depend on the QCD scale parameter Λ, renormalization scale μ, and the quark masses m_b, m_c, m_u etc. With Λ = 200 MeV, $\mu = m_b$, the dependence of the function Z_c on the masses m_b and m_c is shown in table 5a. For the CKM allowed decays and the mass range 4.8 GeV $\leq m_b \leq$ 5.2 GeV, 1.5 GeV $\leq m_c \leq$ 1.8 GeV, the function Z_c varies in the range $2.0 \leq Z_c \leq 3.6$. For the CKM suppressed decays the dependence of the factor Z_u on the masses m_b and m_u is shown in table 5b. It should be empahsized that the value of the mass m_u needed in the CKM forbidden decays $b \to u + x$ is very probably in the vicinity of 500 MeV, since it is an interpolating mass for a weighted average of the hadron masses m_π, m_ρ, $m_{2\pi}$ etc, which saturate the u quark channel. In the next section, we shall discuss that a similar value for m_u is suggested from the positivity of the lepton spectrum, when one takes $O(\alpha_s)$ corrections into account. In the range 4.8 GeV $\leq m_b \leq$ 5.2 GeV and 0.3 GeV $\leq m_u \leq$ 0.6 GeV, the function Z_u varies in the range $5.73 \leq Z_u \leq 6.55$ and hence is quite stable.

The semileptonic decay width can also be expressed similarly

$$\Gamma^b_{SL} = \frac{G_F^2 m_b^5}{192\pi^3}\left[\,|V_{bc}|^2 L_c + |V_{bu}|^2 L_u\,\right] \qquad (2.38)$$

where the factors L_c and L_u, like their counterparts Z_c and Z_u for Γ^b_{tot}, lump the effect of the $O(\alpha_s)$ QCD corrections as well as the quark mass effects. For the quark mass range considered for Γ^b_{tot} , the functions L_c and L_u are given in tables 5a and 5b respectively. Since the present upper bound on the ratio $|V_{bu}|/|V_{bc}|$ is already very stringent for the purpose of determining Γ^b_{SL} and Γ^b_{tot} , namely

$$\frac{|V_{bu}|^2}{|V_{bc}|^2} \lesssim 3\times10^{-2} \ .$$

The numerical effect of dropping the $|V_{bu}|$ dependent term in eqs.(2.37) and (2.38) is negligible. The semileptonic branching ratio is given by the expression (keeping only terms of order $|V_{bu}|/|V_{bc}|^2$)

$$BR(b \to lx) \simeq \frac{L_c}{Z_c}\left[1 + \left|\frac{V_{bu}}{V_{bc}}\right|^2\left(\frac{L_u}{L_c} - \frac{Z_u}{Z_c}\right)\right] \qquad (2.39)$$

The numerical values of the semileptonic branching ratios BR(e) are given in table 5a. For the quark mass range considered, BR(e) varies in the range $13.2\% \lesssim BR(e) \lesssim 15.8\%$. This is to be compared with the measured branching ratios[11]

$$\begin{aligned} BR(B \to xl\nu_l) &= (11.7 \pm 0.6)\% \text{ at } I(4s) \\ &= (12.2 \pm 0.8)\% \text{ at PETRA/PEP} \end{aligned} \qquad (2.40)$$

The measured numbers are approximately 15% lower than the estimates presented here. This represents a fair description of the semileptonic branching ratios since non-perturbative effects certainly have to be taken into account at this level.

The average life-time of the bottom hadrons has also been measured[3]

$$\tau_b = (1.26 \pm 0.16)\times10^{-12} \text{ sec} \qquad (2.41)$$

This information can be combined with the present upper limit on the ratio $\bar{R}$ and eq. (2.37) to determine the CKM matrix element $|V_{bc}|$. However, as we have seen there exists ~ 15% discrepancy between the theoretical prediction of BR(e) based on eq.(2.37) and the experimental measurements. Though this is not a big deal but a somewhat preferred procedure is to use the measured quantities BR(e) and $\tau(b)$ and the relation

$$\Gamma_{SL} = \frac{BR(e)}{\tau} \qquad (2.42)$$

and use instead the theoretical predictions for Γ_{SL} . This needs a precise determination of the masses m_b and m_c , which can in principle be determined from the lepton energy spectrum. We defer further discussion of this point to the next section.

We briefly discuss another method to determine the CKM matrix element V_{bu}. This involves the decay $B^\pm \to \tau^\pm\nu_\tau$. The formula for the width is given in eq.(2.30). Numerically,

$$\Gamma(B^\pm \to \tau^\pm\nu_\tau) \simeq 30\left(\frac{f_B}{m_B}\right)^2 \frac{G_F^2 m_b^5}{192\pi^3}\left|V_{bu}\right|^2 \qquad (2.43)$$

which leads to the branching ratio

$$BR(B^\pm \to \tau^\pm\nu_\tau) \simeq \frac{30\left(\frac{f_b}{m_B}\right)^2\left|\frac{V_{bu}}{V_{bc}}\right|^2}{\left[Z_c + \left|\frac{V_{bu}}{V_{bc}}\right|^2 Z_u\right]} \qquad (2.44)$$

using $f_{B_u} \sim f_\pi = 130$ MeV and $\left|\frac{V_{bu}}{V_{bc}}\right| \lesssim 0.16$, this leads to an upper bound

$$BR(B^\pm \to \tau^\pm\nu_c) \lesssim 2\times10^{-4} \qquad (2.45)$$

which indeed is comparable to the present upper bounds on hadronic two body decays involving $b \to u$ transitons. The signature of the decay $B^\pm \to \tau^\pm\nu_\tau$ would be somewhat striking. One would observe the topology

$$\begin{array}{ccccc} Z^0 & \to & b\bar{b} & \to & (B)_{jet} + (\bar{B})_{jet} \\ & & \Big\downarrow & & \downarrow \\ & & & & \tau\nu_\tau \\ & & \Big\downarrow & & \\ & & (D,F + n\pi,\ldots) & & \end{array} \qquad (2.46)$$

resulting in a very asymmetric hadron energy deposition in the two jets. The jet with lower hadron energy deposition will have a $\tau^{\pm}$, which can be identified either through topology or in vertex detectors. An association of such topologies with the decays $B^{\pm} \to \tau^{\pm}\nu_{\tau}$ however, would need very extensive analysis due to the much more copious process $F^{\pm} \to \tau^{\pm}\nu_{\tau}$ and the semileptonic decays $b \to c\tau^{-}\nu_{\tau}$, both involving $\tau^{\pm}$ in hadronic jets. This, however, can be studied with the help of the existing monte carlo programmes. In any case the final states $l^{-}x$ in jets with $l^{-} = e^{-}$, μ^{-} have led to very important information in the study of weak interactions; we believe that the final state $\tau^{\pm}x$ will certainly provide another useful tag on heavy hadrons, and we would like to emphasize a good detection ability for $\tau^{\pm}x$ states.

Next, we discuss the decays of the top quark. In the CKM model the decays of the top quark are dominated by the transition $t \to bx$. The next allowed transition $t \to sx$ is expected to have a relative branching ratio $\sim |V_{ts}|^2/|V_{tb}|^2 \sim |V_{bc}|^2 \sim 3 \times 10^{-3}$, and the twice forbidden transition $t \to dx$ is expected to give an inclusive branching ratio of $O(10^{-4})$ or less. The present evidence of the top quark is rather sparse and the present determination of m_t allows a range[15] 30 GeV $\lesssim m_t \lesssim$ 50 GeV. We shall take this bound seriously and present calculations for m_t in this range. The total decay width of the top quark can be expressed as

$$\Gamma^t_{tot} = \frac{G_F^2 m_t^5}{192\pi^3} \bar{\Gamma}^t \qquad (2.47)$$

where the reduced width $\bar{\Gamma}^t$ is defined as

$$\bar{\Gamma}^t = \sum_i \bar{\Gamma}^t_i \qquad (2.48)$$

and the sum is over all allowed decay modes i. The partial reduced widths $\bar{\Gamma}_i$ can be defined just as the total reduced width $\bar{\Gamma}^t$, namely via the relation

$$\Gamma^t_i = \frac{G_F^2 m_t^5}{192\pi^3} \bar{\Gamma}^t_i \qquad (2.49)$$

The numerical values of $\bar{\Gamma}^t_i$ together with the CKM angle dependence are shown in table 7 for the leading sixteen inclusive partial decay modes, involving leptons and quarks. The branching ratios for all of these partial decay modes are also shown in table 7 for $m_t = 40$ GeV, $V_{tb} = 0.997$, $V_{ts} = 0.05$ and $|V_{td}|/|V_{tb}| \lesssim 0.01$. These branching ratios depend very weakly on m_t in the mass range 30 GeV $\lesssim m_t \lesssim$ 50 GeV, and in particular the semileptonic branching ratio is very stable with $BR(t \to l^{+}\nu x) \approx 10.7\%$. The dependence of the reduced width $\bar{\Gamma}^t$ on m_t is shown in table 8, where the factors Z_b, Z_s and $Z_d (\approx Z_s)$ are defined via the relation

$$\bar{\Gamma}^t = \left[|V_{tb}|^2 Z_b + |V_{ts}|^2 Z_s + |V_{td}|^2 Z_d \right] \qquad (2.50)$$

The dependence of $\bar{\Gamma}^t$ on m_t as shown in table 8 is also rather mild. Note that for $m_t = 40$ GeV the width $\Gamma^t_{tot} \approx 17.2$ KeV, a number already comparable to the combined electromagnetic and strong widths of the bound toponium state $0(t\bar{t})$. The large width of Γ^t_{tot} and its rapid rise with m_t has several important phenomenological consequences for the search of bound toponium states. This is the subject of the toponium study group to which we refer for details.

There are several remarks that we would like to make here about top quark decays. Top quarks are copious sources of tau leptons: $BR(t \to b\tau^{+}\nu_{\tau}) \approx 10.5\%$. In addition since b decays also involve $\tau^{\pm}$ leptons with a branching ratio $BR(b \to c\tau^{-}\nu_{\tau}) \approx 2.5\%$, one expects an inclusive branching ratio $BR(t \to \tau^{\pm}x) \approx 13\%$. Since $\tau^{\pm}$ can well be tagged in a good vertex detector, one has an additional method to tag top quark decays; $\tau^{\pm}$ at a large angle from a hadronic jet are not expected from background processes. In particular, the processes $b \to \tau^{\pm}\nu X$ would lead to $\tau^{\pm}$ within the jet. Next, we note that the dominant decay modes of the top quark are expected to result in the inclusive states $t \to l^{\pm}x (l = e,\mu)$. This is obvious from table 7 and the fact that in almost all decays a bottom quark will be produced with large energy, the subsequent decays $b \to l^{-}x$, as well as $c \to l^{+}x$, $\tau^{\pm} \to l^{\pm}x$ decays will result in a very large inclusive branching ratio for $t \to l^{\pm}x$. In fact even the decays involving dileptons $t \to l^{\pm}l^{\mp}x$ are expected to be quite significant. The dilepton ($e + \mu$) branching ratio for the decays $t \to l^{\pm}l^{\mp}x$ is expected to be $\sim 1\%$! This provides another very useful signature for detecting the threshold of the top quark. We give in table 9, the branching ratios for the inclusive final states $t \to$

$(nl^{\pm})x$ for n = 0,..,5. Of course, the actual measurements would depend on the lepton detection efficiency and we don't attempt to make a guess about them, since detailed monte carlo programmes[49] are available which can be used at LEP energies to estimate these efficiencies.

We would especially like to emphasize here the decay mode $t \to l^{\pm}l^{+}x$, which is expected to receive contribution from the decays $t \to bl^{+}\nu_l$ + charge conjugate. Since one of the leptons i.e. from the cascade $b \to c \to l^{+}\nu_l$, will be very soft, it will probably not contribute very much to the measured process $t \to l^{\pm}l^{+}x$. As we shall discuss later, we do expect substantial weak mixings in the B_s $\bar{B}_s$ sector, which should also show itself indirectly in the decays of charged top mesons $T_Q^{\pm}$:

$$t(\bar{s}) \to b(\bar{s})l^{+}\nu_l$$
$$\downarrow$$
$$B_s \leftrightarrow \bar{B}_s \to l^{+}\nu_l x$$

leading to energetic $l^{\pm}l^{\pm}x$. Thus, it is extremely important to have a good measurement of the energy of $l^{\pm}$ and its charge.

2.4 Semileptonic decay distributions of heavy quarks and hadrons

The interest in the semileptonic decay distributions of heavy quarks is manifold. The shape of the lepton energy distribution is sensitive to the Michel parameter, ρ_M, which for example has the value $\rho_M = 3/4(0)$ for the standard V-A(V+A) current, in $\tau^{\pm} \to l^{\pm}\nu_l\nu_\tau$ (l = e,μ) decays. The shape of the $l^{\pm}$ spectrum in the semileptonic decays of heavy quarks $Q \to ql^{\pm}\nu_l$ is then by analogy with $\mu^{\pm}$ and $\tau^{\pm}$ decays also sensitive to the chirality of the charged weak current. Experimental measurements of the inclusive lepton energy spectra for the charmed and bottom hadrons have led to the validity of (V-A) currents of the standard model for c and b quark sector. In addition, the lepton energy spectrum in the decays $Q \to ql\nu_l$ is sensitive to the mass of the decaying quark, m_Q, and to the ratio m_q/m_Q. In particular, the peak position of the distribution $d\Gamma/dE_l$, denoted by E_l^{peak} is sensitive to m_Q (to a lesser extent also on m_q/m_Q), and the end point $l^{\pm}$ - spectrum

to the ratio m_q/m_Q. Precise measurement of $d\Gamma/dE_l$ then is a good method to determine both m_Q and m_q, and the relative strength of the CKM allowed and suppressed transitions. We shall review here some of the points involved in using the inclusive lepton spectra for determining m_t from the top quark decays and the ratio V_{bu}/V_{bc} in the bottom quark decays.

In quark-parton model, the $l^{\pm}$-energy spectra in semileptonic decays of heavy hadrons are calculated in the free quark decay approximation from the process $Q \to ql^{\pm}\nu_l$. The normalized lepton energy distributions are well known for c and b decays[50].

$$\frac{1}{\Gamma_o}\frac{d\Gamma}{dx_e} = H(x_l, r_q)$$

$$= \frac{12x_l^2(1 - x_l - r_q^2)^2}{(1 - x_l)} \quad \text{(for c and t decays)} \tag{2.51}$$

$$= \frac{2x_l^2(1 - x_l - r_q^2)^2}{(1 - x_l)^3}\left[\left(1 - x_l\right)\left(1 - r_q^2 - x_l\right) + \left(2 - x_l\right)\left(1 + 2r_q^2 - x_l\right)\right]$$

$$\text{(for b decays)} \tag{2.52}$$

where $x_l = 2E_l/m_Q$, $r_q = m_q/m_Q$ and Γ_o is the semileptonic decay width in the free quark decay model

$$\Gamma_o = \frac{G^2 m_Q^5}{192\pi^3}\sum_q |V_{Qq}|^2 \, g(m_q/m_Q)$$

The maximum of x_l is given by: $x_l^{max} = 1 - r_q^2$, which, for example, has the values 0.87 and 0.99 for the $b \to c$ and $b \to u$ decays, respectively, for $m_b = 5$ GeV, $m_c = 1.8$ GeV and $m_u = 0.5$ GeV. The corresponding values for the top quark decays $t \to bl\nu_l$ and $t \to (s,d)l\nu_l$ are ~ 0.984 and ~ 1.0 respectively for $m_t = 40$ GeV. The difference $\Delta x_l^{max} \simeq 0.015$ translates into ~ 300 MeV in ΔE_l for $E_l = 20$ GeV, for top decays with $m_t = 40$ GeV. Thus, an experimental $l^{\pm}$ energy resolution in $\frac{\Delta E_l}{E_l}$ of better than 1% is needed to measure the difference in the $l^{\pm}$ end point energy

spectra in the decays $t \to b l \nu_l$ and $t \to (s,d) l \nu_l$. This circumstance by itself puts enormous limitation on the feasibility of measuring the ratio of the CKM matrix elements $|V_{ts}/V_{tb}|$, more so since one expects $|V_{ts}/V_{tb}|^2 \sim 3\times10^{-3}$! Given enough statistics, it certainly is doable but in view of the rates for top production, the prospects are not very encouraging. The quantity x_l^{peak} is sensitive to the mass m_Q, and in the free-quark model it is given by the expression (for t decays)

$$x_l^{peak} = \frac{(5 - r_q) - (1 + 14r_q + r_q^2)^{1/2}}{6} \qquad (2.53)$$

$$\longrightarrow 2/3$$

$$r_q \to 0$$

This corresponds to E_l^{peak} = 10.71, 11.03, 11.35 GeV for m_t = 40,41 and 42 GeV, respectively. Thus, an experimental determination of E_l^{peak} within ± 0.10 GeV will determine m_t within ± 0.5 GeV. Of course, this is a somewhat idealized situation. The experimental distributions depend on the lorentz boost (and hence on the fragmentation of t quark → T-hadron), on the polarization of the top hadrons[51], and on their hadronic wave functions. In addition one should take into account perturbative QCD corrections. The $O(\alpha_s)$ corrections to the inclusive lepton spectrum in the decays $Q \to l^{\pm}x$ have been calculated and compared with the data from the $\psi''(3.77)$[43] and $\Upsilon(4s)$ decays. In leading order QCD, the $l^{\pm}$ energy distribution for the standard V-A currents can be expressed as

$$\frac{1}{\Gamma_0}\frac{d\Gamma}{dx_l} = \sum_q |V_{Qq}|^2 \left[H(x_l, r_q) + \frac{2\alpha_s(m_Q^2)}{\pi} h(x_l, r_q) \right] \qquad (2.54)$$

with the normalization

$$\int_0^{x_{max}} h(x_l, r_q)\, dx_l = -f(r_q) \qquad (2.55)$$

where $f(r_q)$ is shown in fig.(5). The function $h(x_l, r_q)$ is in general a complicated function for $r_q \neq 0$. For $r_q = 0$, it has been calculated analytically by Cabibbo et al[4] for c-quark decays and corbo[4] for b quark decays. It was shown in ref. (4) that the normalized distribution $\frac{1}{\Gamma}\frac{d\Gamma}{dx_l}$ is remarkably stable against $O(\alpha_s)$ radiative corrections for $m_q/m_Q \neq 0$, which is the case in the dominant decays $c \to s$, $b \to c$, $t \to b$. The endpoint spectra in the decays $b \to u$, $t \to s,d$ however become negative in $O(\alpha_s)$. The remedy of this is either to exponentiate the leading terms for the endpoint spectrum, or else assume that the effective mass of the u and d quark is not zero but of O(500) MeV[4]. For such values of m_u, m_d, which seem to be very reasonable, the normalized lepton energy spectra are also very stable for the CKM suppressed transitions. We shall not show the QCD corrected spectra here since they are practically indistinguishable from the uncorrected ones and refer to refs. (4) for relevant comparisons.

We would like to point out here that precise measurements of the $l^{\pm}$-energy spectra can also be used in the continuum e^+e^- production, e.g. in the processes $e^+e^- \to \gamma, Z^0 \to b\bar{b} \to l^{\pm}x$, to study the CKM suppressed decays $b \to u l \nu_l$. The interesting distribution in this context is the transverse lepton-momentum distribution, $\frac{1}{\sigma}\frac{d\sigma}{dx_T l}$, where $x_T^l = 2P_T^l/\sqrt{s}$ is measured with respect to the botton jet axis. Since the angular radius of a hadronic jet shrinks with increasing $\sqrt{s}$[52], one expects fairly collimated bottom quark jets at LEP/SLC energies. Thus, errors on the determination of jet axis are not expected to pose a severe problem. We quote here from ref. (50) the corrected expressions for the normalized transverse lepton-momentum distribution, measured with respect to the parent quark (jet) axis in the decays $Q \to q l \nu_l$,

$$\frac{1}{N}\frac{dN}{dp_T^l} = c\int_{(p_T^{min})_H}^{\infty} (dp_T)_H \frac{f(p_T^H)}{E_T^H} \int_{\chi^{min}}^{\chi^{max}} d\chi \frac{m_Q}{\chi} H(\chi, r_q) \qquad (2.56)$$

where

$$\chi = P_Q \cdot P_l \,, \quad E_T^H = \left(P_T^{H^2} + m^{H^2} \right)^{1/2}$$

$$(P_T^{min})_H = \max.\left\{ 0, (P_{T_1}^2 - \Delta^2 m_Q^2)/2\Delta P_{T_1} \right\}$$

$$\chi^{min} = (P_T)_1 \left\{ (E_T)_H - (P_T)_H \right\}$$

$$\chi^{max} = m_Q^2 \Lambda$$

$$\Lambda = \frac{1}{2}(1 - r_q^2) \qquad (2.57)$$

and $c = \left\{ \frac{32}{m_Q^6 g(r_q)} ; \frac{192}{m_Q^6 g(r_q)} \right\}$ for (b; c,t) decays

Here $H = Q\bar{q}$ is the heavy (decaying) hadron and $f(P_T^H)$ is an intrinsic P_T^H distribution function, usually taken as a gaussian. The function $H(\chi = P_Q \cdot P_l, r_q = m_q/m_Q)$ is given by the expression in eq. (2.51), for c and t decays, and eq. (2.52) for b decays, and the function g(x) is given by $g(x) = 1 - 8x^2 - 24x^4 \ln x + 8x^6 - x^8$.

The measurements of the distribution $\frac{1}{N}\frac{dN}{dp_T}$ in high energy e^+e^- experiments have led to the determination of branching ratios for $b \to lx$, which are in good agreement with the measurements at the $\Upsilon(4s)$[53]. Present bottom hadron statistics at PETRA/PEP is typically an order of magnitude smaller than at DORIS and CESR, and this fact therefore has limited the scope of the PETRA/PEP experiments in setting a meaningful limit on the quantity V_{bu}/V_{bc}. However, with an expected $\sim 10^6$ bottom hadrons per experiment per year at LEP, detectors having good lepton energy resolutions would be very competitive with experiments at DORIS and CESR.

With this possibility in mind we show the distributions $\frac{1}{N}\frac{dN}{dp_T}$ from the decays $b \to cl^-\nu_l$ and $b \to ul^-\nu_l$ in fig. (6) using a gaussian p_T^H-distribution with $\langle p_T^B \rangle \simeq 400$ MeV, a number suggested by the present e^+e^- data [54]. One can see that the p_T^l-distributions depend on the choice of the intrinsic-P_T^H function and hence

the quality of such measurements is not quite the same as the ones from the $\Upsilon(4s) \to b\bar{b} \to l^\pm x$ decays. It should, however, be pointed out that the function $f(p_T^H)$ is measurable independently in the same experiment, by for example measuring $d\sigma/dp_T^{B,B^*}$ and this would eliminate the uncertainty in discussion. A word of caution about the relative normalization of dN/dP_T^l ($b \to u/b \to c$) in an experiment; it is given by $\bar{K}(\ldots|V_{bu}/V_{bc}|^2 g(r_u)/g(r_c)$ in the quark parton model.)

2.5 Top quark polarization effects

In the preceding sections the effects of the heavy quark polarization on the production and decay distributions were neglected. For charm and bottom quarks, the polarization effects are expected to be very small since it is predominantly a pseudoscalar meson that eventually decays weakly. Clearly, the spin-1/2 nature of the quarks leading to a $(1 + \cos^2\theta)$ distribution for the quark jets is still maintained but the heavy quark decays isotropically in its rest frame. The distributions measured in the processes $e^+e^- \to c\bar{c}$, $b\bar{b} \to l^\pm x$, $h^\pm x$ are in good agreement with the assumption of neglecting the polarization effects in the weak decays of the c and b quarks.

This assumption would still be correct if the top quark fragmentation process $t \to T, T^*, + x$ were either dominated by the pseudoscalar top mesons T_q^0, T_q^+ etc, which is somewhat unlikely, or else if the vector meson T^* decayed via electromagnetic or strong interactions leading to $T^* \to T\gamma$, $T\pi$, which, [illegible] the case for D^* and B^* decays. However, this latter scenario is also very unlikely since the hyperfine splitting between T and T^* is expected to be very small and the M1 transition rate $\Gamma(T^* \to T + \gamma)$ would become much smaller compared to the weak decay width $\Gamma(T^* \to BX)$[55]. This certainly would be the case for the top quark with $m_t > 30$ GeV. This means that the polarization of the top quark will result in a polarization of T^* and, through the parity violating weak decays of T^*, will be visible in the energy and angular distributions of its decay products. In addition, for the process $e^+e^- \to T^*(s_z)\bar{T}^*(s_z) + x$, one expects spin-spin correlation effects, leading to some coherence in the fragmentation of top quark jets[56].

It is evident from this discussion that an additional parameter, namely the degree of polarization that survives the fragmentation process, f, would be needed to compare theoretical distributions with the data on top quark production and

decays. Of course, f is à priori not known, but it can be determined by a single measurement. The data from the top quark decays then should be compared with theoretical calculations including polarization effects, with the depolarization parameter f. We shall discuss the t-polarization effects both in production and decays, borrowing calculations reported in refs. (56) and (57).

Top quarks will be produced in e^+e^- annihilation with a high degree of polarization. Defining the t quark polarization vector $\vec{P}_t = (P_L, P_T, P_N)$, one has the following expressions for the three components[57,58]

$$P_L = \frac{1}{N_1}\left\{ 2\, v_t\, a_t\, \beta\, (1 + \cos^2\theta) + 2\, r_e\, (v_t^2 + a_t^2\beta^2)\cos\theta \right\}$$

$$P_T = \frac{m_t}{m_Z}\frac{1}{N_1}\left\{ 4 \sin\theta\, (v_t\, a_t\, \beta \cos\theta + r_e\, a_t^2 \right\} \qquad (2.58)$$

Neglecting γ-z interference and QCD loop corrections the vector $\vec{P}_t$ lies in the t-production plane, i.e. its normal component P_N vanishes. In eq. (2.58), the functions N_1 and r_e are given by

$$N_1 = (v_t^2 + a_t^2)\,\beta^2\,(1 + \cos^2\theta) + 2v_t^2\,(1 - \beta^2) + 4r_e\, v_t\, a_t\, \beta \cos\theta$$

$$r_e = \frac{2v_e\, a_e}{(v_e^2 + a_e^2)} \qquad (2.59)$$

$$\beta = (1-4m_t^2/s)^{1/2}$$

where a_i, v_i are given in table (1). Both P_L and P_T are sensitive functions of m_t. For m_t not very close to $m_Z/2$, P_L is large, negative and only slowly varying with θ. The transverse component P_T has a strong forward-backward asymmetry in θ. Both components are displayed in fig. (7) for m_t = 40 GeV. Averaged over the polar angle, $\langle P_L \rangle$ and $\langle P_T \rangle$ are given by

$$\langle P_L \rangle = -\frac{2v_t\, a_t \beta}{N_2}$$

$$\langle P_T \rangle = \frac{3\pi}{4}\frac{m_t}{m_Z}\frac{r_e v_t^2}{N_2} \qquad (2.60)$$

$\longrightarrow 0$

$r_e = 0$

and the function N_2 is given by

$$N_2 = (v_t^2 + a_t^2)\beta^2 + \frac{3}{2}\, v_t^2\, (1 - \beta^2) \qquad (2.61)$$

The quantities $\langle P_L \rangle$ and $\langle P_T \rangle$ are shown in fig. (8) as a function of $\sqrt{s}$ for m_t = 40 GeV and the values of the standard model parameters corresponding to set (1) in table (2).

The component of t-quark polarization normal to the t-quark production plane, P_N, gets a non-zero contribution from interference between non-real Z exchange and real γ exchange amplitudes[59], and between Born amplitudes and non-real vertex QCD corrections. The relevant Feynman diagrams are shown in fig. (9). Writing

$$P_N = P_N(\gamma Z) + P_N(QCD) \qquad (2.62)$$

one has

$$P_N(\gamma Z) = -\frac{16\pi\alpha}{G_F m_Z^2/2\sqrt{2}}\,\frac{m_Z\Gamma_Z}{Q^2}\,\frac{m_t}{\sqrt{Q}}2\,\beta\sin\theta\,(Q_e\, a_e\, Q_t\, a_t)/N_1 \qquad (2.63)$$

where $Q_e(Q_t)$ is the electric charge of the electron (top quark) and the normalization N_1 is given by eq. (2.59). The $P_N(QCD)$ part is given by

$$P_N(QCD) = -\frac{4\alpha_s}{3}\frac{m_t}{\sqrt{Q}}2\,\sin\theta\left\{(v_e^2 + a_e^2)v_t^2\,\beta\cos\theta + 2v_e\, a_e\, v_t\, a_t\, (2 - \beta^2)\right\} / N_1 \qquad (2.64)$$

The dependence of P_N on θ is also shown in fig. (7). The numerical value of P_N is very small for all values of θ and it is not going to be easy to measure it. The effects of beam polarization on P_N have been studied in ref. (57), where it is shown that both $P_N(\gamma z)$ and $P_N(QCD)$ are dramatically enhanced for longitudinally polarized beams, though in angular regions of small production rate. For this reason we don't show them here.

The measurement of final state correlations among leptons and jets requires the knowledge of spin-spin correlations between t and $\bar{t}$. Dropping terms of $O(r_e)$ (=0 for $\sin^2\theta_w$=1/4), one has

$$\frac{d\sigma(s,\bar{s})}{d\Omega} = \frac{d\sigma}{d\Omega}\frac{1}{4}\left\{ 1 + b_\mu s_\mu + \bar{b}_\mu \bar{s}_\mu + b_{\mu\nu} s_\mu \bar{s}_\nu \right\} \tag{2.65}$$

where the coefficients of the spin terms are given by

$$b_\mu = -\frac{4m_t}{Q^2} a_t v_t \left\{ (1 - \beta\cos\theta)k_\mu + (1 + \beta\cos\theta)k'_\mu \right\} / N_1$$

$$\bar{b}_\mu = \frac{4m_t}{Q^2} a_t v_t \left\{ (1+\beta\cos\theta)k_\mu + (1-\beta\cos\theta)k'_\mu \right\} / N_1$$

$$\begin{aligned} b_{\mu\nu} = & \left\{ (v_t^2 - a_t^2)\,\beta^2(1 - \cos^2\theta)g_{\mu\nu} \right. \\ & - 4(v_t^2 - \beta^2 a_t^2)\,(k_\mu k'_\nu + k_\nu k'_\mu) / Q^2 \\ & \left. - 4(v_t^2 - a_t^2)\,\beta\cos\theta\,(k_\mu k'_\nu - k_\nu k'_\mu) / Q^2 \right\} / N_1 \end{aligned} \tag{2.66}$$

where k_μ and k'_μ denote the 4-momenta of the initial state electron and positron. In the preceding section we have presented detailed distribution based on the unpolarized top quark. Including the polarization of the t quark, one has

$$d\Gamma(s) = d\Gamma(1 + c_\mu s_\mu) \tag{2.67}$$

where $d\Gamma$ is the differential width for unpolarized t-decay. Restricting to the semileptonic decays $t \to bl^+\nu_l$, one has[57]

$$d\Gamma = \frac{G_F^2 m_t^5}{128\pi^3} \frac{x_l\left\{1 - x_l - (m_b/m_w)^2\right\} dx_l dx_b d\Omega_l}{\left\{1 - (m_l/m_w)^2 - (m_t/m_w)^2\,(1 - x_b)\right\}^2} \tag{2.68}$$

The vector c_μ can be chosen for top quark as

$$c_\mu = -\frac{1}{m_{t/2}}\left(\frac{1}{x_l} p_{l\mu} - \frac{1}{2} p_{t\mu} \right) \tag{2.69}$$

and for $\bar{t}$ decays

$$\bar{c}_\mu = +\frac{1}{m_{t/2}}\left(\frac{1}{x_l} p_{l\mu} - \frac{1}{2} p_{t\mu} \right) \tag{2.70}$$

The treatment of $t\bar{t}$ production and decays so far is in close analogy with, for example, the one for the process $e^+e^- \to \tau^+\tau^- \to l^\pm l^\mp x$, $l^\pm h^\mp x$ discussed in ref. (61). The essential difference here arises from the unknown mixture of top hadron polarization states surviving fragmentation effects. The actual cross section is a weighted average of configurations in which both top quarks are depolarized, t or $\bar{t}$ is depolarized, or no quark is depolarized. This will happen, for example, for the configurations $T\bar{T}X$, $(T\bar{T}^* + T^*\bar{T})x$ and $T^*\bar{T}^*x$ respectively. Assuming that a polarized quark with $s_z = +1/2$ will convert into $T^*(s_z = 1)$, $T^*(s_z = 0)$, $T^*(s_z = -1)$ and $T(s = 0)$ with relative weights 2:1:0:1 would give $f = 0.5$. The combined effect of production, fragmentation depolarization, and weak decays can then be expressed as

$$d\sigma_{final} \propto d_\sigma\, D_t\, D_{\bar{t}} \left\{ 1 - f\,[b_\mu c_\mu + b_\mu \bar{c}_\mu] + f^2\, b_{\mu\nu}\, c_\mu \bar{c}_\nu \right\} d\Gamma(t) d\Gamma(\bar{t}) \tag{2.71}$$

where $D_t(D_{\bar{t}})$ is the top quark (anti-quark) fragmentation function, usually parametrized by the Peterson et al. function[62]

$$D_t(z) \sim \frac{4\sqrt{\varepsilon_t}\,/\,\pi}{z\left(1 - \frac{1}{z} - \frac{\varepsilon_t}{1-z}\right)^2}$$

$$\varepsilon_t \sim 0.15(m_c/m_t)^2$$
$$z = 2E_H / \sqrt{s}$$

To show the kind of polarization effects that are expected at LEP and SLC energies, we show from ref. (57) the effect of varying the ε_t and f parameters on the primary lepton energy distribution in the process $e^+e^- \to z^0 \to t\bar{t} \to l^\pm x$ in figs. (10a)...(10c). It is clear that the effect of varying ε_t in the region $0 < \varepsilon_t < 10^{-3}$ on $d\sigma/dE_l^\pm$ is not very important, however this distribution is rather sensitive to the depolarization parameter f. In particular, the end-point spectrum is dependent on f in a measurable way. This is a complication worth remembering if attempts are made to determine the CKM ratio V_{ts}/V_{tb} from precise measurements of the end-point spectrum in the top quark semi-leptonic decays. In fig. (10c), the combined effect of the variations on ε and f on $d\sigma/dE_l^\pm$ are shown for two values of m_t = 42.5 and 37.5 GeV. We note that E_l^{peak}, which we recall is a good measure of m_t, though somewhat smeared is still rather sharp. Thus, polarization effects on the lepton energy spectra, though by no means small, still leave the shape sensitive to m_t, and a good measurement of $\frac{d\sigma}{dE_l^\pm}$ could allow a determination of m_t to within 1 GeV. The measurement of m_t through lepton energy measurements is also studied by the working group on toponium at LEP.

We will conclude this section by a brief discussion of coherence effects in the production of top quarks, which are absent for light quark process $e^+e^- \to \gamma,z \to q\bar{q} \to 2$jets. The coherence effects in the top quark fragmentation would reveal themselves in a production angle dependence of the fragmentation function, quite contrary to the common incoherent approach. This can be seen by introducing the helicity density matrix $\rho(t\bar{t})$ for the process $e^+e^- \to \gamma,z \to t\bar{t}$

$$\rho_{\nu\mu\nu'\mu'} = \frac{1}{N'} \sum_{\lambda_1,\lambda_2} T_{\nu\mu\lambda_1\lambda_2} T^*_{\nu'\mu'\lambda_1\lambda_2} \qquad (2.73)$$

Here T is the helicity amplitude calculated from the Born diagram shown in fig. (11), where the definition of helicities can also be seen. The condition $\mathrm{Tr}\,\rho = 1$ fixes the normalization N'. The cross-section for the inclusive production of a top hadron is given by

$$\frac{d\sigma(e^+e^- \to t\bar{t} \to Hx)}{d\cos\theta dz} = \frac{d\hat{\sigma}}{d\cos\theta} D_t^H(\theta,z) \qquad (2.74)$$

where, in the coherent picture, the fragmentation function is given by

$$D_t^H(\theta,z) = \int dx \sum_{\substack{\lambda\lambda_x \\ \nu\nu'\mu\mu'}} M_{\lambda\lambda_x\nu\mu}(t\bar{t} \to Hx)\, \rho^{(\theta)}_{\nu\mu\nu'\mu'}\, M^*_{\lambda\lambda_x\nu'\mu'} \qquad (2.75)$$

Eq. (2.74) describes the inclusive cross-section for the production of H in $t\bar{t} \to Hx$, starting with a $t\bar{t}$ system whose spin state is described by $\rho(t\bar{t})$, which is a function of θ, hence the dependence of D_t^H on θ and z. It is easy to show (in the approximation of neglecting p_t^H) that the coherent fragmentation function is given by the expression[57]

$$D_t^H(\theta,z) = \int dx \sum_{\lambda\lambda_x} \Big\{ (1 - 2\rho_{++++}) |M_{\lambda\lambda_x+-}|^2 + 2\rho_{++++} \big[|M_{\lambda\lambda_x++}|^2 + \mathrm{Re}\, M_{\lambda\lambda_x++}\, M^*_{\lambda\bar{\lambda}_x--} \big] \Big\} \qquad (2.76)$$

where

$$\rho_{++++} = \frac{4}{N} \sin^2\theta \frac{m_t^2}{s} \left(Q_t^2 + \frac{16}{9} |D_z|^2 V_t^2 (a_e^2 + v_e^2) \right) \qquad (2.77)$$

where $|D_z|^2 = s^2/[(s^2 + m_z^2)^2 + m_z^2 \Gamma_z^2]$

For light quarks, $\rho_{++++} = 0$ and so the fragmentation function $D_t^H(\theta,z)$ has no θ-dependence, recovering the usual incoherent fragmentation picture. To have a detailed prediction one should know the non-perturbative function $M_{\lambda\lambda_x+-}$, $M_{\lambda\lambda_x\pm\pm}$ etc., which, for example are functions of ε_t and the depolarization parameter f for the model we discussed earlier.

It is obvious that detailed predictions of the coherence effects are model

dependent. However, it is possible to get firm predictions for exclusive final states like for example $e^+e^- \to \gamma,z \to T\bar{T}$, $T\bar{T}^*$ etc. In particular, one has

$$D_t^T (e^+e^- \to T\bar{T}^*) \sim (1 - 2\rho_{++++})|M_{01-+}|^2$$

$$D_t^T (e^+e^- \to T\bar{T}) \sim 4\rho_{++++} |M_{00++}|^2$$

The quantities $1-2\rho_{++++}$ and $4\rho_{++++}$ are shown as functions of θ in fig. (12), which serves as an example of the t-quark fragmentation dependence of θ. The effect that such angular dependence can have on some of the physical observables could be dramatic. For example, the forward-backward asymmetry A_{FB}^t (θ) is zero for the exclusive state $e^+e^- \to T\bar{T}$ and gets enhanced for the exclusive state $e^+e^- \to T\bar{T}^*$, compared to the A_{FB}^t (θ) for the process $e^+e^- \to t\bar{t}$. This is shown in fig. (13). Measurement of these effects would constitute a test of the spin-spin effects of top quarks in hadronic channels.

3. The Cabibbo-Kobayashi-Maskawa Matrix

The flavour mixing matrix V, relating the eigenstates of the quark masses to those of the weak currents J_μ^q in eq. (2.21) can be symbolically written as

$$V = \begin{pmatrix} V_{ud} & V_{us} & V_{ub} \\ V_{cd} & V_{cs} & V_{cb} \\ V_{td} & V_{ts} & V_{tb} \end{pmatrix} \qquad (3.1)$$

There are various parametrizations of the matrix V abailable[64], involving three angles and a phase. The first of these parametrization, given by Kobayashi and Maskawa[12], has the form

$$V_{KM} = \begin{pmatrix} c_1 & -s_1c_3 & -s_1s_3 \\ s_1c_2 & c_1c_2c_3-s_2s_3e^{i\delta_{KM}} & c_1c_2s_3+s_2c_3e^{i\delta_{KM}} \\ s_1s_2 & c_1s_2c_3+c_2c_3e^{i\delta_{KM}} & c_1s_2s_3-c_2c_3e^{i\delta_{KM}} \end{pmatrix} \qquad (3.2)$$

where $c_i(s_i) = \cos\theta_i(\sin\theta_i)$ and δ_{KM} is a phase, inducing CP violation. Despite its pioneering character, there is a general feeling among the practitioners of weak

interaction phenomenology that the Kobayashi-Maskawa form, V_{KM}, is not particularly handy in the analysis of experimental results in terms of simple deductions of the CKM angles. This is obvious from a comparison of eqs. (3.1) and (3.2); only the measurements of the matrix element V_{ud} can be directly transformed into the determination of the CKM angle θ_1. All other elements involve functions of at least two angles and some involve all the four CKM parameters. Not surprisingly, almost all quantities related to the elements V_{cs}, V_{cb}, V_{ts}, and V_{tb} directly or indirectly have an involved dependence on the phase δ_{KM}. Examples of such behaviour are $K^0 - \bar{K}^0$ mass differences, the CP violating parameters ϵ, ϵ', mixing parameters in the neutral bottom meson sector as well as CP violations. In several of the cases mentioned above this is an unnecessary complication and can be avoided by a more judicious choice of rotation axes and quark phases. One can make use of the recent measurements of $|V_{bc}|$ and the bounds on $|V_{bu}|$ to write much simpler and practical parametrizations of the matrix V. We shall discuss some popular alternative representations for the matrix V in a while after discussing the present experimental status of the V_{KM} matrix elements.

We list here the matrix elements governing the 2x2 (d,s) part of the matrix V. They are taken from a recent compilation in ref. (65) (see also refs. (66)).

$$|V_{ud}| = 0.9735 \pm 0.0015 \qquad (3.3)$$

$$|V_{us}| = 0.231 \pm 0.003$$

$$|V_{cd}| = 0.24 \pm 0.03$$

$$|Vcs| = 0.85 \pm 0.15$$

The matrix elements $|V_{bc}|$ and $|V_{bu}|$ are the focus of very intense experimental research at the existing e^+e^- machines. As we have discussed in detail in the preceeding sections, the most optimistic place to measure $|V_{bu}|$ is in the analysis of the end-point lepton energy spectrum (equivalently transverse lepton energy spectrum). The present best limit on the ratio $|V_{bu}/V_{bc}|$ is from the analyses of the process $e^+e^- \to \Upsilon(4s) \to B\bar{B} \to l^\pm X$[3]. Unfortunately, the tail of the lepton energy spectrum is sensitive to the bottom hadron wave function and the extraction of

$|V_{bu}/V_{bc}|$ at present is a model dependent enterprise. Probably, the present best limit on the quantity $\bar{R} \equiv \Gamma(b\to u l\nu_l)/\Gamma(b\to c l\nu_l)$ is[67]

$$\bar{R} < 0.04 \quad (90\ \%\ \text{c.L.}) \tag{3.4}$$

obtained by analysing the events with the mass of the hadronic system produced with the lepton, $m_X < 1.0$ GeV. Analysing the lepton energy region beyond the $b \to c l\nu_l$ kinematic limit gives $\bar{R} < 0.08$[3]. Theoretical models used in such analyses are by no means exhaustive or compelling. There is certainly a lot of experimental and theoretical work to be done to get out $|V_{bu}/V_{bc}|$ from e^+e^- data. However, it is obvious from eqs. (2.37) - (2.39) that the upper bound $\bar{R} < 0.08$ already pushes the contributions of the $b \to u$ transitions below a significant level in the semileptonic decay branching ratios and life-times for bottom hadrons. This fact can be used (and has been used) to determine the matrix element $|V_{bc}|$ from the measurements of $\langle\tau_B\rangle$ and $\langle BR\rangle_{SL}$. Using the relation

$$\Gamma^B_{SL} = \frac{BR(l)}{\tau_B}$$

the QCD improved expression (2.37) for Γ^B_{SL} and the measured values for $\langle\tau_B\rangle$ and BR(l) one gets

$$|V_{bc}| = 0.050\ {}^{+\,0.011}_{-\,0.006} \pm 0.002 \tag{3.5}$$

for $m_b = 4.95 \pm 0.04$ GeV and $m_c = 1.65 \pm 0.05$ GeV. We have discussed the dependence of Γ^B_{SL} on m_b and m_c in detail in the preceding section and will not repeat the arguments here. It seems, however, safe to deduce that the present e^+e^- experiments give

$$0.04 < |V_{bc}| < 0.07 \tag{3.6}$$

using $\bar{R} < 0.08$, this gives the upper bound

$$|V_{bu}| < 0.01 \tag{3.7}$$

This is roughly a factor 2 worse limit that one often sees in literature, which are

based on much smaller values for $\bar{R}$. The matrix elements $|V_{bc}|$ and $|V_{bu}|$ are so small that it is possible to predict the element $|V_{tb}|$ to a precision better than 2 p.p.m., with the error dominated by the one on $|V_{bc}|$. Unitarity can be used to predict the range of all the rest of the matrix elements of V. Thus, the present knowledge of the CKM matrix can be summarised as follows

$$V = \begin{pmatrix} 0.973 \pm 0.001 & 0.231 \pm 0.003 & < 0.01 \\ 0.24 \pm 0.03 & 0.85 \pm 0.15 & 0.055 \pm 0.015 \\ < 0.04 & < 0.06 & 0.9992 > V_{tb} > 0.9975 \end{pmatrix} \tag{3.8}$$

We would like to point out that the errors on the matrix elements $|V_{cd}|$ and $|V_{cs}|$ are still quite large to make more definitive statements about V_{td} and V_{ts} and we have used the safer present limit $\bar{R} < 0.08$.

We shall make a digression here and point out that in particular theoretical scenarios it is possible to relate the matrix elements V_{ij} and the quark masses. For example, it was pointed out by Stech[68] that if the up-quark mass matrix M_u and the down-quark mass matrix M_d have the form

$$M_u = M_u^\dagger = M_u^T \tag{3.9}$$

$$M_d = M_d^\dagger = \alpha M_u + A$$

where α is a constant and A is an antisymmetric matrix, then one can show that

$$\alpha = \frac{m_d - m_s + m_b}{m_u - m_c + m_t} \approx \frac{m_b}{m_t} \tag{3.10}$$

$$|V_{12}|^2 \approx m_d/m_s = (0.055)^2$$

$$|V_{23}|^2 \approx m_s/m_b - m_c/m_t = (0.23)^2$$

The predictions and postdictions (3.10) are in remarkable agreement with the

experimental measurements and someday may eventually help to disentangle the complicated structure of symmetry breaking giving rise to the quark matrices M_u and M_d. While still on the trail of theoretical speculations, one should remark that it is possible to predict the ratio $|V_{bu}/V_{bc}|$ in specific models for quark mass matrices. For example, in the generalized Fritzsch model[60] the quark mass matrices M_u and M_d each have the form[70]

$$M_{ij} = e^{i\lambda i} \; F_{ij} \; e^{i\rho j} \; , \quad F = \begin{pmatrix} 0 & A & 0 \\ A & 0 & B \\ 0 & & C \end{pmatrix} \tag{3.11}$$

where A, B, C are positive constants and λ_i and ρ_j are some phases. The matrix elements of F can be written in terms of the quark masses

$$A \approx (m_1 m_2)^{1/2} \; , \; B \approx (m_2 m_3)^{1/2} \; , \; C \approx m_3 \; (m_3 >> m_2 >> m_1) \tag{3.12}$$

One then has the prediction[70,71]

$$|V_{bu}/V_{bc}| \approx \left(\frac{m_u}{m_c} \right)^{1/2} \approx 1/16 \tag{3.13}$$

for the quark masses $m_u = 5.1$ MeV and $m_c = 1.35$ GeV, taken from ref. (72). This predicts $|V_{bu}| \approx 0.004$, which is a factor 2.5 smaller than the present limit given in (3.7). It has been argued in ref. (70) that both the Stech and Fritzsch mass matrices can be made compatable to each other. Confirming (or ruling out) the prediction (3.13) is probably one of the tasks of the LEP experiments. Seen in this perspective, precision measurements of bottom hadron decay properties is an enormously rewarding enterprise.

Returning to other parametrization of the CKM matrix, V, there are two which deserve special mention here. Wofenstein[73] has observed that the matrix elements V_{ij} show a certain pattern, which suggests a perturbative expansion of the matrix elements. Defining $|V_{us}| = \cos\theta_c \equiv \lambda$, one has numerically

$$\lambda = 0,23 \tag{3.14}$$

$$|V_{bc}| = \lambda^2 = 0.05$$

$$|V_{bu}| \leq \lambda^3$$

Then, expanding V_{ij} in powers of λ and keeping terms upto $O(\lambda^3)$, one has a perturbative form for V

$$V_{\text{Wolfenstein}} = \begin{pmatrix} 1 - \frac{1}{2}\lambda^2 & \lambda & A\lambda^3(\rho - i\eta) \\ -\lambda & 1 - \frac{1}{2}\lambda^2 & A\lambda^2 \\ A\lambda^3(1 - \rho - i\eta) & -A\lambda^2 & 1 \end{pmatrix} \tag{3.15}$$

The present experimental information then gives (for $\bar{R} < 0.08$)

$$\lambda = 0.23 \tag{3.16}$$

$$A = 1.0 \pm 0.2$$

$$\rho^2 + \eta^2 < 0.65$$

For $\bar{R} < 0.04$, one would have $\rho^2 + \eta^2 < 0.30$. This parametrization has the simple features that (i) the elements V_{us} and V_{cd} have the same interpretation (to $O(\lambda)$) as in the (2x2) Cabibbo-GIM matrix[74], (ii) $|V_{cb}| = |V_{ts}|$ and (iii) CP violation enters at $O(\lambda^3)$. Of course, the ansatz eq. (3.15) is a very convenient construct for analysing experimental results as we shall see below. Any deeper theoretical understanding of the pattern (3.14) is not at present available.

Another representation of the CKM matrix is given by Gronau and Schechter[75] which, to practical accuracy has the form ($c_{12}(s_{12}) = \cos\theta_{12}(\sin\theta_{12})$ etc.).

$$V_{GS} = \begin{pmatrix} c_{12} & s_{12}e^{i\phi_{12}} & s_{13}e^{i\phi_{13}} \\ -s_{12}e^{-i\phi_{12}} & c_{12} & s_{23}e^{i\phi_{23}} \\ -s_{13}e^{-i\phi_{13}} + s_{12}s_{23}e^{-i(\phi_{12}+\phi_{23})} & -s_{23}e^{-i\phi_{23}} & 1 \end{pmatrix} \qquad (3.17)$$

Here the three mixing angles coincide with the measurable transition amplitudes $s_{12} = |V_{us}|$, $s_{23} = |V_{cb}|$, $s_{13} = |V_{ub}|$. The physical CP nonconservation is measured by the invariant phase[74]

$$\phi = \phi_{12} + \phi_{23} - \phi_{13} \qquad (3.18)$$

All CP-nonconserving amplitudes are proportional to $|V_{us}V_{cb}V_{ub}|\sin\phi$. For fixed values $|V_{us}|$, $|V_{cb}|$ and $|V_{ub}|$, the CP non-conserving amplitudes will be maximized for $|\phi| = \pi/2$. Using the freedom in defining the quark phases one can rotate away the phases ϕ_{12} and ϕ_{23} in (3.17) getting

$$V'_{GS} = \begin{pmatrix} c_{12} & s_{12} & s_{13}e^{i\phi} \\ -s_{12} & c_{12} & s_{23} \\ s_{12}s_{23} - s_{13}e^{-i\phi} & -s_{23} & 1 \end{pmatrix} \qquad (3.19)$$

which is very similar to $V_{Wolfenstein}$. We shall use the form (3.15) in discussing our results. Some other representations of the CKM are discussed in refs. (71) and (76).

We would like to end this section with some remarks on the potential of LEP experiments in measuring the CKM matrix elements. Judging from the present safe limit $\bar{R} < 0.08$, one may need an order of magnitude larger bottom hadron sample than presently available to measure the matrix element $|V_{bu}|$ at a level $|V_{bu}| \approx 0.004$.

This may or may not be available by the LEP turn on. With an anticipated 10^6 bottom hadrons per year per experiment at LEP, it should certainly be possible to test this limit. We have already stressed the importance of having good lepton energy resolution in this context. Measurements of exclusive bottom hadron decay modes $B^{\pm} \to \tau^{\pm}\nu_{\tau}$, $B \to \pi\pi$, $\rho\pi$, 3π, $\Lambda_t\pi$ etc.[77] may also help, though the interpretation of data would be somewhat model dependent. Compared to the experiments at DORIS and CESR, the experiments at LEP have an advantage and a disadvantage in the reconstruction of bottom hadrons. Since the bottom quark and antiquark jets will be separated at LEP enrgies, the problem of cross-over of the two bottom hadron decay products is much less severe, increasing the bottom hadron reconstruction efficiency. The disadvantage at LEP is combinatorics due to the bottom quark fragmentation, giving rise to addidional hadrons before the decay of the bottom hadron, a feature which is absent at the $\Upsilon(4s)$. Luckily, the fragmentation $b \to Bx$ is very hard and this should help in distinguishing the bottom hadron decay products from the remnants of the bottom quark jet. Thus, for $\langle z\rangle_B = 0.8$ and for the case of twobody or quase two-body decays in $b\to u$ transitions, a cut of $E_{track} > 10$ GeV, for example, should remove the fragmentation products. Here having good particle identification will be a particular advantage.

Turning to the measurements of the CKM matrix elements $V_{ti}(i=d,s,b)$, the experiments at LEP and SLC have no obvious rival! However, as can be seen from eq. (3.15), one expects

$$\left|\frac{V_{ts}}{V_{tb}}\right| \sim \lambda^2 = 0.05 \qquad (3.20)$$

$$\left|\frac{V_{td}}{V_{tb}}\right| \lesssim \lambda^3 = 0.01$$

It seems that if $m_t \approx O(30\ \text{GeV})$, then there might be enough top hadrons available in the decay $Z^0 \to t\bar{t}$ to measure $|V_{ts}|$. The element $|V_{td}|$ is, however, by no means

trivial to measure, though identification of the hadrons (π,ρ,Λ_1) recoiling in the decay $t \to lx$ may provide some useful trigger for the $t \to d$ decays. The topology of $t \to (s,d)l^{\pm}\nu_l \to (\pi,\rho,K,K^*)l^{\pm}\nu_l$ is also quite striking.

4. Weak Mass Mixings and their Implications at LEP

A non-trivial test of the standard model lies in measuring the strength of the flavour changing $|\Delta F|=2$, $\Delta Q=0$ transitions among the neutral meson systems $K^0-\bar{K}^0$, $D^0-\bar{D}^0$, $B^0-\bar{B}^0$ and $B_S^0-\bar{B}_S^0$. Experimantally, such transitions have been measured in the $K^0-\bar{K}^0$ sector only, though there exists some preliminary evidence from the CERN $\bar{p}p$ collider[78] that such mixings may also be present among the neutral bottom mesons[20].

Concentrating on the interest at LEP, we will discuss the $D^0-\bar{D}^0$, $B^0-\bar{B}^0$, $B_S^0-\bar{B}_S^0$ and $T_U^0-\bar{T}_U^0$ oscillations and their phenomenological implications in this section. We start with a discussion of the formalism which is needed to describe $M^0-\bar{M}^0$ mixing, where M is any neutral meson, assumed to be a pseudoscalar. Defining the mass eigenstates by M_H and M_L (for heavy and light) having definite decay widths Γ_H and Γ_L (and hence life-times), we will primarily be interested in the quantities ΔM, $\Delta\Gamma$ and ϵ_M defined below

$$\Delta M \equiv M_H - M_L \tag{4.1}$$

$$\Delta\Gamma \equiv \Gamma_H - \Gamma_L$$

$$M_{H,L} = \frac{(1+\epsilon_M)M^0 \pm (1-\epsilon_M)\bar{M}^0}{\sqrt{2(1+|\epsilon_M|^2)}}$$

where ΔM and $\Delta\Gamma$ are obtained by diagonalizing the Hamiltonian

$$H\begin{pmatrix} M^0 \\ \bar{M}^0 \end{pmatrix} = \begin{pmatrix} M - \frac{1}{2}i\Gamma & M_{12} - i\Gamma_{12} \\ M_{12}^* - \frac{1}{2}\Gamma_{12}^* & M - \frac{1}{2}i\Gamma \end{pmatrix} \begin{pmatrix} M^0 \\ \bar{M}^0 \end{pmatrix} \tag{4.2}$$

This exercise gives

$$\Delta M = 2\mathrm{Re}\left[\left(M_{12} - \frac{i}{2}\Gamma_{12}\right)\left(M_{12}^* - \frac{i}{2}\Gamma_{12}^*\right) \right]^{1/2} \tag{4.3}$$

$$\Delta\Gamma = -4\,\mathrm{Im}\left[\left(M_{12} - \frac{i}{2}\Gamma_{12}\right)\left(M_{12}^* - \frac{i}{2}\Gamma_{12}^*\right) \right]^{1/2} .$$

In this notation $M_{12} - \frac{i}{2}\Gamma_{12} = \langle M^0|H|\bar{M}^0\rangle$, and one needs to compute the transition amplitude $M^0(\bar{Q}q) \leftrightarrow \bar{M}^0(\bar{Q}q)$ to get M_{12} and Γ_{12}. Since in the standard model, both the photon and Z^0 have manifestly diagonal couplings, the lowest non-trivial contribution to the amplitude $M^0 \leftrightarrow \bar{M}^0$ is via the exchange of W^+W^- diagrams. These box type diagrams are assumed to represent the inclusive sum of all flavour neutral intermediate states to which both M^0 and $\bar{M}^0$ can contribute.

4.1 $D^0-\bar{D}^0$ Mixings

The calculations for $\Delta M(D^0)$ and $\Delta\Gamma(D^0)$ are given in refs. (8). The contribution to $\Delta\Gamma(D^0)$ is suppressed due to the Cabibbo angle and one expects $\frac{\Delta\Gamma(D^0)}{\Gamma(D^0)} \approx 10^{-2}$. Theoretical predictions for $\Delta M(D^0)$ are rather fluid. The standard prodedure is to calculate the $\Delta C = 2$ box diagrams and relate the result to the $\Delta S = 2$ result of Lee and Gaillard[79]. The result (ignoring the small contribution from the b and t quarks) is

$$\frac{\Delta M_D}{\Delta M_K} = \left(\frac{m_s}{m_c}\right)^2 \frac{f_D^2}{f_K^2}\,\frac{m_D}{m_K} \tag{4.4}$$

Using the current quark masses[72] and $f_D = f_K$ gives

$$\Delta M(D) = 2\times10^{8}\ \mathrm{sec}^{-1}\ , \quad \frac{\Delta M(D)}{\Gamma(D)} \approx 10^{-4} \tag{4.5}$$

If, however, one uses the constituent quark mass m_s = 500 MeV, then

$$\Delta M(D^0) = 2\times10^9 \text{ sec}^{-1}, \quad \frac{\Delta M(D)}{\Gamma(D)} \approx 10^{-3} \tag{4.6}$$

It has also been argued recently[8] that $\Delta M(D)/\Gamma(D)$ is further suppressed if one includes quark masses on the external lines of the $\Delta c=2$ box diagrams giving $\Delta M(D)/\Gamma(D) \propto 10^{-6}$! Wolfenstein has taken up this issue recently and questioned the use of box diagrams to estimate $\Delta M(D^0)$ because of the smallness of m_s^2, since non-perturbative effects are expected to be important. The problem is that the alternative way of calculating $\Delta M(D)$ via the Cabibbo suppressed decays $D^0 \to \pi^+\pi^-$, K^+K^-,...,etc. leads at best to an upper bound $\Delta M(D)/\Gamma(D) < 10^{-2}$ and it is very difficult to make a definitive quantitative statement. It seems that this issue will keep the D^0-$\bar{D}^0$ issue lively for some time to come! Any way, the $D^0 \leftrightarrow \bar{D}^0$ transition probability, despite large charmed hadron statistics at LEP, would be difficult to detect.

4.2 B^0-$\bar{B}^0$ Mixings

We shall now discuss the mixings in the bottom meson sector and for the time being will not discuss the CP violation parameter ε_B. The box diagrams shown in fig. (14) give the following results for the mass differences

$$\Delta M(B_d^0) = \frac{G_F^2 f_{Bd}^2 m_{Bd}}{6\pi^2} M_W^2 \hat{B} F_d(m_b,m_t,\lambda) \tag{4.7}$$

$$\Delta M(B_s^0) = \frac{G_F^2 f_{Bs}^2 m_{Bs}}{6\pi^2} M_W^2 \hat{B} F_s(m_b,m_t,\lambda)$$

where $\hat{B}$ is the so-called bag constant, which enters through the definition

$$\langle B_d^0 | (\bar{b}\gamma_\mu(1-\gamma_5)d)^2 | \bar{B}_d^0 \rangle \equiv \frac{4}{3}\hat{B} f_{Bd}^2 m_{Bd} \tag{4.8}$$

$$\langle B_s^0 | (\bar{b}\gamma_\mu(1-\gamma_5)s)^2 | \bar{B}_s^0 \rangle \equiv \frac{4}{3}\hat{B} f_{Bs}^2 m_{Bs}$$

and has the value $\hat{B} = 1$ in the vacuum insertion approximation; f_{B_d} and f_{B_s} are the bottom meson pseudoscalar constants defined in section 2 and the functions F_d and F_s are given by

$$F_d(m_b,m_t,\lambda) = (\lambda_c^d)^2 u_1 + (\lambda_t^d)^2 u_2 + 2(\lambda_t^d)(\lambda_c^d) u_3$$

$$F_s(m_b,m_t,\lambda) = (\lambda_c^s)^2 u_1 + (\lambda_t^s)^2 u_2 + 2(\lambda_t^s)(\lambda_c^s) u_3 \tag{4.9}$$

The CKM-angle dependent factor λ_i^j assume the following values in the Wolfenstein parametrization:

$$|\lambda_c^d| \equiv |V_{cb}^* V_{cd}| \propto \lambda^3 \tag{4.10}$$

$$|\lambda_t^d| \equiv |V_{tb}^* V_{td}| \propto \lambda^3 \sqrt{(1-\rho)^2+\eta^2} < \lambda^3$$

$$|\lambda_c^s| \equiv |V_{cb}^* V_{cs}| \propto \lambda^2$$

$$|\lambda_t^s| \equiv |V_{tb}^* V_{ts}| \propto \lambda^2$$

The quark mass dependent factors u_i have been recently recalculated by Buras et al.[19] including QCD calculations to which we refer for details. We shall show simple and approximate formulae for u_i for intuitive reason. The leading contributions to u_i

are given by

$$u_1 \sim m_c^2 / m_W^2 \qquad (4.11)$$

$$u_2 \sim m_t^2 / m_W^2$$

$$u_3 \sim m_t m_c / m_W^2$$

In the expected top quark mass range 30 GeV $< m_t <$ 50 GeV, eq. (4.11) is within 5% of the exact result. Thus, the dominant contribution in both $\Delta M(B_d^0)$ and $\Delta M(B_s^0)$ is due to the u_2 term. Since in the QCD improved quark decay model for bottom hadrons, one expects $\Gamma(B_d^0) \approx \Gamma(B_s^0) \propto |V_{bc}|^2 \sim \lambda^4$, as we discussed in section 2, the phenomenologically interesting quantity for B-$\bar{B}$ oscillations, $\Delta M/\Gamma$, has the following CKM angle dependence[20]

$$\frac{\Delta M}{\Gamma}(B_d^0) \propto \lambda^2 \qquad (4.12)$$

$$\frac{\Delta M}{\Gamma}(B_s^0) \propto \frac{\lambda^4}{\lambda^4} = 1$$

Eq. (4.12) gives a simple pattern for the mass mixings in the bottom meson sector, namely $(B_d^0 - \bar{B}_d^0)$ oscillations are CKM forbidden and $(B_s^0 - \bar{B}_s^0)$ are CKM allowed. In fig. (15) we show $\frac{\Delta M}{\Gamma}(B_d^0)$ and $\frac{\Delta M}{\Gamma}(B_s^0)$ as a function of m_t for $\hat{B} = 1$. For all these values $\frac{\Delta M}{\Gamma}(B_d^0) < 10^{-1}$ and $\frac{\Delta M}{\Gamma}(B_s^0) > 1$. Thus, we expect substantial mixings in the B_s^0-$\bar{B}_s^0$ and very little in the B_d^0-$\bar{B}_d^0$ sector.

There exists a general consensus in literature that the quantity $\frac{\Delta\Gamma}{\Gamma}$ is suppressed for both the B_d^0-$\bar{B}_d^0$ and B_s-$\bar{B}_d^0$ mixings; in the former case it is a consequence of CKM suppression in the decay $b\bar{d} \to (u\bar{d})(\bar{u}d)$, and in the latter of phase space in the decay $b\bar{s} \to (c\bar{s})(\bar{c}s)$. Thus $\frac{\Delta\Gamma}{\Gamma}(B_d^0, B_s^0) \ll 1$ and we shall ignore this quantitiy in numerical calculations.

A good method to investigate B-$\bar{B}$ mixing is to measure the semileptonic decay of a B(or $\bar{B}$) meson in the "wrong-sign" lepton. Defining the ratios r and $\bar{r}$ as follows (note our convention $B \equiv b\bar{q}$, $\bar{B} \equiv \bar{b}q$)

$$r = \frac{\Gamma(B^0 \to l^+ \nu_l x)}{\Gamma(B^0 \to l^- \nu_l x)} \qquad (4.13)$$

$$\bar{r} = \frac{\Gamma(B^0 \to l^- \nu_l x)}{\Gamma(B^0 \to l^+ \nu_l x)}$$

then one can show[81]

$$r = \eta^2 \frac{\left(\frac{\Delta M}{\Gamma}\right)^2 + \left(\frac{\Delta\Gamma}{2\Gamma}\right)^2}{2 + \left(\frac{\Delta M}{\Gamma}\right)^2 - \left(\frac{\Delta\Gamma}{2\Gamma}\right)^2} \approx \frac{\eta^2 \left(\frac{\Delta M}{\Gamma}\right)^2}{2 + \left(\frac{\Delta M}{\Gamma}\right)^2} \qquad (4.14)$$

$$\bar{r} = r/\eta^4$$

where η is a measure of CP-violation defined via the convention independent relation

$$\langle B_H \mid B_L \rangle = \frac{1-\eta^2}{1+\eta^2} \qquad (4.15)$$

We shall set $\eta = 1$ for the time being. For complete mixing i.e.for $\left(\frac{\Delta M}{\Gamma}\right)^2 \gg 1$, $r = 1$ leading to equal number of "right sign" and "wrong sign" leptons in neutral B decays. However, since only the B_s^0-$\bar{B}_s^0$ oscillation is expected to be significant, only the ratio r_s will deviate significantly from 0. We define a quantity which takes into account the relative rate for B_s^0 production and hence is more relevant for the experimental measurements in the continuum than the quantities $r(B_d^0)$ and $r(B_s^0)$ which were defined in (4.13). The experimental measure of B-$\bar{B}$ mixing involving the wrong sign lepton in the semileptonic B decays is χ, defined as

$$\chi \equiv \frac{\Gamma(B \to l^+ x)}{\Gamma(B \to l^\pm x)} \tag{4.16}$$

One can relate χ to the individual mixing parameters χ_d and χ_s of B_d^0 and B_s^0 mesons defined as

$$\chi_{d(s)} \equiv \frac{\Gamma(B^0_{d(s)} \to l^+ x)}{\Gamma(B^0_{d(s)} \to l^\pm x)} = \frac{r_{d(s)}}{1+r_{d(s)}} \tag{4.17}$$

via the relation

$$\chi = \frac{(BR)_d}{\langle BR\rangle} P_d \chi_d + \frac{(BR)_s P_s \chi_s}{\langle BR\rangle} \tag{4.18}$$

where $P_d(P_s)$ is the fraction of $B_d^0(B_s^0)$ meson production at a given centre of mass energy, $(BR)_d[(BR)_s]$ is the semileptonic branching ratio for the $B_d^0[B_s^0]$ meson and $\langle BR\rangle$ is the average semileptonic branching ratio of bottom hadrons measured at that energy. Since $P_s = 0$ at $\Upsilon(4s)$, the $\Upsilon(4s)$ data can measure only χ_d. However, as can be calculated from fig. (16), one expects $\chi_d \leq 10^{-2}$ in the standard model. The present best limit on χ_d from experiments at CESR is $\chi_d < 0.22$[3], which is roughly two orders of magnitude larger than the expected value of the same quantity in the standard model. (Experiments at CESR and DORIS are well advised to run above $\Upsilon(4s)$ to be able to measure weak mass mixing effects in the bottom meson sector!)

Since χ_d is very small, we set $\chi_d \approx 0$ in (4.18). Then, one has a simple expression for χ[20],

$$\chi = \frac{(BR)_s P_s \chi_s}{\langle BR\rangle} \approx P_s \chi_s \approx f(s\bar{s})\chi_s \tag{4.19}$$

where the last two equalities emerge from the assumptions (i) $(BR)_s \approx \langle BR\rangle$ and (ii) $P_s = f(s\bar{s})$, which is the probability of producing an $s\bar{s}$ pair in the fragmentation

of the b-quark jet. The quantity $f(s\bar{s})$ has been measured in a large number of high energy physics experiments. The best fit of the related quantity $\gamma_s \equiv f(s\bar{s})/f(d\bar{d})$ in e^+e^- annihilation at PETRA and PEP is: $\gamma_s = 0.33 \pm 0.02$[54], which gives $f(s\bar{s}) \sim 0.13$. The ratio $f(s\bar{s})$ is increasing slowly with $\sqrt{s}$, so we expect $f(s\bar{s})_{LEP/SLC} \approx 0.15$. Thus, for maximum B_s-$\bar{B}_s$ mixing, $\chi_s = 0.5$ and for experiments involving $b\bar{b}$ production in the continuum, one expects

$$\chi_{max} \approx \frac{1}{2} f(s\bar{s}) \tag{4.20}$$

which gives a ratio of (7-8)% for the relative probability of producing a wrong-sign lepton in the primary semileptonic decays of a bottom quark (jet).

4.3 Inclusive dilepton rates in $e^+e^- \to b\bar{b} \to llx$

Next we calculate the dilepton rates from the primary B decays. Denoting by N_{21} the predicted dilepton rate, the expected rate for opposite and same charge combination is $N_{+-} = ((1-\chi)^2 + \chi^2)N_{21}$ and $N_{\pm\pm} = 2\chi(1-\chi)N_{21}$. Then[20]

$$R(\pm\pm/+-) \equiv \frac{N_{\pm\pm}}{N_{+-}} = \frac{2\chi(1-\chi)}{(1-\chi)^2 + \chi^2}$$

$$\approx \frac{2\chi_s(1 - \chi_s f(s\bar{s}))}{[1 - \chi_s f(s\bar{s})]^2 + \chi_s^2 f(s\bar{s})^2} \tag{4.21}$$

$$\xrightarrow[\chi_s \to 0.5]{} \frac{2f(s\bar{s})(2 - f(s\bar{s}))}{(2 - f(s\bar{s}))^2 + f^2(s\bar{s})}$$

$$\approx 0.16 \quad \text{for} \quad f(s\bar{s}) = 0.15$$

The number quoted is for maximum B_s-$\bar{B}_s$ mixing at LEP/SLC energies. To compare the above ratio with data one should add to this the contributions due to the bottom hadron cascades $b \to cx \to l^+x'$, which obviously depend on the specific experimental conditions.

Let us briefly take stock of the present experimental results on the quantity $R(\pm\pm/+-)$. There is some preliminary evidence[78] from the UA1 (1983+1984)

data that in high p_t dimuons from $\bar{p}p$ collisions $R(\pm\pm/+-) \neq 0$. An analysis of this data, taking into account experimental conditions is given in refs. (20) and (82). After subtracting the bottom cascades and other backgrounds one finds[20] $R(\pm\pm/+-) = 0.25 \pm 0.09$, which is consistent with the expectations (4.21) and suggests substantial B_s-$\bar{B}_s$ mixing. The least that one can do with the UA1 data is set a 90% C.L. lower limit on the mixing parameter. This gives $\chi > 0.04$. In fig. (17) we show contours of constant χ in a two-dimensional $f(s\bar{s})$ - r_s plot. For $f(s\bar{s}) \leq 0.2$ at the CERN collider one gets a lower bound on B_s-$\bar{B}_s$ mixing parameter r_s, namely $r_s > 0.25$. From e^+e^- annihilation, there are two null results available from PEP and CESR for the quantity $R(\pm\pm/+-)$. We have already discussed the bound from CESR. The Mark-II collaboration at PEP[83] have set a limit on χ, $\chi<0.12$ at 90% C.L. We show the excluded area in the $f(s\bar{s})$ - r_s plot (fig. (17)). As indicated in eq. (4.20), in the standard model, one expects $\chi_{max} = 1/2\ f(s\bar{s}) \approx 0.07$ at PEP energies. Thus, the present e^+e^- data both at PEP and CESR[84] do not yet have enough statistics to test bottom meson mixing in a significant way. On the other hand, the limits on χ can be used to rule out non-standard models, which predict substantial B^0_d-$\bar{B}^0_d$ mixing. This, for example, is the case in SUSY models with relatively light gluino and squarks.

4.4 Weak mixing effects in forward-backward bottom charge asymmetry

Another place to detect the presence of $|\Delta B|=2$, $|\Delta Q|=0$ transitions is the electroweak forward-backward charge asymmetry in the process $e^+e^- \to b\bar{b}$[34]. At PETRA, the charge asymmetry in $e^+e^- \to b\bar{b}$ is measured via the final state $e^+e^- \to b\bar{b} \to l^{\pm}x$. The presence of B-$\bar{B}$ mixing will lead to wrong-sigh lepton and hence will decrease this asymmetry. At LEP, one could use in addition reconstructed B^0_s mesons and/or information from the vertex detectors to directly measure the asymmetry in $e^+e^- \to B^0_s x$. We have discussed at length the electroweak charge asymmetry in the standard model including QCD radiative and mass corrections. That in fact was a prelude to the overriding interest in the $e^+e^- \to b\bar{b}$ asymmetry due to B-$\bar{B}$ mixings. De-Denoting by A^b_{FB} the standard value and by $\bar{A}^b_{FB}$ the measured value for bottom quarks, one has[20]

$$\frac{\bar{A}^b_{FB}}{A^b_{FB}}\ (e^+e^- \to b\bar{b} \to \bar{l}x) = \left[\frac{BR(b\to l^-x) - BR(\bar{b}\to l^-\bar{x})}{\langle BR\rangle}\right] \qquad (4.22)$$

$$= (1 - 2\chi)$$

$$\approx (1 - 2\chi_s f(s\bar{s}))$$

$$\longrightarrow \quad (1 - f(s\bar{s}))$$

$$\chi_s \to 0.5$$

Thus, for complete B_s-$\bar{B}_s$ mixing, the ratio $\bar{A}^b_{FB}$ / A^b_{FB} is smaller than 1 by the fraction $f(s\bar{s})$. We expect $f(s\bar{s}) \approx 0.15$ at LEP and SLC. Thus, a measurement of $\bar{A}^b_{FB}$ better than 5% is needed to see possible effects of B-$\bar{B}$ mixing through the asymmetry measurements. With 10^6 bottom hadrons expected per year at LEP, the error in the measurements of $\bar{A}^b_{FB}$ will be dominated by systematic errors.

The measurements of the quark charge asymmetry at PETRA and PEP are still very much in a preliminary stage. Despite this the JADE collaboration at DESY have measured the bottom quark asymmetry at 4σ level. Combining all the PETRA data[86], which is dominated by the JADE contribution, yields

$R^b_{asym} \equiv \bar{A}^b_{FB} / A^b_{FB} > 0.74$ at 90% c.L. In fig. (18) we draw contours of constant R^b_{asym}, using the equation $R^b_{asym} = 1 - 2\chi_s f(s\bar{s}) = 1 - 2\,\frac{r_s f(s\bar{s})}{(1+r_s)}$, with the boundary condition $0 \leq f(s\bar{s}) \leq 0.3$. Also shown is the excluded region for $R^b_{asym} > 0.74$, which corresponds to $\chi < 0.13$. This limit is slightly worse than the one set by the Mark-II dimuon data $\chi < 0.12$. Again, the expected effect at PETRA, PEP and LEP for $f(s\bar{s}) = 0.15$ and $r_s \leq 1$ is: $R^b_{asym} > 0.86$ (i.e. $\chi \leq 0.07$).

It is clear from the discussion above that the actual measurements of B-$\bar{B}$ mixing effects would depend on dynamical details, like for example the relative semileptonic branching ratios $(BR)_s$ / $\langle BR\rangle$ and the probability Γ_s (or $f(s\bar{s})$), in addition to the intrinsic measure χ_s (or r_s) which is in principle determined by the weak interactions. Despite the dependence on these dynamical quantities, the

experimental measurements of $R(\pm\pm/+-)$ or R^{b}_{asym} by themselves are not sufficient to tell whether the mixing pertains to $B_d-\bar{B}_d$ or $B^0_s-\bar{B}^0_s$. There certainly is no way to tell the two mixings apart at LEP and SLC experiments, without tagging the B^0_s meson or demanding an extra correlation. Therefore, there is a need to devise tests which, at least in some reasonable limit, are able to distinguish the $B^0_d \leftrightarrow \bar{B}^0_d$ from the $B^0_s-\bar{B}^0_s$ mixings. In this connection, it has been pointed out that measurements of the final states $l^+l^+\Lambda^0$, $l^-l^-\bar{\Lambda}^0$ and $l^\pm l^\pm F^\mp$ in $(e^+e^-, \bar{p}p) \to b\bar{b}$ would be strongly indicative of $B_s-\bar{B}_s$ mixings[6]. One needs good detection efficiencies for both Λ^0 and $F^\pm$. This certainly is going to compromise event rates despite large bottom hadron statistics expected at LEP.

4.5 Weak mixing effects in $\sigma(e^+e^- \to l^\pm K^\mp K^\mp x)$

We would like to discuss the proposal presented in ref. (21) to measure $B_s-\bar{B}_s$ mixing. The proposal consists of measuring the "decay" of an excited bottom quark produced in a hard collision into the following states

$$\text{"b"} \to l^+K^-K^-x,\ l^+K^-\Lambda^0x \tag{4.23}$$

or its charge conjugate $\bar{b} \to l^-K^+K^+x$, $l^-K^+\bar{\Lambda}^0x$. The main idea behind the final states (4.23) is rather simple. Since mixing in the bottom meson sector is expected in the $B^0_s-\bar{B}^0_s$ sector, one expects short range (in rapidity) flavour correlations among the fragments of a single bottom quark jet also. Normally in a bottom quark jet one would have the fragments

$$b \to B^0_s + (K^-,\ \bar{K}^0,\ \bar{\Lambda}^0) + \ldots \tag{4.24}$$

$$\bar{b} \to \bar{B}^0_s + (K^+,\ K^0,\ \Lambda^0) + \ldots$$

In other words one expects final states $B^0_sK^-$, $B^0_s\bar{\Lambda}^0$, $\bar{B}^0_sK^+$ and $\bar{B}^0_s\Lambda^0$. Of course, in general the $K^\pm$ and $\Lambda^0/\bar{\Lambda}^0$ multiplicity in the fragmentation of bottom quark may be large leading, for example, to both the B^0K^-x and B^0K^+x final staes. This however is not the case experimentally. In the jargon of fragmentation model builders, the kaon multiplicity in a jet is governed by an SU(3)-breaking parameter $\gamma_s \equiv \frac{f(ss)}{f(dd)}$ and of the Λ by another $\gamma_s' \equiv \frac{f(sd)}{f(dd)}$. All e^+e^- data at PETRA and PEP as well as in other high energy experiments are in agreement with $\gamma_s = 0.33$ and $\gamma_s' = 0.1 - 0.20$[87,88].

Thus, it is sensible to study flavour correlations of the type $B^0_sK^\pm$, $\bar{B}^0_sK^\pm$, $B^0_s\Lambda/\bar{\Lambda}$ etc. With the normal correlations being (4.25), correlations of the "wrong stangeness" type, namely

$$b \to \bar{B}^0_s + (K^+,K^0,\Lambda^0) + \ldots \tag{4.25}$$

$$\bar{b} \to B^0_s + (\bar{K},\bar{K}^0,\bar{\Lambda}^0) + \ldots$$

would be in the first approximation signs of $B^0_s-\bar{B}^0_s$ mixing. Thus, in leading order in γ_s or γ_s' one has, for example,

$$\frac{b \to \bar{B}^0_sK^-X}{b \to B^0_sK^-X} = \frac{\chi_s}{1-\chi_s} \tag{4.24}$$

$$\frac{b \to \bar{B}^0_s\Lambda^0X}{b \to B^0_s\Lambda^0X} = \frac{\chi_s}{1-\chi_s}$$

Of course, the utility of the short range flavour correlations (4.25) is only in conjunction with the ability to distinguish a B^0_s from $\bar{B}^0_s$. This can be achieved through the semileptonic decays. Recalling that the transition $b \to c$ dominates b decays, the semileptonic decay of a bottom hadron would lead to the following states:

$$B^0_d \to (D^+,D^{*+},\ldots)l^-\nu_l \tag{4.27}$$

$$B^-_u \to (D^0,D^{*0},\ldots)l^-\nu_l$$

$$B^0_s \to (F^+,F^{*+},\ldots)l^-\nu_l$$

Now, since the decays $(D^0,D^+) \to K^+X$ are Cabibbo suppressed but the decays $F^+ \to K^\pm X$ are Cabibbo allowed, a good two-particle inclusive final state to enhance the $B^0_s(\bar{B}^0_s)$ signal should be in the decays $B \to l^-K^+X$ and $\bar{B} \to l^+K^-X$. This would lead to the final

state b-jet → $l^+K^-K^-X$, $l^+K^-\Lambda^0X$ advocated in eq. (4.23). Once again, it is imperative to have the b and $\bar{b}$ jets well separated. Hence, in contrast to $l^\pm l^\pm X$, the final states $l^\pm K^\mp K^\mp$ are useful for experimental situation well above the Υ(4s) resonance region. To quantify this proposal, one could define the following ratio[21]

$$R(l^+K^-K^- \,/\, l^-K^-K^-) \equiv \frac{b \to l^+K^-K^-X}{b \to l^-K^-K^-X} \tag{4.28}$$

Then, quite generally for collisions leading to $b\bar{b}$ production one can express the ratio R as (4.29)

$$R(l^+K^-K^- \,/\, l^-K^-K^-) = \frac{\sum_q \sigma(Bq)\left\{BR(Bq \to l^+K^-X)f(q \to K^-X) + BR(B_q \to l^+X)f(q \to K^-K^-X)\right\}}{\sum_q \sigma(Bq)\left\{BR(Bq \to l^-K^-X)f(q \to K^-X) + BR(Bq \to l^-X)f(q \to K^-K^-X)\right\}}$$

where the sum $\sum_q$ is over all species of the bottom hadrons B_q and $f(q \to K^+x)$ etc. represents the probability of a quark giving a K^+. The decays $B_q \to l^+K^-K^-X$ are completely negligible ($\lesssim 10^{-3}$) and hence not included in (4.29). Now in leading order in $f(s\bar{s})$ (keeping only the valence $K^\pm$ hadrons from the fragmentation $q \to K^\pm X$), one has

$$R(l^+K^-K^- \,/\, l^-K^-K^-) = \frac{\sigma(B_s^0)BR(B_s^0 \to l^+K^-X)f(s \to K^-X)}{\sigma(B_s^0)BR(B_s^0 \to l^-K^-X)f(s \to K^-X)}$$

$$= \frac{BR(B_s^0 \to l^+K^-X)}{BR(B_s^0 \to l^-K^-X)} = \frac{\chi_s}{1-\chi_s}\,\frac{BR(F^- \to K^-X)}{BR(F^+ \to K^-X)} \tag{4.30}$$

Thus, in the limit that eq. (4.30) holds, the quantity $R(l^+K^-K^-X)$ is independent of $\sigma(B_s^0X)$, the probability $f(s \to K^-x)$ and the semileptonic branching ratio for the B_s^0 meson. It depends, however, on the inclusive branching ratio of the $F^\pm$ mesons, namely $BR(F^- \to K^\pm X)$. The quantity $BR(F^- \to K^-X)/BR(F^+ \to K^-X)$ in eq. (4.30) is expected to be around 1 in the quark-parton model description of the $F^\pm$ decays, and hopefully would be available soon.

Of course the discussion above is somewhat idelalized. In real world, Cabibbo suppressed transitions in charmed hadron decays $D^0, D^+ \to K^+X$ and the suppressed fragmentation precesses $u,d \to K^-X$ and $s \to K^+X$ would contribute to the final state $b \to l^-K^+K^+X$, thus giving non-zero contribution to the ratio R defined in (4.28). The signal and background rates have been estimated in ref. (21), from where we retrace the essential steps and results.

The distributions $\frac{d\sigma}{dz}$ ($z = 2E_K/\sqrt{s}$) for the processes $e^+e^- \to \gamma,Z \to b\bar{b} \to (B_d^0, B_u^-, B_s^0, \ldots)K^\pm X$ are calculated in the quark-parton model, which gives $\sigma(e^+e^- \to b\bar{b})$; the inclusive two-particle distributions are then obtained by using a modified fragmentation model of the Field-Feynman type[89]. The essential feature of the modification is in the use of an experimentally observed hard bottom hadron fragmentation function, which we take here to be the one due to Peterson et al[62]. The momentum distributions of the $K^\pm$ mesons in the processes

$$e^+e^- \to BK^\pm x \tag{4.31}$$

are then bound to be rather soft[90]. This is shown in fig. (19) for the fragmentation function $D(z \equiv 2E_K/\sqrt{s})$ for $q \to K^\pm X$, q = u, d, s with $\int_0^1 D(z)dz$ $f(q \to K^\pm X)$ being the inclusive probabilities of producing $K^\pm x$ in the fragmentation $q \to K^\pm x$, taken from the present e^+e^- measurements[34]. The flavour distributions D shown in fig. (18) are quite instructive. They give a concrete meaning to the notion of allowed $s \to K^-X$ and suppressed $s \to K^+X$ transitions.

In fig. (20) we show the two-particle inclusive differential cross-section $\frac{1}{\sigma(b\bar{b})}\frac{d\sigma}{dz}$ ($e^+e^- \to BKX$) for the final states $B_u K^\pm X$ and $B_s^0 K^\pm X$ assuming $f(s\bar{s}) = 0.15$ for $\sqrt{s}$ = 93 GeV. The hierarchy in the cross-sections is very striking, with $\sigma(B_s^0K^+X) \simeq \sigma(B_u^-K^+X)$ being the largest and $\sigma(B_s^0 K^-X)$ the smallest cross-section. For the particular choice of $f(s\bar{s})$, we note that $\sigma(B_s^0K^-X)/\sigma(B_s^0K^+X) \simeq 5$ for $z = \frac{2EK}{\sqrt{s}} > 0.1$ and this ratio becomes > 10 for $z > 0.2$. In the presence of B_s-$\bar{B}_s$ mixing, no change is really expected in the cross-sections $\sigma(B_uK^\pm X)$ and $\sigma(B_d^0K^\pm X)$ but the cross-

section $\sigma(B_s^0 K^\pm X)$ will change in accordance with eq. (4.26). For complete B_s^0-$\bar{B}_s^0$ mixing, one would have $\frac{d\sigma}{dz}(e^+e^- \to B_s^0 K^- X) = \frac{d\sigma}{dz}(e^+e^- \to B_s^0 K^+ X)$ for all values of z. This is an effect hard to miss for detectors having good B_s^0 and $K^\pm$ detection abilities.

To get rates for the ratio R in eq. (4.28) one has to know the inclusive branching ratios for $(D^+, D^0) \to K^\pm X$ and $F^+ \to K^\pm X$. The former are now well measured but the latter are not yet available. The branching ratios used in our calculations are shown in table (11).

We now discuss the results for the final states sensitive to the issue of B_s^0-$\bar{B}_s^0$ mixing, namely the rates for the dileptons $e^+e^- \to b\bar{b} \to l^\pm l^+ X$, $l^+ l^- X$ and $e^+e^- \to b\bar{b} \to l^\pm K^\mp K^\mp X$, $l^\pm K^+ K^- X$. To remove the background from the jet-axis $e^+e^- \to c\bar{c} \to l^\pm X$ and the cascade decays $e^+e^- \to b\bar{b}$, $b \to c \to l^- X$, producing the final states $e^+e^- \to l^\pm l^\pm X$ etc. without any B-$\bar{B}$ mixings, we have put a cut-off on the transverse momentum of the lepton, P_T^l, measured with respect to the jet-axis. Similarly, since the signal/background ratio is expected to improve with the increase in the momentum of the $K^\pm$, P_K, we have put a lower cut-off on P_K. In table (12) we present our results for the final states $e^+e^- \to llX$, $lKKX$ for $\sqrt{s}$ = 93GeV, for all possible charges $l^\pm$ and $K^\pm$, $f(s\bar{s})$ = 0.15, $P_T^l > 1.5$ GeV and $P_K > 0.5$ GeV. The dilepton ratio R(±±/+-) rises from 0.045 to 0.175 as χ_s increases from 0(no mixing) to 0.5 (complete B_s-$\bar{B}_s$ mixing). The ratio $\Delta R(lKK) = \frac{\sigma(l^- K^- K^-) - \sigma(l^- K^+ K^+)}{\sigma(l^- K^- K^-) + \sigma(l^- K^+ K^+)}$ decreases from 0.41 to 0.23 in the same interval. The rates for $l^\pm K^\mp K^\mp X$ states are substantially higher than those for the $l^\pm l^\pm X$ states. The decrease in the ratio $\Delta(lKK)$ as a function of χ_s is a special case of the results shown in fig. (20), where as we have argued before, the cross sections $\sigma(B_s^0 K^+ X)$ and $\sigma(\bar{B}_s^0 K^- X)$ tend to each other with increasing χ_s. It is obvious, for equal number of $b\bar{b}$ events, the change in $\Delta R(lKK)$ due to B-$\bar{B}$ mixing is more marked at lower energies than at higher energies, since the $K^\pm$ multiplicity in a jet is lower at lower $\sqrt{s}$, resulting in smaller background. We show the ratio $\Delta R(lKK)$ in figs. (21) for two representative values (a) at PETRA, $\sqrt{s}$ = 43 GeV and (b) at LEP/SLC, $\sqrt{s}$ = 93 GeV, where we also show the dependence of $\Delta R(lKK)$ on $f(s\bar{s})$ for the range $0.1 < f(s\bar{s}) < 0.15$. In figs. (22) we plot the relative rate of same sign dilepton $R(l^\pm l^\pm) \equiv (N^{++} + N^{--})/(N^{++} + N^{--} + N^{+-})$ as a function of χ_s for $f(s\bar{s})$ in the range $0.1 \leq f(s\bar{s}) \leq 0.15$.

Note that we have used somewhat relaxed P_T^l cut-off in fig. (20a) for lower $\sqrt{s}$.

In figs. (23), we show how to determine $f(s\bar{s})$ in bottom quark jets, where we have plotted the branching ratio for the inclusive final states $\sigma(e^+e^- \to l^\pm K^+ K^- X + l^\pm K^\pm K^\pm X + l^\pm K^\mp K^\mp X)$ involving $l^\pm$ and $K^\pm$, as a function of $f(s\bar{s})$ for the range $0.1 < f(s\bar{s}) < 0.2$. As expected, the cross-section $\sigma(e^+e^- \to lKKX)$ depends lineary on $f(s\bar{s})$ and a measurement of this quantity should already be possible with the existing data at PETRA/PEP energies. This would then provide an independent measurement of $f(s\bar{s})$ for bottom jets in the same experiment where effects of B_s^0-$\bar{B}_s^0$ mixings would be searched. This would fix $f(s\bar{s})$ for both $\Delta(lKK)$ and R(±±/+-) measurements.

The rates presented in table (12) are based on 10^5 $b\bar{b}$ events. The integrated bottom meson sample at LEP could be an order of magnitude larger in a typical year. Measurements of B_s-$\bar{B}_s$ mixings at a level suggested by the recent UA1 dimuon data, as well as by theoretical calculations namely $r_s \geq 0.25$ (or $\chi \geq 0.2$) is within the feasability of LEP experiments. Not only will it be possible to see at LEP statistically significant (>4σ) deviations for $r_s \geq 0.25$, but also the concomittant short range flavour correlations via $\Delta R(lKK)$ measurements will be testable. We would like to close this section with some remarks about direct and induced mixing effects in the top meson sector.

4.6 Direct and induced mixing effects in top hadrons

There are two neutral top mesons T_c^0 which can mix with their charge conjugates via weak interactions and, in principle, one could have T_u-$\bar{T}_u$ and T_c^0-$\bar{T}_c^0$ oscillations. Since the width Γ_t is very large (i.e. top hadrons decay very fast), there is no time for mixing. Consequently, weak mixing effects in the neutral top mesons are expected to be extremely small[91]. These expectations can be given a concrete form by calculating $\frac{\Delta\Gamma}{\Gamma}$ and $\frac{\Delta M}{\Gamma}$ for the two neutral top meson systems. We have already discussed the decays of the top quark in section 2. To a good approximation one expects $\Gamma(T_u) = \Gamma(T_d) = \Gamma(T_s) = \Gamma(T_c) = \Gamma_{tot}^t$, where Γ_{tot}^t is given in eq. (2.47) together with table (8). It is likely that due to the larger phase space $\Gamma(T_c) \approx 2\Gamma(T_u)$. However, for the discussion of $\Delta M/\Gamma$ this difference is not crucial. The

diagrams leding to $\Delta\Gamma(T_u)$ and $\Delta\Gamma(T_u)$ are shown in fig. (24a) and (24b), respectively. They lead to

$$\frac{\Delta\Gamma}{\Gamma}(T_u^0) \simeq \frac{3}{\bar{\Gamma}^t}\left[\,|V_{td}|^2 + |V_{ts}|^2\,|V_{us}|^2\,\right] \tag{4.32}$$

$$\lesssim \frac{1}{2}\lambda^6$$

$$\frac{\Delta\Gamma}{\Gamma}(T_c^0) \simeq \frac{3}{\bar{\Gamma}^t}\left[\,|V_{td}|^2\,|V_{cd}|^2 + |V_{ts}|^2\,|V_{cs}|^2\,\right] \tag{4.33}$$

$$\simeq \frac{1}{2}\lambda^4$$

where $\bar{\Gamma}^t$ is the reduced top width given in table (8) and $\lambda = \sin\theta_c \simeq 0.23$. The mass difference $\Delta M(T_u^0)$ and $\Delta M(T_c^0)$ are calculated by the box diagrams shown in figs. (24c) and (24d) respectively. These can be expressed in a form analogous to $\Delta M(B_s^0)$ in eq. (4.7). (We have ignored the external quark mass effects in $\Delta T = 2$ box diagrams which would further suppress the rates for $\Delta M/\Gamma(T)$).

$$\frac{\Delta M(T_u^0)}{\Gamma} = \frac{32\pi f_{Tu}^2 m_{Tu} m_W^2 \hat{B}}{m_t^5\,\bar{\Gamma}^t} F_u \tag{4.34}$$

$$\frac{\Delta M(T_c^0)}{\Gamma} = \frac{32\pi f_{Tc}^2 m_{Tc} m_W^2 \hat{B}}{m_t^5\,\bar{\Gamma}^t} F_c$$

where

$$F_u = |V_{tb}^* V_{bu}|^2 \frac{m_b^2}{m_W^2} \lesssim \lambda^6 \frac{m_b^2}{m_W^2} \tag{4.35}$$

$$F_c = |V_{tb}^* V_{bc}|^2 \frac{m_b^2}{m_W^2} \simeq \lambda^4 \frac{m_b^2}{m_W^2}$$

which gives for $m_t = 40$ GeV, $f_{Tu} = 0.1$ GeV, $f_{Tc} = 0.3$ GeV

$$\frac{\Delta M}{\Gamma}(T_u^0) \lesssim 2\times10^{-10} \tag{4.36}$$

$$\frac{\Delta M}{\Gamma}(T_c^0) \lesssim 4\times10^{-8}$$

Thus, direct mixing effects in the top meson sector need not be discussed any further. On the other hand there are indirect effects in t-decays (as opposed to the mass mixing effects) which may not be negligible. These induced effects should presumably be marked in the decays of $T_s^{\pm}$ and $T_s^{\pm *}$ mesons, via the decays

$$t(\bar{s}) \to b(\bar{s}) + (q\bar{q},\ l^+\nu_l) \tag{4.37}$$

since a significant fraction of the $\bar{b}(\bar{s})$ topology is expected to give rise to $B_s + X(X = \gamma,\pi,\ldots)$ one could observe effects of B_s^0-$\bar{B}_s^0$ mixing in t quark decays. One could get final states of the following form in the top quark jet

$$t\bar{s} \to (b\bar{s}) + l^+\nu_l$$

$$(\bar{b}s) \longrightarrow F^- l^+ \nu_l \Longrightarrow l^+ l^+ F^- X \tag{4.38}$$

The background to the process $t\bar{s} \to l^+l^+X$ is due to the normal t cascades $t \to l^+b\nu_l \to cx \to l^+\nu_l$. However, in this case the secondary lepton will have very soft energy spectrum and can be removed by an appropriate cut-off. In addition, the dilepton collinearity angle distribution in (4.38) is quite different than for example from the normal process

$$e^+e^- \to t\bar{t} \longrightarrow \bar{b} \to l^+X \qquad \text{(with } t \to l^+X\text{)} \tag{4.39}$$

and should help to distinguish the two sources of $l^{\pm}l^{\pm}X$. One can also use final states in the toponium and $t\bar{t}$ production above threshold to see induced mixing effects in trilepton final states. These latter would require a large $t\bar{t}$ / toponium

data sample as discussed in ref. (92).

5. CP violation in bottom hadrons and prospects of measurements at LEP

In the standard three family model, CP violation effects arise due to the Kobayashi-Maskawa phase, δ_{KM}. The only place where such effects have been experimentally measured is the $K^0-\bar{K}^0$ system[93]. Present measurements of the CP-violation parameters $|\epsilon|$[94] and ϵ'/ϵ[95] are consistent with the standard model[96] predictions, though the situation is tantalizing.

In principle, CP violation in decays and virtual transitions ($M^0-\bar{M}^0$) is expected in the charmed, beauty and top hadrons as well. These effects can be generally classified as (i) decay amplitude differences in partial rates between the particle and its charge conjugate, which are the only sources of CP violation for charged hadrons, and (ii) the ones that may involve $M^0 \leftrightarrow \bar{M}^0$ mixing in addition. The general rule here is that partial rate differences between the decay $M^0 \to f$ and its charge conjugate $\bar{M}^0 \to \bar{f}$ will involve both the $M^0 \leftrightarrow \bar{M}^0$ mixing and decay amplitude differences if the final states f and $\bar{f}$ are CP eigenstates. If f or $\bar{f}$ is not a CP eigenstate then CP violating effects in the partial rates of neutral hadrons will arise only from partial decay amplitude differences. Finally, (iii) CP-violation involving neutral hadrons may arise only from the virtual transitions $M^0 \leftrightarrow \bar{M}^0$.

We will first discuss CP-violating effects in virtual transitions. As we have noted in the last section, the mass- and width differences M_{12} and Γ_{12} for $M^0 \leftrightarrow \bar{M}^0$ transitions are in general complex quantities. Physically, it means that the probability $P(M^0 \to \bar{M}^0) \neq P(\bar{M}^0 \to M)$. The CP-violating effects in this case are proportional to $a(M^0) \equiv [P(M^0 \to \bar{M}^0) - P(\bar{M}^0 \to M)] / [P(M^0 \to \bar{M}^0) + P(\bar{M}^0 \leftrightarrow M)]$. Now, if the mixing probabilities, proportional to $\Delta M/\Gamma$ and $\Delta\Gamma/\Gamma$ are small, then there is no realistic hope to observe CP violations. This, for example, is certainly the case for $D^0-\bar{D}^0$, $T_u^0-\bar{T}_u^0$ and $T_c^0-\bar{T}_c^0$ transitions. Here, CP violating effects are exceedingly difficult to measure since in the first place, the mixing amplitudes are exceedingly small. The smallness of a_M, expected in the standard model, is on top of that. This can be quantified by recalling from eqs. (4.13) and (4.14) that the CP-violating charge asymmetry in the semileptonic decays of neutral hadrons in

the process

$$e^+e^- \to M\bar{M}X \to l^\pm l^\pm X,\ l^+l^-X \tag{5.1}$$

can be expressed as[81]

$$a = \frac{N^{++} - N^{--}}{N^{++} + N^{--}} = \frac{r-\bar{r}}{r+\bar{r}} = \frac{\eta^4-1}{\eta^4+1} \tag{5.2}$$

where η is given by $\eta^2 = 1-z\ /\ 1+z$ with $z = 1/2\ \mathrm{Im}(\Gamma_{12}\ /\ M_{12})$. The counting rates are then determined by the total charge asymmetry in the dilepton final states,

$$\frac{N^{++} - N^{--}}{N_{21}} = 2a\chi(1-\chi) \tag{5.3}$$

where we recall N_{21} is the total number of dileptons from the process (5.1). We have presented estimates and experimental bounds for the quantity $\frac{\Delta M}{\Gamma}$ and $\frac{\Delta\Gamma}{\Gamma}$ related to χ in the last section and in view of this we shall not discuss the cases $M = D^0$, T_u^0 and T_c^0 any more. Concentrating on the bottom sector, we quote the upper bound for 'a' from the calculations in literature[19],

$$a_d^{max} \lesssim 10^{-2} \tag{5.4}$$

$$a_s^{max} \lesssim 5\times10^{-4}$$

with the actual values depending on the CKM matrix element V_{bu} and the phase δ_{KM}, as can be seen in fig. (25). Inserting the expression for χ in terms of χ_d and χ_s from eq. (4.18) in eq. (5.3) one gets

$$\frac{N^{++} - N^{--}}{N_{2l}} = 2a_d \chi_d \frac{(BR)_d P_d \chi_d}{\langle BR\rangle} + 2a_s \chi_s \frac{(BR)_s P_s \chi_s}{\langle BR\rangle} \qquad (5.5)$$

which on using the values

$$\chi_d \leq 10^{-2} \qquad (5.6)$$

$$\chi_s \leq 0.5$$

$$P_d = 0.4$$

$$P_s = 0.15$$

$$(BR)_d = (BR)_s = \langle BR\rangle$$

gives

$$\frac{N^{++} - N^{--}}{N_{2l}} \leq 10^{-4} \qquad (5.7)$$

Now, since the effective branching ratio for the process $e^+e^- \to b\bar{b} \to l^+l^-X$ with primary leptons $b \to l\bar{\chi}$ is $O(10^{-3})$ [83], this would need $O(10^8)b\bar{b}$ events to be able to test CP violating charge asymmetry in the standard model, which looks hopelss despite the large $b\bar{b}$ event rates expected at Z^0.

We shall now discuss other CP violating effects that may emerge due to the differences in decay amplitudes of neutral bottom hadrons. The main idea here is to look into differences in the partial decay rates for the decays $B \to f$ and $\bar{B}^0 \to f$ involving the same final states f. An example of these decays is $B_d^0 \to D^0 + X \to K_s + Y + X$ and $\bar{B}_d^0 \to \bar{D}^0 + X \to K_s + Y + X$ where X and Y are sets of hadrons common to both B_d^0 and $\bar{B}_d^0$ decays. One needs a tag for the bottom hadron,say $b \to l^{\pm}X$, one can then define a CP asymmetry in $e^+e^- \to B^0\bar{B}^0 + X \to l^-Xf$, $l^+\bar{X}f$ [97]

$$\Delta A = \frac{\sigma(l^-Xf) - \sigma(l^+\bar{X}f)}{\sigma(l^-Xf) + \sigma(l^+\bar{X}f)} = \frac{2xu^2\sin 2\phi}{1+y^2+2y\cos 2\phi} \xrightarrow[y=0]{} 2xu^2\sin 2\phi \qquad (5.8)$$

where $u = \frac{1-y^2}{1+\chi^2}$, $x = \frac{\Delta M}{\Gamma}$ and $y = \frac{\Delta\Gamma}{2\Gamma} \ll .1$ and ϕ is the Carter-Sanda phase

defined via the relation

$$\exp(-2i\phi) = -\frac{1}{\eta}\frac{\langle f|\mathcal{L}(\Delta B=1)|B^0\rangle}{\langle f|\mathcal{L}(\Delta B=1)|\bar{B}^0\rangle} \qquad (5.9)$$

since for $B_d^0 - \bar{B}_d^0$, $x^2 < 10^{-2}$, $u \simeq 1$ and one has (for $m_t \leq 50$ GeV) (5.10)
$\Delta A(B_d^0) \simeq 2x\sin(2\phi_d) < 0.1$

Again the CP asymmetry (5.8) is suppressed since the mixing parameter $x(B_d^0)$ is very small. The corresponding asymmetry for the B_s^0 and $\bar{B}_s^0$ decays $\Delta A(B_s^0)$ is tiny [97] because the Carter - Sanda phase factor $\sin 2\phi_s$ in this case is CKM suppressed and hence negligible. Quite apart from the smallness of the CP-violating quantity ΔA in the standard model it would be exceedingly difficult to dig out the state f and construct B_d^0 and $\bar{B}_d^0$ mesons from the debris of a bottom jet at LEP/SLC energies. Either f is an exclusive mode, like for example $B_d^0 \to K_s\pi^0\pi^0$, which has a branching ratio probably less than 10^{-4} , or f is an inclusive state in which case one can just forget about reconstructing B_d^0 / $\bar{B}_d^0$ from it. We are afraid that the prospects of measuring ΔA at LEP and SLC are not terribly bright.

Yet another class of reactions to study CP asymmetry in bottom decays involves the difference in exclusive partial rates, $\Gamma(B^0 \to f)$ and $\Gamma(\bar{B}^0 \to f)$. Examples of such exclusive final states are by now abundant, namely $B_d \to K^-\pi^+$, D^+F^-, $\pi^+\pi^-$, D^+D^-,... and $B_S \to K^+\pi^-$, D^-F^+, K^+K^-, F^+F^- etc. [98]. Denoting such differences in integrated partial decay rates generically by ΔW, defined as

$$\Delta W \equiv \frac{\Gamma(\bar{B}^0 \to f) - \Gamma(B^0 \to f)}{\Gamma(\bar{B}^0 \to f) + \Gamma(B^0 \to f)} \tag{5.11}$$

one can show that[98]

$$\Delta W = \frac{x\sin 2\phi}{1+y\cos 2\phi} \xrightarrow[y=0]{} x\sin 2\phi \tag{5.12}$$

Again for B_d^0-$\bar{B}_d^0$ system, since $v_d \approx 1$, one gets (for $m_t \lesssim 50$ GeV)

$$\Delta W = x\sin 2\phi \lesssim 5\times 10^{-2} \tag{5.13}$$

For the B_s^0 - $\bar{B}_s^0$ system, $\sin 2\phi_s$ is suppressed as for ΔA due to the CKM angles and hence $\Delta W(B_s^0)$ is negligible. We realize that the estimates presented in (5.10) and (5.12) are somewhat smaller as compared to some other estimates of the same quantities found in literature. The reason for this dispersion is the use of larger values by some of them for the quantity $x = \frac{\Delta M}{\Gamma}$ for the B_d^0-$\bar{B}_d^0$ case. This quantity, as we have shown in the last section is CKM suppressed and is naturally of $O(\lambda^2)$ in the standard model.

Apart from this difficulty in rate, the feasibility of ΔW measurements at LEP and SLC is commensurate upon successful reconstruction of the B_d^0 and B_s^0 mesons into the exclusive two body decay modes in which the CP asymmetry is being sought for. Many of these decay modes are suppressed by the CKM ratio $|V_{bu}/V_{bc}|^2$ like, for example, $B_d \to \pi^+\pi^-$, K^+K^-, $B_s \to K^+\pi^-$, K^+K^- or else by $\sin^2\theta_c$ like $B_s^0 \to \bar{D}f^+$ and hence are not expected to have branching ratios in excess of 10^{-4}. This is to be expected if one notes that the present branching ratio upper limits[3] on CKM suppressed decays are already quite stringent, namely $B^0 \to \pi^+\pi^-$, $\rho^0\pi^- \lesssim 2\times 10^{-4}$. The decays $B_d \to D^+F^-$, $B_s \to F^+F^-$, on the other hand, though CKM allowed, demand the reconstruction of two charmed hadrons $D^\pm$ and $F^\mp$, which would render the ΔW asymmetry measurements rather formidable at LEP and SLC energies.

Next, we briefly review the possibilities of observing CP violation in the decays of charged bottom hadrons $B_u^\pm$ and $B_c^\pm$. The decays $B_u^- \to D^0D^-$, D^{-*0} were first descussed in this context in ref. (99). The decay $B_u^- \to K^-J/\Psi$ was pointed out in ref. (100). Recently[101], these decays have been recalculated together with the decays $B_u^- \to \pi^0K^-$ and the decays of the much less frequently produced bottom meson $B_c^\pm$, namely $B_c^- \to K^-\bar{D}^0$, $\pi^-\bar{D}^0$ and π^0D^-. These calculations include interference between the penguin diagrams and the usual $W^\pm$ exchange and decay diagrams. Concentrating, for example, on the decay $B_u^- \to \pi^0K^-$ one can write the decay amplitudes as[101]

$$M(B_u^- \to \pi^0K^-) = V_{cb}V_{cs}^*A_1 + V_{ub}V_{us}^*A_2 \tag{5.14}$$

$$\bar{M}(B_u^+ \to \pi^0K^+) = V_{cb}^*V_{cs}A_1 + V_{ub}^*V_{us}A_2$$

The partial rate difference is then given

$$\Delta W^{(\pm)} \equiv \frac{|\bar{M}|^2 - |M|^2}{|\bar{M}|^2 + |M|^2} \tag{5.15}$$

in the CKM parametrization, one gets[101]

$$\Delta W^{(\pm)} = \frac{-2s_1^2s_2s_3s_\delta \mathrm{Im}_1(A_1A_2^*)}{|M|^2 + |\bar{M}|^2} \tag{5.16}$$

which gives rise to the universal CP non-conserving factor, $s_1^2s_2s_3s_\delta$. In the Wolfenstein parametrization, we get instead

$$\Delta W^{(\pm)} = \frac{+4A^2\lambda^6\eta\mathrm{Im}(A_1A_2^*)}{|M|^2 + |\bar{M}|^2} \tag{5.17}$$

where $A \approx 1$. Thus, in this parametrization the universal CP violating factor is $2\lambda^6\eta$. The amplitudes $|M|^2 + |\bar{M}|^2$ and the interference term $\mathrm{Im}(A_1A_2^*)$ depend on the

particular decay mode. For the reaction in (5.14), one gets

$$|M|^2 + |\bar{M}|^2 \simeq 2|V_{cb}|^2|V_{cs}|^2 A_1^2$$

$$\simeq 2A^2\lambda^4 A_1^2 \qquad (5.18)$$

Thus

$$\Delta W^{(\pm)} \simeq + \frac{2\lambda^2 \eta \mathrm{Im}(A_1 A_2^*)}{|A_1|^2} \qquad (5.19)$$

which gives $\Delta W^{(\pm)} \leq 8\times10^{-2}$ for the bounds on η given in eq. (3.16), assuming $\mathrm{Im}(A_1A_2^*)/(A_1)^2 \simeq O(1)$. Since $A_1 = 0$ in the absence of Penguin diagrams, a definitive estimate of the rates for the asymmetry in the decays $B_u^\pm \to K^\pm\pi^0$ is rather model dependent. To get an order of magnitude we use the calculations in ref. (101), then one gets $BR(B_u^- \to \pi^0 K^-) \simeq 4\times10^{-5}$; thus again one would need $O(10^7)$ $b\bar{b}$ events to be able to observe CP-violation in the decays of $B_u^\pm$ mesons. Observation of CP violation in the other decay mode mentioned earlier namely $B_u^- \to D^-D^*$ would need similar statistics; the case for observing the asymmetry in $B_u^- \to K^-J/\Psi$ decays is even weaker, requiring $O(10^9)$ $b\bar{b}$ events[101]. We shall not present any rates for asymmetries in the $B_c^\pm$ decays since the rates of $B_c^\pm$ production at LEP and SLC energies is expected to be very small, with probably $\sigma(B_c^\pm X) \simeq 10^{-3}\,\sigma(b\bar{b})$ a reasonable guess, judging from[3] $\sigma(e^+e^- \to J/\Psi+X) / \sigma_{tot} < 10^{-3}$. Since the expected charge asymmetry in the standard model is very small, exclusive two body decays provide an interesting but challenging alternative. It is quite possible that the CP-violating difference in some of the partial modes may attain as high a value as 10%. The success in observing such differences, however, hinges entirely on the ability to reconstruct bottom hadrons in the relevant (but alas very much suppressed) exclusive modes.

In summary, in the standard scenario of CP violation in bottom hadrons the general features are qualitatively very clear. The physical quantities in bottom hadron decays, which involve virtual B^0-$\bar{B}^0$ transitions and are sensitive to CP-violation, need both large mixings, i.e. large $x = \Delta M/\Gamma$, and large relative phases, i.e.either large $z = 1/2\ \mathrm{Im}(\Gamma_{12}/M_{12})$ or large ϕ, in order to yield measurable rates. For B_d^0-$\bar{B}_d^0$ transitions, $\Delta M/\Gamma \ll 1$ since the CKM ratio $|V_{td}\ /\ V_{bc}|^2 \leq \lambda^2$.

For B_s^0-$\bar{B}_s^0$ transition , the phases z or ϕ are small due to CKM and GIM suppressions. This is a pattern intrinsic to the standard model and it leaves little room for any educated guesswork within the model. The other class of CP-violating quantities, namely involving $B^0 \to f$, $\bar{B}^0 \to \bar{f}$ decays where f is either not reachable by $\bar{B}$ or it is not a CP eigenstate, do not involve B^0-$\bar{B}^0$ virtual transitions. The problems here, as well as in partial rate differences in $B_u^\pm$ and $B_c^\pm$ decays, are more of practical nature. They require measurements of rate differences of $O(10^{-2})$ for specific bottom hadrons in exclusive decay modes, with effective branching ratios of $O(10^{-4})$ or less. Many, probably all "easy" modes involve $b \to u$ decays. With $O(10^5)$ $e^+e^- \to b\bar{b}$ events at DORIS and CESR, there is not a single inclusive or exclusive decay mode seen involving the CKM suppressed $b \to u$ transition. Measurement of the CKM element V_{bu} will reduce at least one uncertainty. Ability to measure specific decay modes at a rate better than 5% is a lot more demanding goal. It seems reasonable to conclude that measuring CP violations at LEP and SLC is very probably not going to be a first generation experiment. The question is whether it would at all be possible to detect CP violation in botton meson sector at LEP?

It is certainly conceivable that the standard model in not the whole truth! In that case one could have additional effective interactions, like for example in the SUSY extension of the standard model[14], which contribute both to Re (M_{12}) and $\mathrm{Im}(M_{12})$, thereby enhancing $\Delta M/\Gamma$ and $\mathrm{IM}(M_{12}\ /\ \Gamma_{12})$ both in the B_d^0-$\bar{B}_d^0$ and B_s^0-$\bar{B}_s^0$ transitions. This would lead, among other things, to a measurable rate for the charge asymmetry in the inclusive dilepton states, N^{++}-N^{--}.

Of course, the SUSY interactions are not the only non-standard forces that may lead to such enhancements. It was pointed out in ref. (91) that if CP-violations have a spontaneously broken symmetry origin[102], then CP-violation effects in the bottom and top mesons will be very much enhanced. Like for the SUSY models, in the multi-Higgs models also the delicate cancellation obtaining in the standard model leading to a small value of $z = 1/2\ \mathrm{Im}(\Gamma_{12}\ /\ M_{12})$ in the B_s^0-$\bar{B}_s^0$ sector, will be upset, again leading to observable CP-violation effects in virtual transitions[103]. While on the track of theoretical speculations beyond the standard model, one should also mention left-right symmetric models based on the $SU(2)_L \times SU(2)_R \times U(1)$ group[104], which contain additional gauge bosons $W_R^\pm$, Z_R and Higgses, both

charged and neutral. The implications of these models for mass mixing and CP-violation in heavy hadrons have recently been studied in ref. (105). The scenario in the left-right symmetric models is that the quantity $Re(\Delta M/\Gamma)$ for both $B_d^0-\bar{B}_d^0$ and $B_s^0-\bar{B}_s^0$ systems approximately retains its value in the standard model, but the quantities $Im(M_{12}/\Gamma_{12})$ and ϕ for the $B_s^0-\bar{B}_s^0$ system get enhanced. This could again lead to observable charge asymmetry $N^{++}-N^{--}$ from the $B_s^0-\bar{B}_s^0$ transition. Likewise, additional CP violating phases obtaining in the four-generation quark models[22] can also lead to the enhancement of $Im(M_{12}/\Gamma_{12})$ and ϕ for both the $B_d^0-\bar{B}_d^0$ and $B_s^0-\bar{B}_s^0$ systems.

In view of the multiple "choice" of CP violating non-standard effective interactions, our experimental colleagues are well advised to entertain the possibility of observing CP-violations in bottom physics seriously. Unfortunately, there is no positive indication yet for the existence of these additional interactions anywhere and hence the scales of the non-standard forces are not presently known! Definitive predictions are therefore hard to make. Instead, we have pointed out specific suppression mechanisms for CP violations. These mechanisms are endemic to the standard three-family model and are expected to fail in an extended theory, thereby making the CP-violation phenomena experimentally accessible at machines with high bottom hadron yield and good taggings, like for example LEP. It may be that like the kaon beams one would need extracted bottom hadron beams to study CP-violation. This however is possible only in large hadron fixed target machines[106].

6. Summary and Conclusions

In the preceeding sections we have discussed some salient features of heavy quark physics expected at LEP and SLC energies. Though most of the rate calculations presented above are made for LEP, the theoretical framework on which these calculations are based has a wider range of interest. In particular, most aspects of charm and bottom physics discussed above are also relevant for physics below the LEP energies. For example, sections 3-5 contain a systematic study of rare transitions and decays of bottom hadrons, which is also the main thrust of the physics research programme at CESR and DORIS.

This report can be broadly divided into three main categories. In section 2, we have reviewed the general features of the production and decays of heavy quarks, in the framework of QCD and standard model. This includes measurements of the total hadronic cross-section, forward backward quark charge asymmetry, inclusive leptonic and hadronic decay rates of the bottom and top hadrons and their lepton energy spectra, rates for multileptonic states in top decays, measurements of m_t through semileptonic spectra and effects of the top quark polarization on the final states. This is the main fare of the physics programme involving unbound heavy quarks at LEP. The interest here lies in the precise determination of the vector and axial vector couplings of the heavy quarks, many of which are either not accessible at lower energies or are presently poorly determined for lack of statistics. Experiments at LEP hopefully would complete the fermionic sector of the standard model and confirm that the t-quark really belongs to an $SU(2)_L$ doublet, with expected couplings.

The second category of effects involving heavy quarks are the ones that aim at measuring suppressed transitions, involving the CKM matrix elements $|V_{bu}|$, $|V_{ts}|$ and $|V_{td}|$. Only the element $|V_{bu}|$ is, in principle, measurable at CESR and DORIS. The present reliable limit on the ratio $\bar{R} = \frac{\Gamma(b\to u l \nu_e)}{\Gamma(b\to c l \nu_e)}$ is $\bar{R} < 0.08$. In particular theoretical scenarios, one expects $|V_{bu}/V_{bc}| \approx 0.05 - 0.1$. We discussed the prospects of measuring the ratio $|V_{bu}/V_{bc}|$ at LEP through the transverse lepton energy distributions, $\frac{d\sigma}{dp_T^l}$, measured with respect to the jet axis. With $O(10^6)$ $Z^0 \to b\bar{b}$ events per year per detector it would certainly be possible to measure $|V_{bu}/V_{bc}|$ at the 0.1 level. Beyond that the systematic errors, both from p_T^l measurements and jet axis determination as well as from theoretical uncertainties, will dominate. We have only presented the gross features of the experimental method here. This problem deserves further theoretical study.

Measurements of the matrix elements $|V_{ts}|$ and $|V_{td}|$ are the uncontested domain of experiments at LEP, though such measurements are by no means going to be easy. In the standard model one expects $|V_{ts}| \approx |V_{bc}| \approx 0.05$ and $|V_{td}| \approx 0.01$. There is some hope of measuring $|V_{ts}|$ if the top quark is accessible in $Z^0 \to t\bar{t}$ decays, without any appreciable suppression. Unfortunately the end-point spectra in

the rest frame decays $t \to bl^+\nu_l$ and $t \to sl^+\nu_l$ differ by an amount $\frac{m_b^2 - m_s^2}{2m_t}$ (GeV/c). for $m_t \simeq 40$ GeV. This would require a lepton energy resolution $\frac{\Delta E_l}{E_l}$ of better than 1%. One will have to combine E_l measurements with identification of the hadrons in the process $t \to l^+X$. Again, the fragmentation uncertainties can be avoided if it becomes possible to construct the top quark jet axis, which should be possible in the decays $Z^0 \to t\bar{t}$ if m_t is not very high, say $m_t \simeq 30$ GeV. The branching ratio in any specific channel involving $t \to d$ transition is expected to be $< 10^{-5}$. That looks prohibitively small and very probably $|V_{td}|$ will only be determined indirectly through precise measurements of V_{ud}, V_{sd} and unitarity.

In section (4), we discussed the virtual transitions $M^0 \leftrightarrow \bar{M}^0$. The interest here is mainly in the B_s^0-$\bar{B}_s^0$ and B_d^0-$\bar{B}_d^0$ mixings. Such transitions can also lead to induced mixing effects in the decays of charged top mesons $T_d^\pm$, $T_s^\pm$ etc. There are three final states in which effects of the virtual B^0-$\bar{B}^0$ transitions are expected to manifest themselves: (i) same sign dilepton production in the process $e^+e^- \to b\bar{b} \to l^\pm l^\pm X$ (ii) reduction in the bottom quarks electroweak charge asymmetry measured, for example, in the process $e^+e^- \to b\bar{b} \to l^\pm X$ and (iii) lepton-kaon correlations in $e^+e^- \to b\bar{b} \to l^\pm K^\mp K^\mp X$. In terms of the mixing measure χ defined in the text, the present limits from the final states (i) and (ii) are $\chi < 0.12$ [83] and $\chi < 0.13$ [85] from e^+e^- annihilation experiments at PEP and PETRA, respectively. Present data from the CERN collider for the process $p\bar{p} \to \mu^\pm\mu^\pm X$ [78] suggest $\chi > 0.04$ [20]. There are no limits on χ from the process (iii) yet. Our conclusion is that with the large bottom statistics expected at LEP, it would be possible to test B-$\bar{B}$ mixings in all these final states at the level $\chi > 0.04$, suggested by the UA1 data. The correlation (iii) is sensitive only to the B_s^0-$\bar{B}_s^0$ mixing and a positive measurement of it would confirm the standard model prediction $r_s \gg r_d$.

The third category of effects at LEP are related to CP violations in the bottom hadron sector. These were reviewed in section 5 and involve measurements of either the charge asymmetry $a = \frac{N^{++} - N^{--}}{N^{++} + N^{--}}$ in the process $e^+e^- \to b\bar{b} \to l^\pm l^\pm X$, l^+l^-X, or else differences in partial decay rates. The quantity which determines the rates

for the former is the total charged asymmetry $\frac{N^{++} - N^{--}}{N_{21}} = 2a\chi\,(1-\chi)$. We estimate this to be $< 10^{-4}$ in the standard model which makes it unaccessible at LEP with realistic running time. The differences in the partial rates ΔW and $\Delta W^{(\pm)}$, defined in the text, could be as large as 10% in some specific channels of bottom hadrons. Unfortunately, most of these partial modes have small branching ratios $< O(10^{-3} - 10^{-4})$. The ability to reconstruct bottom hadrons in specific decay modes is going to be of crucial importance here. Realistic estimates would have $O(10^6 - 10^7)$ $b\bar{b}$ events for CP violation to be measurable in partial decay rates, given a good bottom hadron reconstruction efficiency. There are a number of non-standard scenario which could enhance $\frac{N^{++} - N^{--}}{N_{21}}$ by an order of magnitude, as well as enhance the asymmetry in other CP violating partial rates. This would bring CP violation measurements within the reach of LEP experiments in long and dedicated runs over several years. It will not surprise many of us if CP violation becomes the Achilles heel of the standard model. LEP experiments are certainly well equipped to take an aim at that!

Acknowledgements

I would like to thank my collegues in the working group on " QCD, γγ and Heavy Quark Physics at LEP" for many stimulating discussions. I warmly thank F.Barreiro, B.v.Eijk, G.Ingelman, R.Rückl and D.Saxon for frequent discussions and Frau M.Hausser for her patient typing of the manuscript.

References

1. LEP Design Report, CERN-LEP/84-01 (1984); C.Y. Prescott, SLAC-PUB 2854 (1981); Proceedings of the SLC Workshop, SLAC-247 (1982). For estimates of $\sigma(Z)$ including radiative corrections see R. Kleiss, these proceedings.

2. J. Ellis, Proceedings of the LEP Summer Study, CERN Report 79-01 (1979); Report of the "New Particles Working Group", H. Baer et al, these proceedings; Report of the "Physics at LEP at High Energies", G. Barbiellini et al., these proceedings.

3. For a recent review of experimental charmed and bottom hadron decay properties see, for example, E. Thorndike, talk presented at the 1985 International Symposium on Lepton and Photon Interactions at High Energies, Kyoto, Japan (1985).

4. A. Ali and E. Pietarinen, Nucl. Phys. B154, 519 (1979); N. Cabibbo, G. Corbo and L. Maiani, Nucl. Phys. B155, 93 (1979); G. Altarelli, N. Cabibbo, G. Corbo, L. Maiani and G. Martinelli, Nucl. Phys. B208, 365 (1982); G. Corbo, Phys. Lett. 116B, 298 (1982).

5. K. Hayes, "B Tagging at the SLC", MARK II/SLC Note # 73.

6. A. Ali and Z.Z. Aydin, Nucl. Phys. B148, 165 (1978); A. Ali and C. Jarlskog, Phys. Lett. 114B, 266 (1984).

7. C. Büno et al., Phys. Rev. Lett., to be published (1986). See also A.C. Benvenuti et al., Phys. Lett. 158B, 531 (1985).

8. For recent theoretical discussions on D^0-$\bar{D}^0$ mixing see L. Wolfenstein, Carnegie Mellon University Report CMU-HEP85-10 (1985); A. Dutta and P. Kumbhakar, Zeit. f. Physik C27 515 (1985); L.L. Chau, Phys. Rep. 95C, 1 (1983) and references quoted therein; G. Ecker and W. Grimus, Universität Wien Preprint UWThPh-1985-14 (1985).

9. R. Settles, these proceedings.

10. J.M. Dorfan, SLAC Report, SLAC-PUB-3407 (1984) and references quoted therein. See also refs. (1) and (3).

11. A. Chen et al. (CLEO Collaboration), Phys. Rev. Lett. 52, 1084 (1984); R. Giles et al. (CLEO Collaboration), Phys. Rev. D30, 2279 (1984); See also ref. 3.

12. N. Cabibbo, Phys. Rev. Lett. 10, 531 (1963); M. Kobayashi and K. Maskawa, Prog. Theor. Phys. 49, 652 (1973).

13. Large-p_T inclusive bottom hadron cross sections at the CERN and Fermilab anti-proton proton colliders are estimated to be of O(1μb) for p_T^B 5 GeV. For a theoretical update see, for example, A. Ali, Proceedings of the International Symposium on Physics of Proton-antiproton Collision, Tsukuba, 1985 (Ed. Y. Shimizu and K. Takikawa) p. 456.

14. For CP violation effects in bottom hadron sector in supersymmetric models, see J.-M. Gérard et al., Phys. Lett. 140B, 349 (1984); M.B. Gavela et al., CERN Report TH-4093/85 (1985); M. Dugan, B. Grinstein and L. Hall, Nucl. Phys. B255, 413 (1985); A.I. Sanda, Phys. Rev. Lett. 56, 298 (1986).

15. G. Arnison et al. (UA1 Collaboration), Phys. Lett. 147B, 493 (1984).

16. "Toponium Physics at LEP", W. Buchmüller et al., these proceedings.

17. J. Kim, P. Langacker, M. Levine and H. Williams, Rev. Mod. Phys. 53, 211 (1980). See also W.J. Marciano and A. Sirlin, Brookhaven Report BNL-33819 (1983).

18. M. Veltman, Nucl. Phys. B123, 89 (1977); M.B. Einhorn, D.R.T. Jones and M. Veltman, Nucl. Phys. B191, 146 (1981).

19. For earlier works on B-$\bar{B}$ mixings see J. Ellis, M.K. Gaillard, D.V. Nanopoulos and S. Rudaz, Nucl. Phys. B131, 285 (1977); A. Ali and Z.Z. Aydin, Nucl. Phys. B148, 165 (1978); J.S. Hagelin, Nucl. Phys. B193, 123 (1981); I.I. Bigi and A.I. Sanda, Nucl. Phys. B193, 85 (1981), Phys. Rev. D29, 1393 (1984); F.J. Gilman and J.S. Hagelin, Phys. Lett. 133B, 443 (1983); E. Ma, W.A. Simmons and S.F. Tuan, Phys. Rev. D20, 2893 (1979); E. Franco, M. Lusignoli and A. Pugliese, Nucl. Phys. B194, 403 (1982); H.Y. Cheng, Phys. Rev. D26, 143 (1982); L.-L. Chau, Phys. Reports 95C (1983) 1; L.-L. Chau, W.-Y. Keung and M.D. Tran, Phys. Rev. D27, 2145 (1983); D. Hochberg and R. G. Sachs, Phys. Rev. D27, 606 (1983); E.A. Paschos, B. Stech and U. Türke, Phys. Lett. 128B 240 (1983); E.A. Paschos and U. Türke, Nucl. Phys. B243, 29 (1984). A.J. Buras, W. Slominski and H. Steger, Nucl. Phys. B245, 369 (1984). The list is by no means complete.

20. A. Ali, DESY Report 85-107 (1985); to be published in the Proceedings of the XVI Symposium on Multiparticle Dynamics, Kiryat Anavim, Israel (1985).

21. A. Ali and F. Barreiro, DESY Report 85-127 (1985) (to be published in Zeit. f. Physik C).

22. X.-G. He and S. Pakvasa, Univ. of Hawaii Report UH-511-553-85 (1985); T. Hayashi, M. Tanimoto, S. Wakaizumi, Kure Technical College Report KCTP-8501/HUPO-8505 (1985).

23. V. Barger, H. Baer, K. Hagiwara and R.J.N. Phillips, Phys. Rev. D30, 947 (1984); A. Ali et al., CERN Report, CERN-TH. 3959/84 (1984) and proceedings of the ECFA-CERN Workshop; M. Gronau and J. Schechter, SLAC Report SLAC-PUB-3451 (1984).

24. G. Altarelli et al., these proceedings; B.W. Lynn, M.E. Peskin and R.G. Stuart, SLAC-PUB-3725 (1985); W. Hollik and H.-J. Timme, DESY Report DESY 85-099 (1985) and references quoted therein.

25. M. Dine and J. Sapirstein, Phys. Rev. Lett. 43, 668 (1979); K.G. Chetyrkin, A.L. Kataev and F.V. Tkachov, Phys. Lett. 85B, 277 (1979); W. Celmaster and R.J. Gonsalves, Phys. Rev. Lett. 44, 560 (1980).

26. W.E. Caswell, Phys. Rev. Lett. 33, 244 (1974); D.R.T. Jones, Nucl. Phys. B75, 531 (1974). A.A. Belavin and A.A. Migdal, JETP Lett. 19, 181 (1974).

27. W.A. Bardeen, A.J. Buras, D.W. Duke and T. Muta, Phys. Rev. D18, 3998 (1978).

28. J. Schwinger, Particles, Sources and Fields, Vol. II (Addison-Wesley, New York 1973) Chap. 5-4. See also G. Källen and A. Sabry, K. Dansk Vidensk. Slesk. Mat.-Fys. Medd. 29, No. 17 (1955).

29. A. De Rujula and H. Georgi, Phys. Rev. D13, 1296 (1976); T.W. Appelquist and H.D. Politzer, Phys. Rev. Lett. 34, 43 (1975); Phys. Rev. D12, 1404 (1975).

30. J.H. Kühn and S. Ono, Zeit. f. Physik C21, 395 (1984). J. Jersak, E. Laermann and P. Zerwas, Phys. Rev. D25, 1219 (1982); S. Güsken, J.H. Kühn and P.M. Zerwas, Phys. Lett. 155B, 185 (1985).

31. This is close to the present world average of the QCD parameter, $\Lambda_{\overline{MS}}$.

32. G. Rudolph, these proceedings.

33. See, for example, Lynn, Peskin and Stuart in ref. (24).

34. R. Barlow, Proceedings of the XX Recontre de Moriond, "Heavy Quarks, Flavour Mixing and CP-Violation" (La Plagne, France, 1985) p. 187; W. Bartel et al. (JADE Collaboration), Phys. Lett. 146B, 437 (1984); I.I. Bigi, Phys. Lett. 155B, 125 (1985).

35. M.K. Gaillard and B.W. Lee, Phys. Rev. Lett. 33, 108 (1974); G. Altarelli and L. Maiani, Phys. Lett. 52B, 351 (1974).

36. N. Cabibbo and L. Maiani, Phys. Lett. 79B, 109 (1978); M. Suzuki, Nucl. Phys. B145, 420 (1978).

37. G. Altarelli, G. Curci, G. Martinelli and R. Petrarca, Phys. Lett. 99B, 141 (1981) and Nucl. Phys. B187, 461 (1981).

38. For a discussion of the variation of μ on various physical parameters in charm decays see, for example, A.J. Buras, J.-M. Gérard and R. Rückl, Max-Planck-Institute Report MPI-PAE/PTh 41/85 (1985).

39. J. Lee-Franzini, Proceedings of the Europhysics Conference on "Flavor Mixing in Weak Interactions", Ettore Majorana International Science 20 (1984) (Ed. L.-L. Chau).

40. B. Guberina, S. Nussinov, R.D. Peccei and R. Rückl, Phys. Lett. 89B, 111 (1979); Y. Koide, Phys. Rev. D20, 1739 (1979); K. Jagannathan and V.S. Mathur, Phys. Rev. D21, 3165 (1980).

41. W. Bernreuther, O. Nachtmann and B. Stech, Zeit. f. Physik C4, 257 (1980); H. Fritzsch and P. Minkowski, Phys. Lett. 90B, 455 (1980); S.P. Rosen, Phys. Rev. Lett. 44, 4 (1980); M. Bander, D. Silvermann and A. Soni, Phys. Rev. Lett. 44, 7 (1980) and Erratum Phys. Rev. Lett. 44, 962 (1980).

42. See, for example, Y. Eisenberg, DESY Report 85-116 (1985) and references quoted therein.

43. H. Krasemann, Phys. Lett. 96B, 397 (1980); M. Suzuki, Nucl. Phys. B177, 413 (1981); Phys. Lett. 142B, 207 (1984) and 162B, 392 (1985); A. Ali and C. Jarlskog in ref. 6.

44. V.A. Novikov et al., Phys. Rev. Lett. 38, 626 (1977); E.V. Shuryak, Nucl. Phys. B198, 83 (1982); S. Narison, Zeit. f. Physik C14, 263 (1982); L.J. Reinders et al., CERN Report-TH-4079 (1984).

45. E. Golowich, Phys. Lett. 91B, 271 (1980); M. Claudson, Harvard University Preprint HUTP-81/A016, unpublished.

46. J.P. Leveille, University of Michigan Preprint, UMHE 81-18 (1981).

47. Our results are quite close to the ones calculated by R. Rückl, Habilitationsschrift, Universität München (1983).

48. V. Barger, J.P. Leveille, P.M. Stevenson and R.J.N. Phillips, Phys. Rev. Lett. 45, 83 (1980).

49. P. Hoyer et al., Nucl. Phys. B161, 349 (1979); A. Ali, E. Pietarinen, G. Kramer and J. Willrodt, Phys. Lett. 93B, 155 (1980); B. Andersson et al., Phys. Rep. 97, 33 (1983).

50. A. Ali, Zeit. f. Physik C1, 25 (1979).

51. J.H. Kühn, Nucl. Phys. B237, 77 (1984).

52. Ch. Berger et al. (PLUTO Collaboration), Zeit f. Phys. C12, 297 (1982).

53. See, for example, J.M. Izen, DESY Report 84-104 (1984) and proceedings of the XV Symposium on Multiparticle Dynamics, Lund Sweden (1984).

54. For a recent review of jet fragmentation properties see D.H. Saxon, Rutherford Lab. Report RAL-85-077 (1985).

55. I.I. Bigi and H. Krasemann, Zeit. f. Physik C7, 127 (1981).

56. N. Anselmino, P. Kroll and B. Pire, Zeit. f. Physik C29, 135 (1985) and CERN Report, CERN-TH-4172/85 (1985).

57. J.H. Kühn, A. Reither and P.M. Zerwas, SLAC PUB-3746 (1985).

58. M. Gourdin, University of Paris Report PAR-LPTHE 78/17 (1978) (unpublished).

59. J. Kühn (unpublished). For a related calculation see B. Pire and J.P. Ralston, Phys. Rev. D28, 260 (1983).

60. J. Jersak, E. Laerman and P.M. Zerwas, Phys. Rev. D25, 1218 (1982).

61. Y.S. Tsai, Phys. Rev. D4, 2821 (1971).

62. C. Peterson, D. Schlatter, I. Schmitt and P.M. Zerwas, Phys. Rev. D27, 105 (1983). For comparison with e^+e^- data see S. Bethke, DESY Report 85/067 (1985).

63. B. Naroska, DESY Report 85-090 (1985) and proceedings of the meeting: "Physics in Collisions V", Autun, France (1985).

64. L. Maiani, Proc. of the 8th Int. Symp. on Leptons and Photon Interactions at High Energy, Hamburg, Fed. Rep. of Germany (1979). See also refs. (70), (71) and (73) below.

65. G. Barbiellini and C. Santoni, CERN Report EP/85-117 (1985) and references quoted therein.

66. For earlier attempts on the determination of V_{KM} elements see K. Kleinknecht and B. Renk, Phys. Lett. 130B, 459 (1983); K. Kleinknecht, in "Flavor Mixing in Weak Interactions", Plenum Press New York and London, 1984 (Ed. Ling-Lie Chau) p. 459.

67. C. Klopfenstein et al. (CUSB Collaboration), Phys. Lett. 130B (1983) 444; A. Chen et al., Phys. Rev. Lett. 52, 1084 (1984).

68. B. Stech, Phys. Lett. 130B, 189 (1983); See also G. Ecker, Zeit. f. Phys. C24, 353 (1984).

69. H. Fritzsch, Phys. Lett. 73B, 317 (1978) and Nucl. Phys. B155, 189 (1979).

70. M. Gronau, R. Johnson and J. Schechter; Phys. Rev. Lett. 54, 2176 (1985).

71. H. Fritzsch, Max-Planck-Institut Report MPI-PAE/PTh 32/85 (1985).

72. J. Gasser and H. Leutwyler, Phys. Rep. 87C, 77 (1982).

73. L. Wolfenstein, Phys. Rev. Lett. 51, 1945 (1984).

74. N. Cabibbo in ref. (12); S.L. Glashow, J. Illiopoulos and L. Maiani, Phys. Rev. D2, 1285 (1970).

75. M. Gronau and J. Schechter, Phys. Rev. Lett. 54, 385 (1985).

76. L. Maiani, in ref. 64; L. Chau and K. Keung, Phys. Rev. Lett. 53, 1802 (1984).

77. For a recent calculation of exclusive semileptonic and nonleptonic bottom meson decays see M. Wirbel, B. Stech and M. Bauer, Universität Heidelberg Report HD-THEP-85-19 (1985); B. Grinstein, M.B. Wise and N. Isgur, Phys. Rev. Lett. 56, 298 (1986).

78. C. Rubbia, Proceedings of the International Symposium on Lepton and Photon Interactions at High Energies, Kyoto, Japan (1985).

79. M.K. Gaillard and B.W. Lee, Phys. Rev. D10, 897 (1974).

80. L. Wolfenstein, Carnegie-Mellon Univer. Report CMU-HEP85-10 (1985).

81. L.B. Okun, V.I. Zakharov and B.M. Pontecorvo, Lett. Nuovo Cim. 13, 218 (1975); A. Pais and S.B. Treiman, Phys. Rev. D12, 244 (1975).

82. V. Barger and R.J.N. Phillips, Madison Report MAP/PH/155 (1984).

83. T. Schaad et al. (MARK-II Collaboration), Phys. Lett. 160B, 188 (1985).

84. P. Avery et al. (CLEO Collaboration), Phys. Rev. Lett. 53, 1309 (1984).

85. W. Bartel et al. (JADE Collaboration), Phys. Lett. 146B, 437 (1984).

86. B. Adeva et al. (MARK-J Collaboration), Phys. Rep. 109, 181 (1984); W. Bartel et al. (JADE Collaboration) in ref. 85; M. Althoff et al. TASSO Collaboration), Zeit. f. Phys. C22, 219 (1984).

87. G.J. Alner et al. (UA5 Collaboration), CERN Report EP/85-81 (1985); M. Banner et al. (UA2 Collaboration), Phys. Lett. 122B, 322 (1983) and the preprint D PH PE 84-07 (1984).

88. R. Brandelik et al. (TASSO Collaboration), Phys. Lett. 94B, 91 (1980); W. Bartel et al. (JADE Collaboration), Zeit. f. Phys. C20, 187 (1983); H. Aihara et al., Phys. Rev. Lett. 53, 2378 (1984); E. Fernandez et al. (HRS Collaboration), ANL Report ANL-HEP-CP-85-69 (1985).

89. R.D. Field and R.P. Feynman, Nucl. Phys. B136, 1 (1978).

90. This feature is common to the fragmentation models in vogue at PETRA and PEP energies. For a sampling see, for example, refs. 49.

91. See Ali and Aydin in ref. (6).

92. A. Fridman, SLAC Report, SLAC-PUB-3830 (1985).

93. J.H. Christenson et al., Phys. Rev. Lett. 13, 138 (1964).

94. Review of Particle Properties, Rev. of Mod. Phys. 56, No. 2 (1984).

95. R.-H. Bernstein et al., Phys. Rev. Lett. 54, 1631 (1985); J.K. Black et al., Phys. Rev. Lett. 54, 1628 (1985).

96. For a recent review see, for example, A. Buras, Max-Planck-Institut Report MPI-PAE/PTh 64/85 (1985).

97. A.B. Carter and A.I. Sanda, Phys. Rev. Lett. 45, 952 (1980); Phys. Rev. D23, 1567 (1981);

98. L.-L. Chau and H.-Y. Cheng, Phys. Lett. 165B, 429 (1985); M. Bander, D. Silverman and A. Soni, Phys. Rev. Lett. 43, 242 (1979). See also, Dan-di Wu et al., Institute of High Energy Physics, Peking, Reports BIHEP-TH-85-24 and BIHEP-TH-85-27 (1985).

99. J. Bernabeu and C. Jarlskog, Zeit. f. Physik C8, 233 (1981).

100. T. Brown, S. Pakvasa and S.-F. Tuan, Phys. Lett. 136B, 117 (1984).

101. L.-L. Chau and H.-Y. Cheng, Phys. Rev. Lett. 53, 1037 (1984).

102. T.D. Lee, Phys. Rev. D8, 1226 (1973); S. Weinberg, Phys. Rev. Lett. 37, 657 (1976).

103. For a classification of CP violations in models with several Higgs doublets see G.C. Branco, A.J. Buras and J.-M. Gérard, Phys. Lett. 155B, 192 (1985) and Nucl. Phys. B259, 306 (1985).

104. R.N. Mohapatra and G. Senjanović, Phys. Rev. Lett. 40, 912 (1980); Phys. Rev. D23, 165 (1981).

105. G. Ecker and W. Grimus in ref. (8).

106. N. Reay, in proceedings of the SSC Fixed Target Workshop, Woodlands, Texas, U.S.A. (1984).

Fermion	N_f	a_f	v_f
ν_e, ν_μ, ν_τ	1	1/2	1/2
e, μ, τ	1	-1/2	$-1/2+2\sin^2\theta_W$
u, c, t	3	1/2	$1/2-4/3\sin^2\theta_W$
d, s, b	3	-1/2	$-1/2+2/3\sin^2\theta_W$

Table 1: The coefficients N_f, a_f and v_f in the standard model of electroweak interactions.

Decay modes	BR(Z) (i)	BR(Z) (ii)	BR(Z) (iii)
$\nu\bar{\nu}$	6.3	6.2	6.1
$e^+e^- = \mu^+\mu^- = \tau^+\tau^-$	3.1	3.1	3.1
$d\bar{d} = s\bar{s}$	14.4	14.4	14.4
$b\bar{b}$	14.3	14.3	14.3
$u\bar{u} = c\bar{c}$	11.2	11.2	11.2
$t\bar{t}$	6.3	6.5	6.7
Γ_{tot} (Z) (GeV)	2.69	2.78	2.92

Table 2a: Branching ratios for the decays $Z^0 \to f\bar{f}$ and the Z^0 decay width including $O(\alpha_s)$ and mass corrections. (i) m_Z = 92 GeV, $\sin^2\theta_W$ = 0.23, (ii) m_Z = 93 GeV, $\sin^2\theta_W$ = 0.225, (iii) m_Z = 94 GeV, $\sin^2\theta_W$ = 0.217. All entries correspond to the values m_t = 30 GeV, $\Lambda_{\overline{MS}}$ = 0.2 GeV with n_f = 5.

Decay modes	BR(Z) (i)	BR(Z) (ii)	BR(Z) (iii)
$\nu\bar{\nu}$	6.5	6.4	6.4
$e^+e^- = \mu^+\mu^- = \tau^+\tau^-$	3.3	3.2	3.1
$d\bar{d} = s\bar{s}$	14.9	14.9	14.9
$b\bar{b}$	14.8	14.8	14.8
$u\bar{u} = c\bar{c}$	11.6	11.6	11.6
$t\bar{t}$	2.8	3.1	3.4
Γ_{tot} (Z) (GeV)	2.59	2.68	2.82

Table 2b: Same as table 2a except for m_t = 40 GeV

Decay modes	BR(Z) (i)	BR(Z) (ii)	BR(Z) (iii)
$\nu\bar{\nu}$	6.6	6.5	6.5
l^+l^-	3.3	3.3	3.2
$d\bar{d} = s\bar{s}$	15.1	15.1	15.1
$b\bar{b}$	15.0	15.0	15.0
$u\bar{u} = c\bar{c}$	11.8	11.8	11.8
$t\bar{t}$	1.4	1.7	2.0
Γ_{tot} (Z) (GeV)	2.55	2.64	2.77

Table 2c: Same as table 2a except for m_t = 44 GeV

Fermion	a_f	Standard Model
u	0.50 ± 0.03	0.5
d	-0.49 ± 0.05	-0.5
c	0.55 ± 0.17	0.5
s	-	-0.5
b	-0.54 ± 0.12	-0.5
t	-	0.5
e	-0.49 ± 0.03	-0.5
μ	-0.51 ± 0.05	-0.5
τ	-0.44 ± 0.07	±0.5

Table 3 : Present status of the axial vector coupling constants a_f and the standard model predictions (from ref. (49))

m_b (GeV)	c_+	c_-	K_{NL}
4.8	0.855	1.369	1.128
4.9	0.856	1.365	1.124
5.0	0.857	1.360	1.120
5.1	0.859	1.356	1.116
5.2	0.860	1.352	1.120

Table 4: QCD correction factors for the non-leptonic decay width of the bottom quark.

m_b (GeV)	m_c (GeV)	K_{SL}	I_c	Z_c	BR(e) %
4.8	1.5	0.868	0.427	3.075	13.9
	1.6	0.872	0.390	2.687	14.5
	1.7	0.874	0.353	2.333	15.1
	1.8	0.878	0.318	2.018	15.8
4.9	1.5	0.867	0.439	3.203	13.7
	1.6	0.871	0.402	2.812	14.3
	1.7	0.874	0.366	2.455	14.9
	1.8	0.877	0.331	2.132	15.5
5.0	1.5	0.868	0.451	3.331	13.5
	1.6	0.871	0.414	2.937	14.1
	1.7	0.874	0.379	2.575	14.7
	1.8	0.877	0.344	2.247	15.3
5.1	1.5	0.868	0.462	3.454	13.4
	1.6	0.870	0.426	3.06	13.9
	1.7	0.875	0.391	2.696	14.5
	1.8	0.876	0.356	2.361	15.1
5.2	1.5	0.868	0.473	3.574	13.2
	1.6	0.871	0.438	3.181	13.8
	1.7	0.873	0.403	2.813	14.3
	1.8	0.876	0.368	2.474	14.9

Table 5a: QCD correction factor in $O(\alpha_s)$ for the semileptonic decay width, K_{SL}, and the functions I_c and Z_c defined in the text for the $b \to c$ transitions. Also shown are the semileptonic branching ratios for the b-quark decays.

m_b(GeV)	m_u(GeV)	K_{SL}	I_u	Z_u
4.8	0.3	0.818	0.793	6.331
	0.4	0.823	0.779	6.169
	0.5	0.827	0.761	5.968
	0.6	0.831	0.738	5.731
4.9	0.3	0.817	0.793	6.387
	0.4	0.824	0.782	6.235
	0.5	0.828	0.764	6.039
	0.6	0.832	0.742	5.810
5.0	0.3	0.817	0.794	6.442
	0.4	0.824	0.784	6.297
	0.5	0.829	0.767	6.109
	0.6	0.832	0.745	5.885
5.1	0.3	0.818	0.796	6.496
	0.4	0.825	0.786	6.357
	0.5	0.829	0.770	6.175
	0.6	0.833	0.749	5.957
5.2	0.3	0.820	0.798	6.550
	0.4	0.826	0.788	6.414
	0.5	0.830	0.773	6.238
	0.6	0.833	0.752	6.027

Table 5b: QCD corrections factor in $O(\alpha_s)$ for the semileptonic decays, K_{SL}, and the functions I_u and Z_u defined in the text for the $b \to u$ transitions.

m_t (GeV)	c_+	c_-	K_{NL}
30.0	0.955	1.097	0.951
35.0	0.962	1.080	0.946
40.0	0.968	1.067	0.943
45.0	0.974	1.055	0.940
50.0	0.978	1.045	0.938

Table 6: QCD correction factors for the non-leptonic decays of the top quark.

Modes	Widths $\bar{\Gamma}_i^t$	BR(Z)
$t \to be\nu_e$	$0.79 \lvert V_{bt}\rvert^2$	10.7
$\to b\mu\nu_\mu$	$0.79 \lvert V_{bt}\rvert^2$	10.7
$\to b\tau\nu_\tau$	$0.77 \lvert V_{bt}\rvert^2$	10.50
$\to bu\bar{d}$	$2.38 \lvert V_{bt}\rvert^2$	32.4
$\to bu\bar{s}$	$0.13 \lvert V_{bt}\rvert^2$	1.7
$\to bc\bar{s}$	$2.34 \lvert V_{bt}\rvert^2$	31.9
$\to bc\bar{d}$	$0.12 \lvert V_{bt}\rvert^2$	1.7
$\to b\bar{b}c$	$2.16 \lvert V_{bt}\rvert^2 \lvert V_{bc}\rvert^2$	7.5×10^{-2}
$\to se\nu_e$	$0.87 \lvert V_{ts}\rvert^2$	3×10^{-2}
$\to s\mu\nu_\mu$	$0.87 \lvert V_{ts}\rvert^2$	3×10^{-2}
$\to s\tau\nu_\tau$	$0.86 \lvert V_{ts}\rvert^2$	2.9×10^{-2}
$\to su\bar{d}$	$2.68 \lvert V_{ts}\rvert^2$	9.1×10^{-2}
$\to su\bar{s}$	$0.14 \lvert V_{ts}\rvert^2$	4.8×10^{-3}
$\to sc\bar{s}$	$2.44 \lvert V_{ts}\rvert^2$	9.0×10^{-2}
$\to sc\bar{d}$	$0.13 \lvert V_{ts}\rvert^2$	4.7×10^{-3}
$\to dx$	$8.3 \lvert V_{td}\rvert^2$	$\leq 1\times10^{-2}$

Table 7: Reduced Widths, $\bar{\Gamma}_i$, for the top quark decays as defined in text and the expected branching ratios, for m_t = 40 GeV.

m_t (GeV)	Z_b	Z_s	$\bar{\Gamma}^t$
30.0	6.69	8.17	6.71
35.0	7.07	8.19	7.09
40.0	7.34	8.20	7.36
45.0	7.51	8.20	7.53
50.0	7.65	8.21	7.67

Table 8: The functions Z_b and Z_s and the reduced width $\bar{\Gamma}^t$ for the top quark decays

Decay Mode	Branching ratio (%)
$t \to 0lx$	41.4
$\to 1lx$	42.8
$\to 2lx$	14.3
$\to 3lx$	1.5
$\to 4lx$	2.8×10^{-4}
$\to 5lx$	3×10^{-5}
$\langle \#l/t \rangle$	0.76

Table 9: Branching ratio for the decays $t \to (nl^{\pm}x)$ using the measured semileptonic branching ratios for the bottom and charm quarks and $\tau^{\pm} \to l^{\pm}\nu_l\dot{\nu}_{\tau}$.

Decay Modes	$c\bar{c}$	$b\bar{b}$	$t\bar{t}$	$\sum$
$Z^0 \to 1lx$	3.7	6.2	1.0	10.9
$\to 2lx$	0.46	2.27	.85	3.58
$\to 3lx$	-	.49	.38	.87
$\to 4lx$	-	.034	.09	0.124
$\to 5lx$	-	-	.011	0.011
$\to 6lx$	-	-	8×10^{-4}	8×10^{-4}

Table 10: Branching ratios (%) for the inclusive decays $Z^0 \to nlx$ $(n=1,\ldots,6)$ from the decays $Z^0 \to c\bar{c}$, $b\bar{b}$, $t\bar{t} \to nlx$, for m_t 40 GeV.

Modes	Branching Ratios (%)
$D^0 \to K^-X$	55.0
$D^0 \to K^+X$	9.5
$D^+ \to K^-X$	30.0
$D^+ \to K^+X$	6.5
$F^+ \to K^-X$	20.0
$F^+ \to K^+X$	30.0

Table 11: Inclusive branching ratios for the charmed meson decays $D,F \to K\ X$ used in the calculation.

χ_s	$l^{\pm}l^{\pm}X$	l^+l^-X	$l^{\pm}l^{\pm}X/l^+l^-X$	$\bar{l}^+K^{\pm}K^{\pm}X$	$l^-K^+K^+X$	$\bar{l}^+K^+K^-X$	$\Delta(lKK)$
0.0	3S	73S	0.04S	420	1000	3640	0.41
0.20	5S	71S	0.07S	47S	96S	3620	0.34
0.30	90	680	0.130	52S	93S	3600	0.28
0.40	10S	66S	0.16	S40	92S	359S	0.2S
0.50	11S	65S	0.17S	S70	900	3590	0.23

Table 12: Estimated rates based on 10^5 $b\bar{b}$ events for the production of dilepton and lepton kaon kaon states in $e^+e^- \to b\bar{b} \to ll\ X$, $lKKX$ ($l = e + \mu$) at $\sqrt{s}$ = 93 GeV with cuts described in the text.

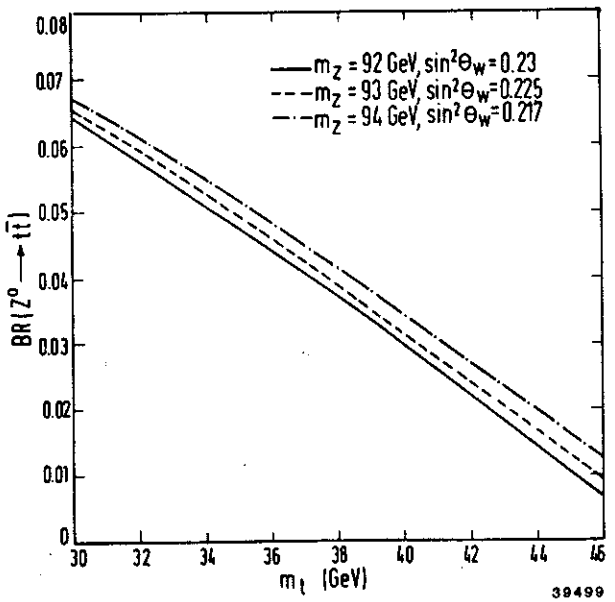

Fig 1: The $O(\alpha_s)$ corrected branching ratio, $BR(Z^0 \rightarrow t\bar{t})$, as a function of top quark mass, values for m_z and $\sin^2\theta_W$ as indicated.

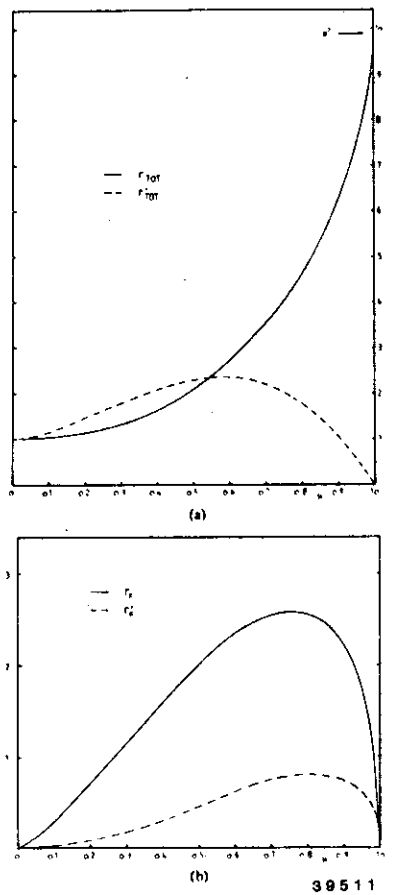

Fig 2: The coefficients γ_{tot} (= R_V^q), γ'_{tot} (= R_A^q), γ_F and γ'_F for the cross sections σ_q and Δ_q as functions of μ (= quark mass/beam energy) (from ref. 33).

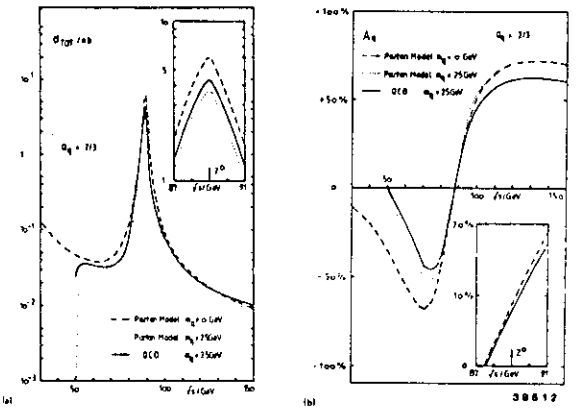

Fig 3: (a) s-dependence of the cross section σ_q with threshold suppression and QCD corrections for charge 2/3 quarks and quark mass m_q = 25 GeV;
(b) The same for the forward-backward asymmetry A_q (= A_{FB}^{q}) (from ref. 33).

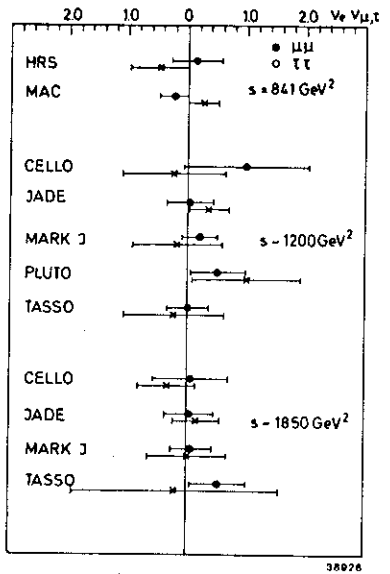

Fig 4: The present status of the leptonic vector coupling constant product $V_e(V_\mu, V_\tau)$, measured at PETRA/PEP energies (from ref. 63).

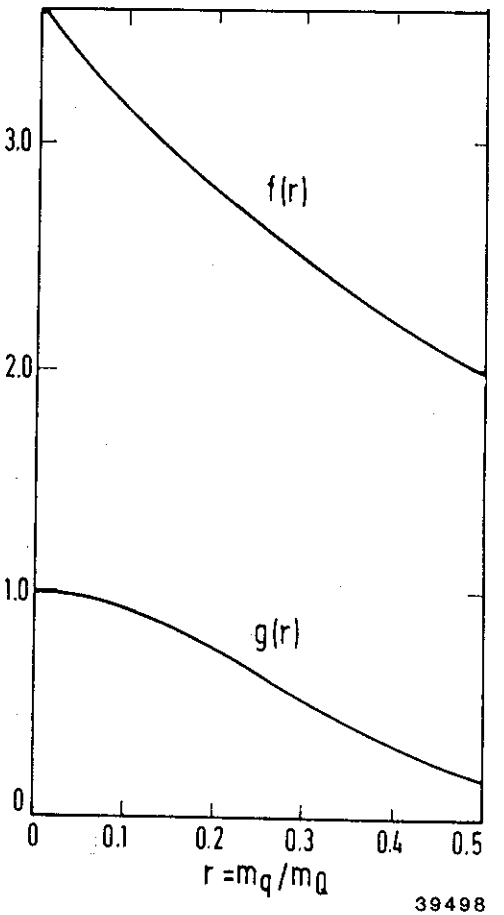

Fig 5: The Phase space functions g(r) and f(r) in the semileptonic decays of heavy quarks as a function of $r = m_q/m_Q$ (from Ali and Pietarinen in ref. 4).

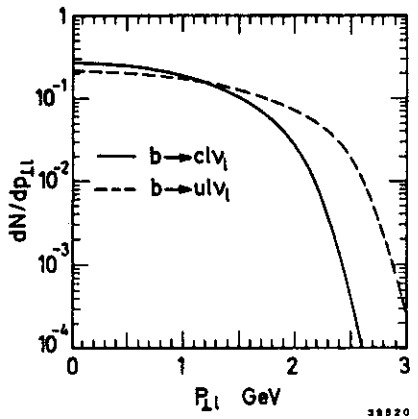

Fig 6: The transverse lepton energy distribution $\frac{1}{N}\frac{dN}{dP_\perp^l}$ based on eq. (2.56) for the decays $b \to c l \nu_l$ and $b \to u l \nu_l$.

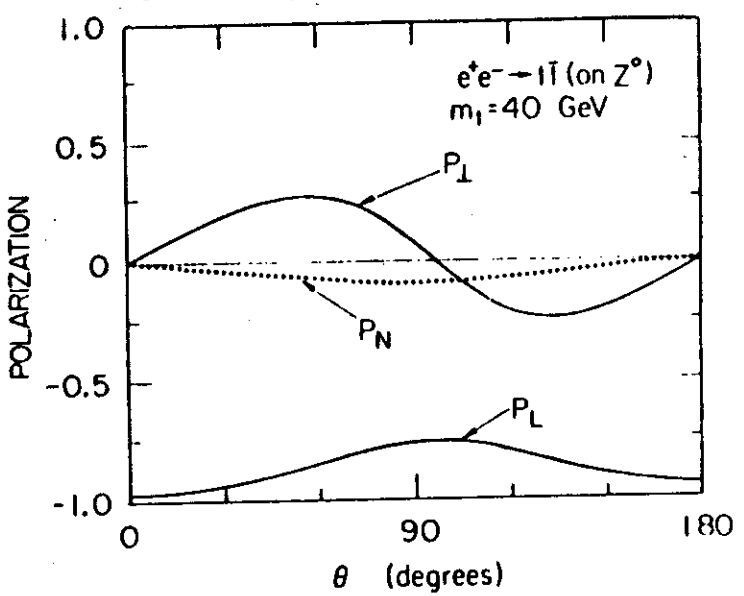

Fig 7: The longitudinal polarization P_L, transverse polarization P_T and normal polarization PN of the top quark in $e^+e^- \to t\bar{t}$ on Z^0 for unpolarized beams as functions of the scattering angle θ (from ref. 57).

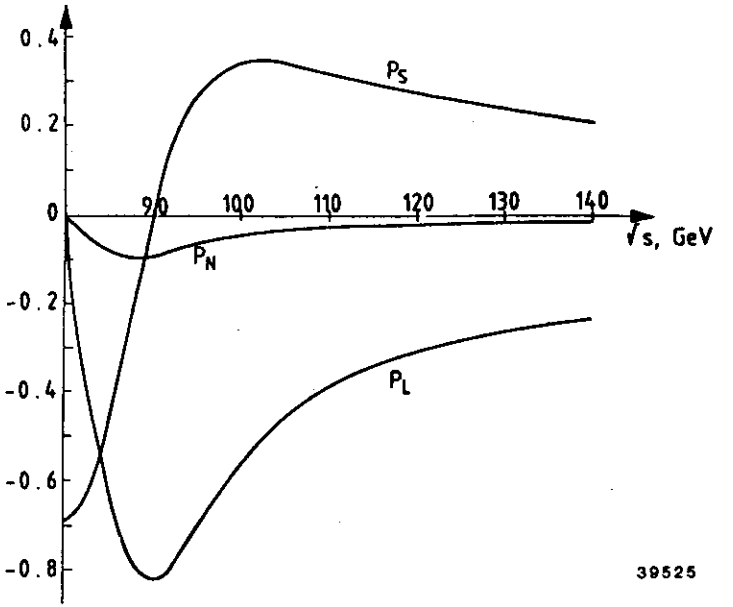

Fig 8: The average values of the polarization components $\langle P_L \rangle$, $\langle P_S \rangle$ (=$\langle P_T \rangle$ and $\langle P_N \rangle$ for the top quark as function of √s (from ref. 56).

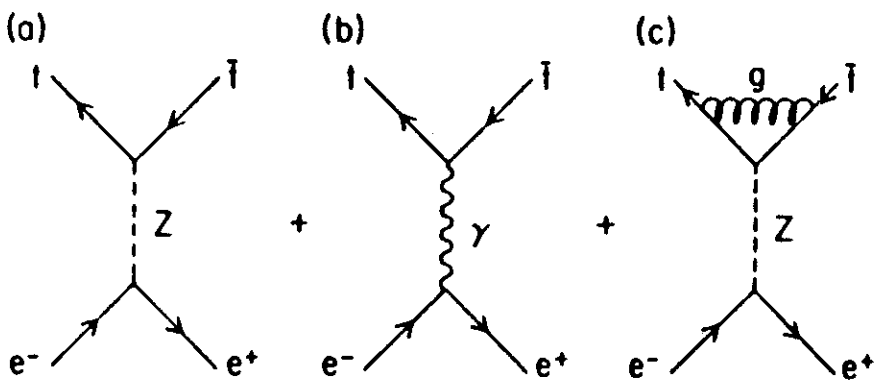

Fig 9: Feynman diagrams contributing to the normal polarization P_N of the top quark in $e^+e^- \to Z^0, \gamma \to t\bar{t}$
(a) Z^0 -exchange Born graph
(b) γ -exchange Born graph
(c) Z^0 -exchange including QCD corrections.

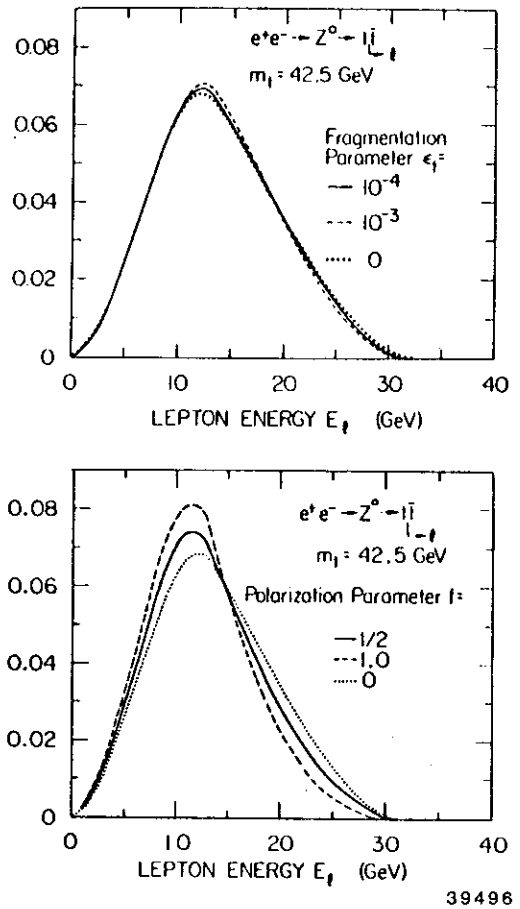

Fig 10: Energy distributions of the charged lepton in $e^+e^- \to Z^0 \to t\bar{t} \to l^\pm X$ due to the semileptonic decay of the t (or $\bar{t}$) quark (from ref. 57).

(a) Dependence on the fragmentation parameter ϵ_l.

(b) Dependence on polarization effects with the fragmentation parameter ϵ_l 10^{-4}. f = 0 indicates complete depolarization, f = 1 no depolarization.

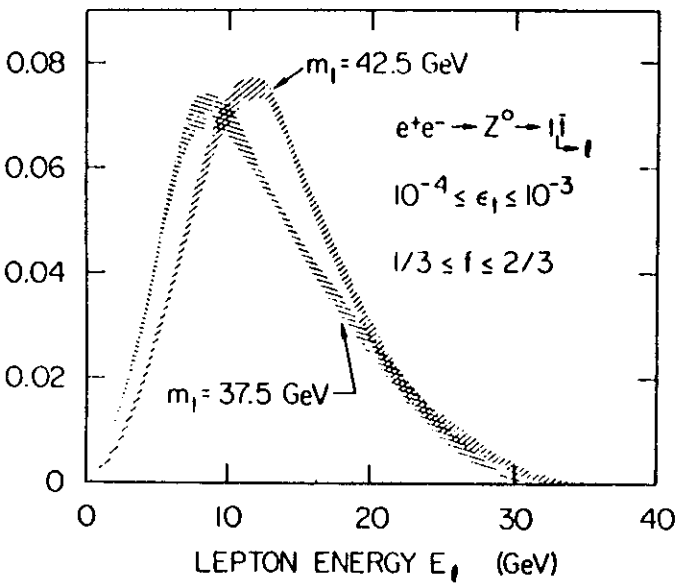

(c) Dependence on polarization and fragmentation effects. The shaded areas indicate bounds of the lepton energy distribution for the values of the parameters in the indicated range.

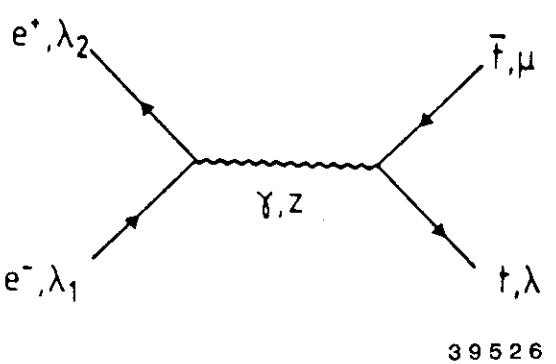

Fig 11: Definition of helicities for the Born diagram for $e^+e^- \to \gamma, Z \to f\bar{f}$.

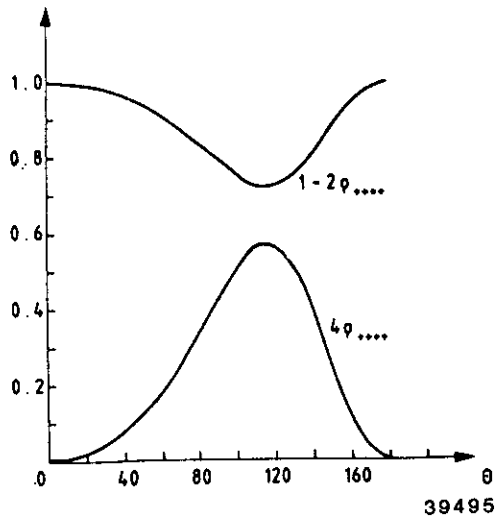

Fig 12: The dependence of the quantities 1-2 ρ_{++++} $(t\bar{t})$ and 4 $\rho_{++++}(t\bar{t})$ on the production angle, θ for m_t = 40 GeV, m_z = 90 GeV and Γ_z = 3 GeV (from ref. 56)

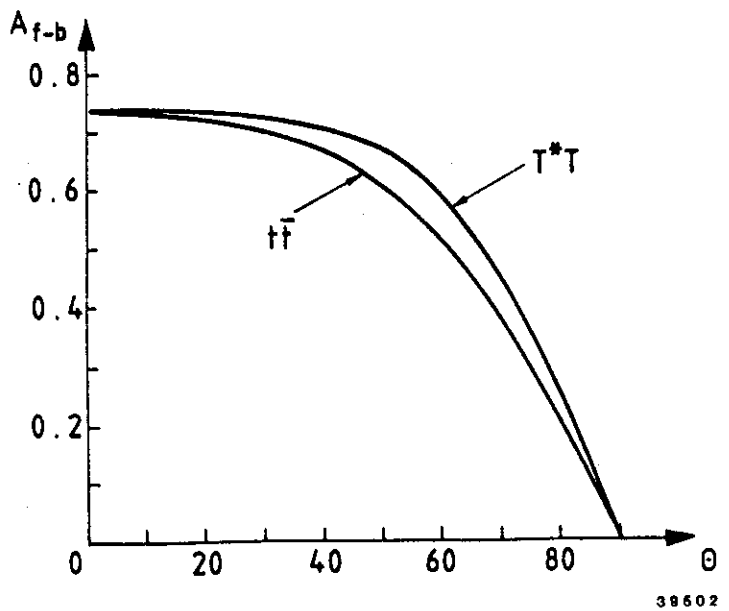

Fig 13: Forward-backward asymmetries for the two processes $e^+e^- \to t\bar{t}$ and $e^+e^- \to T\bar{T}^*$ $(T^*\bar{T})$ with the same parameters as in fig. 12 (from ref. 56).

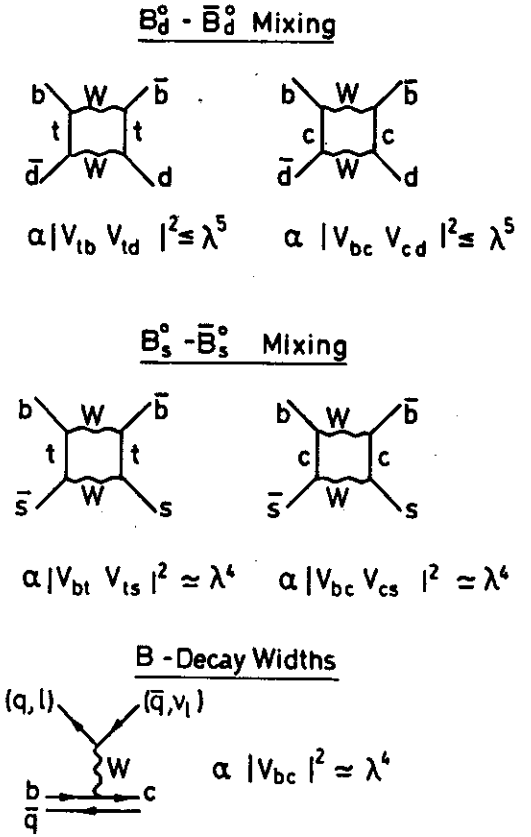

Fig 14: Feynman diagrams contributing to the mass difference ΔM in the neutral bottom meson sector. Also shown is the quark decay diagram for B decays.

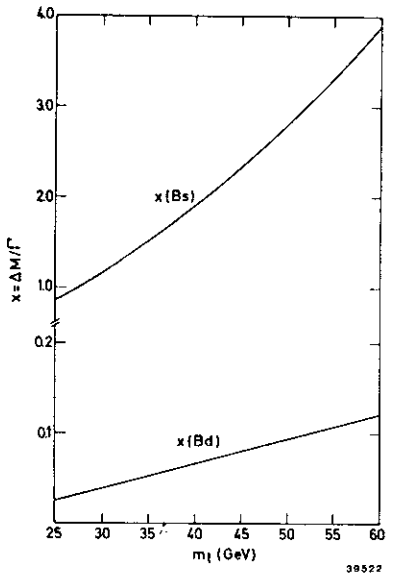

Fig 15: The quantity $x = \Delta M/\Gamma$ for the $B_s^0-\bar{B}_s^0$ system as a function of the top quark mass, m_t.

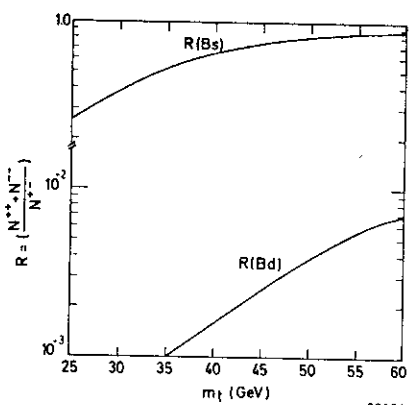

Fig 16: The dilepton ratio $R = N^{\pm\pm}/N^{\pm\mp}$ for the bottom meson production processes $e^+e^- \to B_d^0X \to l^\pm l^\pm X$, $l^\pm l^\mp X$ and $e^+e^- \to B_s^0X \to l^\pm l^\pm X$, $l^\pm l^\mp X$ as a function of the top quark mass, m_t.

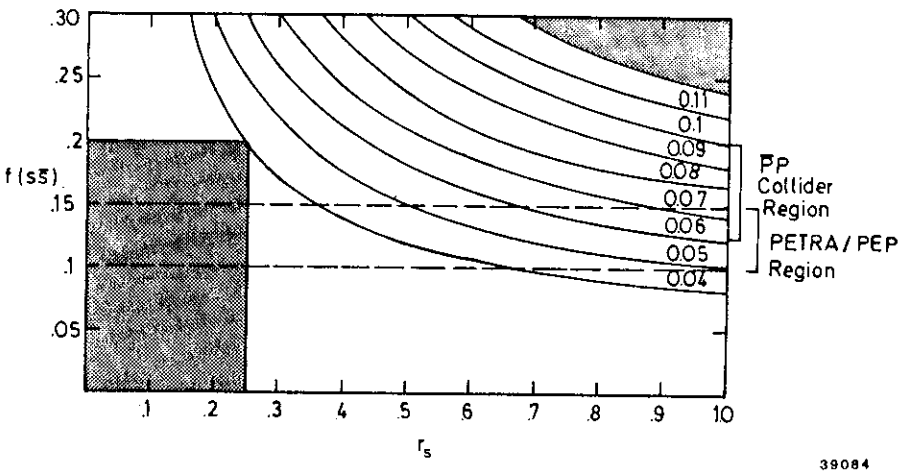

Fig 17: Contours of constant χ in the $f(s\bar{s})$ - r_s plane. The shaded area on the upper right hand corner is excluded by the Mark-II upper limit $\chi < 0.12$. The 90% C.L. lower limit from the UA1 data, $\chi > 0.04$ excludes the left hand shaded area. The most likely regions of $f(s\bar{s})$ for PETRA/PEP and collider data are also indicated. At LEP one expects $f(s\bar{s}) = 0.15$ (from ref. 20).

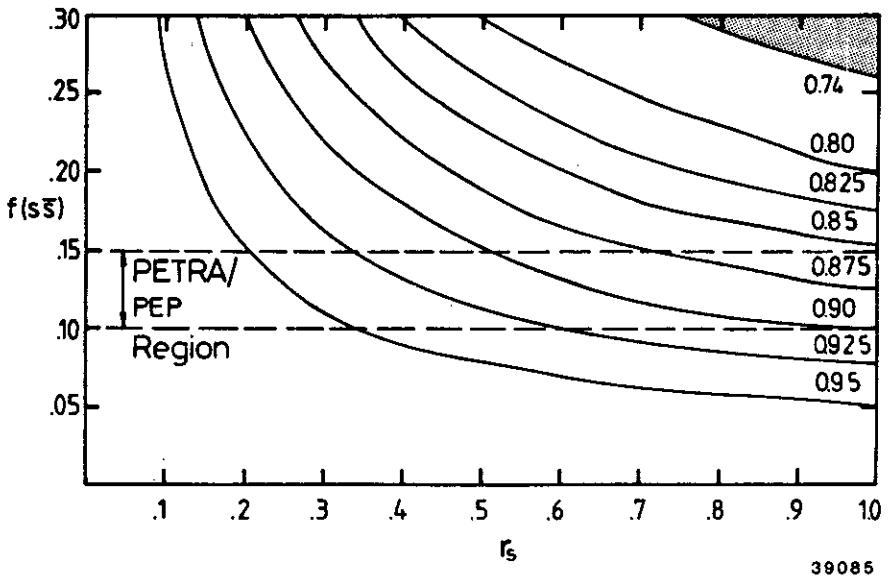

Fig 18: Contours of constant $R^b_{asym} = \bar{A}^b_{FB} / A^b_{FB}$ in the $f(s\bar{s})$-r_s plane. The shaded area on the upper right hand corner is excluded by the electroweak charge asymmetry measurements $\bar{A}^b_{FB} > 0.74$ (90% C.L.) from experiments at DESY (from ref. 20).

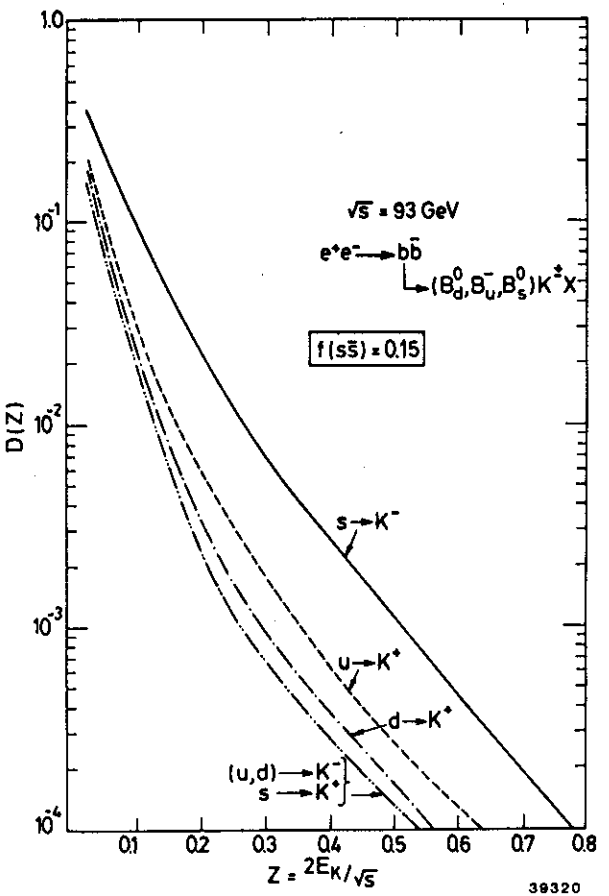

Fig 19: Fragmentation function D(Z) for the associated production of charged kaons from $q \rightarrow K^\pm X$ in the process $e^+e^- \rightarrow b\bar{b} \rightarrow (B^0_d, B^-_u, B^0_s) K^\pm X$ at $\sqrt{s}$ = 93 GeV. Note that for the bottom quark fragmentation we have used the Peterson function[62] but D(Z) has a functional form like in the Field-Feynman model[82] (from ref. 21).

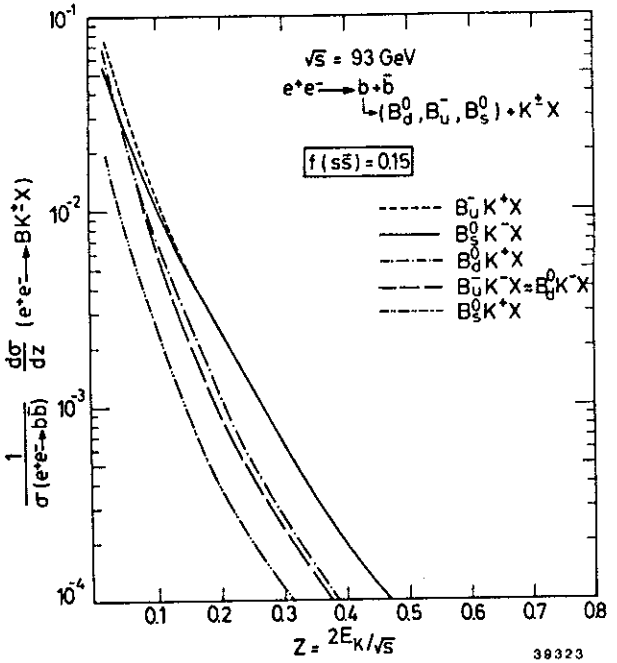

Fig 20: The differential cross section $(1/\sigma(b\bar{b}))(d\sigma/dz)(e^+e^- \to \gamma,Z \to PE^{\pm}X)$ for the various bottom mesons with $f(s\bar{s}) = 0.15$. Note that the P and $K^{\pm}$ mesons belong to the same jet (hemisphere) (from ref. 21).

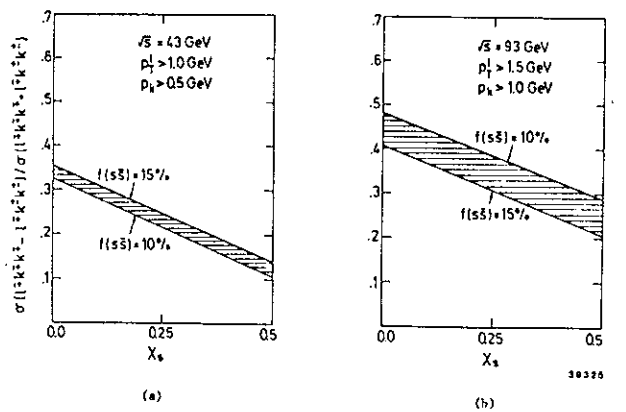

Fig 21: The ratio $\Delta R(lKK) = [\sigma(e^+e^- \to l^{\mp}K^{\mp}K^{\mp}X) - \sigma(e^+e^- \to l^{\mp}K^{\pm}K^{\pm}X)] / [\sigma_+e^+e^- \to l^{\mp}K^{\mp}K^{\mp}X) + \sigma(e^+e^- \to l^{\mp}K^{\pm}K^{\pm}X)]$ as a function of the weak mixing measure, with the indicated values of the parameters (from ref. 21).

(a) $\sqrt{s}$ = 43 GeV

(b) $\sqrt{s}$ = 93 GeV

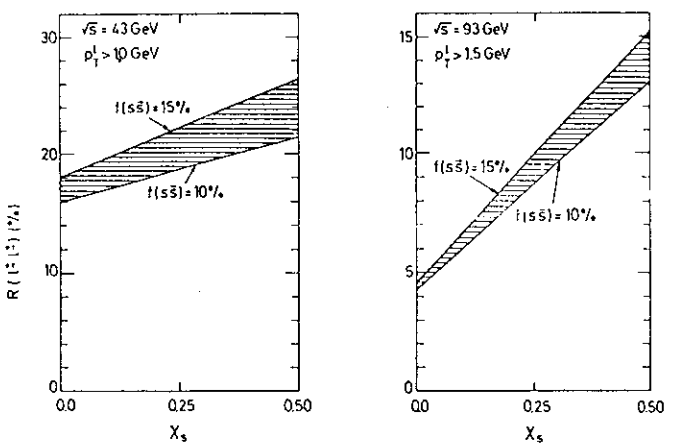

Fig 22: The dilepton ratio $R = (N^{++}+N^{--}/N^{++}+N^{--}+N^{+-})$ with the indicated values of the parameter (from ref. 21)

(a) $\sqrt{s}$ = 43 GeV

(b) $\sqrt{s}$ = 93 GeV

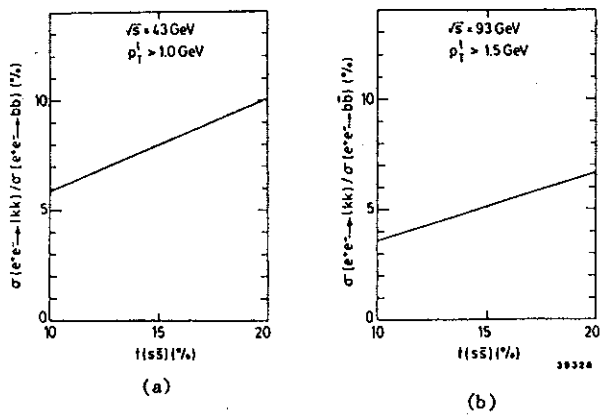

Fig 23: $\sigma(e^+e^- \to lKKX)/\sigma(e^+e^- \to b\bar{b})$ summed over all charged combinations of $l^{\pm}$ and $K^{\pm}$ as a function of $f(s\bar{s})$ with the indicated cuts. Note that (lKK) belong to the same hemisphere (jet) (from ref. 21).

(a) $\sqrt{s}$ = 43 GeV

(b) $\sqrt{s}$ = 93 GeV

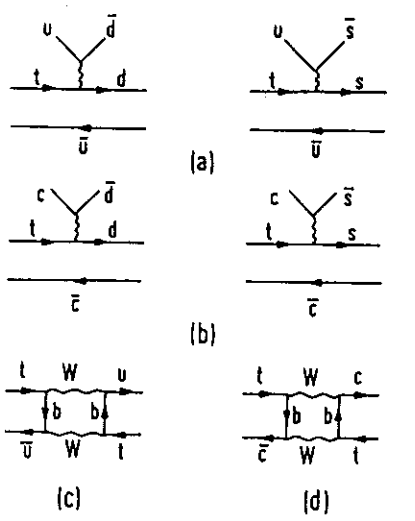

Fig 24. Feynman diagrams contributing to the width and mass differences $\Delta\Gamma$ and ΔM for the neutral top mesons $\bar{T}_u$ and $\bar{T}_c$.

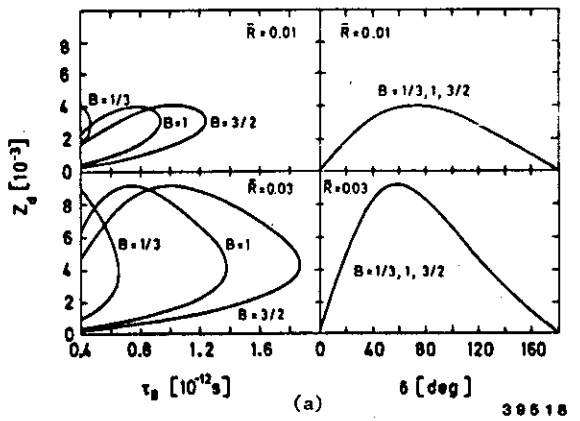

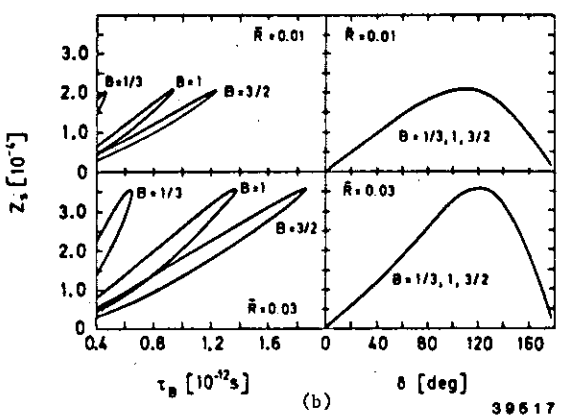

Fig 25: The CP-violating parameter Z defined as Z_d = 1/2 Im Γ_{12} / M_{12} for the neutral bottom meson sector with the indicated values of the Bag constant, B, and the ratio $\tilde{R}$ (from Buras et al. in ref. 19).

(a) Z_d for B_d^0-$\bar{B}_d^0$ mixings

(b) Z_s for B_s^0-$\bar{B}_s^0$ mixings